PLATINUM COMPLEXES OF NEW BORANE-CONTAINING LIGANDS

BORANE-CONTAINING LIGANDS BASED ON THIOXANTHENE, XANTHENE AND ACRIDINE: SYNTHESES AND PLATINUM COORDINATION CHEMISTRY

By

NATALIE L. BLACKWELL, B. Sc.

A Thesis

Submitted to the School of Graduate Studies

in Partial Fulfillment of the Requirements

for the Degree

Master of Science

McMaster University

Master of Science (2006) McMaster University

(Chemistry) Hamilton, Ontario

TITLE: Borane-Containing Ligands Based on Thioxanthene, Xanthene and Acridine: Syntheses and Platinum Coordination Chemistry

AUTHOR: Natalie L. Blackwell, B. Sc. (Windsor University)

SUPERVISOR: Dr D. J. H. Emslie

NUMBER OR PAGES: xviii, 137, XX

Abstract

Ligand backbones based on xanthene, thioxanthene and acridine (XPB, TXPB and APB) have been targeted as scaffolds for the formation of rare compounds containing Lewis basic phosphine and Lewis acidic borane moieties. The resulting complexes with Pt(0) and Pt(II) reagents are expected to possess diverse reactivity compared to traditional platinum phosphine adducts owing to the strategically appended borane Lewis acid.

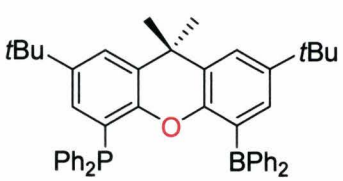

XPB

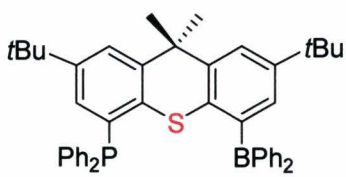

TXPB

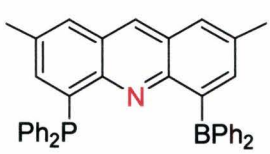

APB

Two ligands, 2,7-di-(*tert*-butyl)-4-diphenylboryl-5-diphenylphosphino-9,9-dimethylthioxanthene (**TXPB**) and 2,7-di-(*tert*-butyl)-4-diphenylboryl-5-diphenylphosphino-9,9-dimethylxanthene (**XPB**), have been synthesized and reacted with the platinum reagents $[PtCl_2(COD)]$, $[PtMe_2(COD)]$ and $[Pt(nbe)_3]$. In the case of **TXPB**, two new Pt(II) compounds $[PtCl(\mu\text{-}Cl)(TXPB)]$ and $[PtMePh(TXPB^{Ph,Me})]$ have been formed, isolated and characterized. In both compounds, X-Ray analysis shows that the S

and the P atoms bind to the Pt center drawing the metal into the vicinity of the B group. In [PtCl(μ-Cl)(TXPB)], a chloride is seen to bridge between the Pt and B, whereas [PtMePh(TXPB^{Ph,Me})] shows that a methyl groups has been transferred to the boron with concomitant transfer of a phenyl group to Pt. Reaction with the platinum(0) precursor [Pt(nbe)$_3$] led to formation of an unstable complex, tentatively assigned as [Pt(nbe)TXPB]. Analogous studies with the new xanthene-derived ligand, **XPB**, led to starkly different results. In the reaction with [PtCl$_2$(COD)], an insoluble product, perhaps a dinuclear complex with bridging chlorides, was formed. No reaction occurred with [PtMe$_2$(COD)], presumably because of non-participation of the O ligand. However, with [Pt(nbe)$_3$], a stable complex, [Pt(nbe)$_2$XPB], was observed.

Synthesis of a third ligand scaffold **APB** has been initiated where the pyridine moiety is expected to allow strong chelation of Pt as observed with TXPB. An advanced intermediate **AFBr** has been synthesised where the backbone has been created through a ring closure reaction positioning two different halides as required for sequential addition of the phosphine and borane groups of the target compound.

Acknowledgements

I would like to thank my supervisor Dr. D. Emslie for allowing me to carry out this research project under his supervision and for all of his help and guidance.

I am grateful to the other members of the group, especially Carlos Cruz for his companionship and sharing of lab space and glassware.

I would like to extend my gratitude to Drs. I. Vargas-Baca and P. Harrison for their help and effort put into being on my committee.

I would also like to thank Drs. Jim Britten and Laura Harrington for X-ray structure determination.

I finally wish to extend my gratitude to my family for their support and perseverance, and especially to my husband James.

Table of Contents

List of Figures

List of Schemes

List of Tables

Abbreviations

Å	Angstroms
Ar	aryl
BINOL	1,1'-binaphthalene-2,2'-diol
br.	broad
Bu	*n*-butyl
Calcd.	calculated
Cat	1,2-$O_2C_6H_4$
COD	cycloocta-1,5-diene
COSY	correlation spectroscopy
COT	1,3,5,7-cyclooctatetraene (C_8H_8 or $C_8H_8^{2-}$)
Cp	cyclopentadienyl
Cp*	pentamethylcyclopentadienyl
CV	cyclic voltammetry
Cy	cyclohexyl
d	doublet
dba	dibenzylidene acetone
dd	doublet of doublets
DEPT	distortionless enhancement by polarization transfer
DCE	1,2-dichloroethane
DMAP	dimethylamino iso-propoxide
DME	1,2-dimethoxyethane

DMSO	dimethylsulfoxide
DiPPE	bis(di(*i*-propyl)phosphino)ethane
DPPE	bis(diphenylphosphino)ethane
DPPM	bis(diphenylphosphino)methane
eq	equivalents
$E_{1/2}$	half-peak potential for a reversible wave, $\frac{[Ep_{(ox)} + Ep_{(red)}]}{2}$
$Ep_{(ox)}$	oxidation peak potential
$Ep_{(red)}$	reduction peak potential
Fc	ferrocenyl
h	hours
hal^-	halide
HMBC	heteronuclear multiple bond correlation
HSQC	heteronuclear single quantum correlation
Hz	Hertz
IR	infrared
J	symbol for coupling constant
LA	Lewis acid
LB	Lewis base
m	multiplet
Mes	mesityl, (2,4,6-trimethylphenyl)
MHz	megahertz
min	minutes

mol	mole
NMR	nuclear magnetic resonance
NOE	nuclear Overhauser effect
nbe	norbornadiene, bicyclo[2.2.1]hepta-2,5-diene
OTf	triflate, trifluoromethanesufonate
ppm	parts per million
t	triplet
tert	tertiary
THF	tetrahydrofuran
TM	transition metal
TMEDA	N,N,N',N'-tetramethylethylenediamine
xyl	2,6-dimethylphenyl

Chapter 1 – Introduction

1.1 Lewis Acids and Lewis Bases

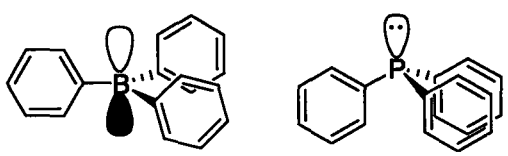

Figure 1.1: Examples of a Lewis Acid and a Lewis Base

In the Lewis acid-base concept, acids and bases are specified in general terms as electron pair-acceptors and electron pair-donors, respectively. Lewis acids are characterized as possessing a vacant orbital whereas Lewis bases are characterized as possessing a lone pair of electrons (see Figure 1.1).[1] The vacant orbital in Lewis acids can accept an electron pair from a Lewis base making these species complementary and fundamental to each other. The importance of Lewis's conceptual approach of acidity is rooted in the fact that it can be applied to compounds which do not contain protons. This is in contrast to the Brønsted definition of acids and bases, which is restricted to proton donors and proton acceptors, respectively. In fact, Lewis acidic molecules can be based on diverse elements form across the periodic table, for example H^+, SnR_3^+, LCu^+; in this discussion, those based on Group 13 elements and metals in higher oxidation states will be emphasized. Lewis basic molecules can also be based on elements from across the

periodic table, such as NH_3, Cl^-, Ph_3P, $[Fe(CO)_4]^{2-}$; in this discussion, those based on Group 15 elements and low oxidation state metals are emphasized.

1.1.1 Group 13 Lewis Acids

Trivalent molecules R_3E based on the Group 13 elements (E = B, Al, Ga, In) are often potent Lewis acids which are susceptible to formation of complexes, $L \rightarrow ER_3$, with a diverse range of Lewis bases. The acceptor behaviour arises because of the presence of a formally vacant p-orbital and the absence of a lone pair of electrons on the group 13 element. The R groups are important in determining the level of Lewis acidity, electron-withdrawing groups generally enhancing the electron deficient character. An important subset are borane derivatives, R_3B, whose electron deficiency results in a tendency for many boranes to form metacentre bonds and Lewis acid-base adducts important in many areas of catalysis. In fact, formation of Lewis acid/Lewis base adducts can be used to activate molecules (for example, carbonyls, imines, epoxides etc) to subsequent reactions with nucleophiles.[2] As shown in Figure 1.2, a Lewis acidic borane forms an adduct with a Lewis basic carbonyl complex, initiating attack at the carbonyl by another Lewis basic (nucleophilic) molecule. This activation pathway is very general and can be found for a wide variety of Lewis acidic and Lewis basic molecules.

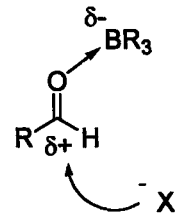

Figure 1.2: An Activated Adduct

In many cases, the nucleophile is contained within the Lewis acid itself (as in H-BR_2, allylBR_2); coordination of the Lewis base triggers an intramolecular ligand transfer (such as H or allyl) from the boron to the activated substrate. Consequently, it is not surprising that borane-Lewis base adducts have been extensively studied from both experimental[3] and theoretical points[4] of view. Of course, many important examples of Al, Ga and In acting as Lewis acids also exist but borane-based Lewis acids are the most common and of most relevance to the research described herein.

1.1.2 Transition Metal Lewis Acids

Metals in high oxidation states which are electronically and coordinatively unsaturated are often strong Lewis acids. It is this electron deficiency which allows them to mediate/catalyse diverse processes including reductions (*e.g.* $TiCl_4$ catalyzed hydrosilations) and oxidations (*e.g.*, $[PdCl_2(MeCN)_2]$ in the cyclisation of ketones and esters[5]), olefin polymerization and other C-C bond forming reactions, and numerous other important processes.[6] Although similar to main group Lewis acids, the presence of

d-orbitals and generally greater coordination numbers, imparts distinct properties to transition metal Lewis acids.

1.1.3 Group 15 Lewis Bases

Some of the most important ligands in inorganic chemistry are based on Group 15 elements, especially those derived from nitrogen and phosphorus. A great number of these are based on trivalent amine and phosphine derivatives, R_3N/R_3P. This is particularly true for phosphines where a low lying electron pair is activated to donation to electron-deficient and coordinatively unsaturated transition metals. This ligand-metal interaction is strengthened in most cases through back-bonding interaction from the metal to the phosphine.[7] Amines and phosphines can also act as catalysts themselves in the field of organocatalysis where again the activity derives from the electron-donating properties of the nitrogen or phosphorus atom.[8]

The differences in reactivity of amines and phosphines towards various Lewis acids can be generalized using Pearson's Hard Soft Lewis acid Lewis base theory (HSAB).[9] Pearson attempted to explain the differential affinity of electron pair donating Lewis bases towards electron pair accepting Lewis acids, (Lewis acid/base complexation) by classifying Lewis acids and Lewis bases as one of hard, borderline or soft. According to HSAB, hard Lewis species are generally small and difficult to polarize, whereas soft Lewis species typically have a large radius and are more easily polarisable. Hard Lewis acids prefer to react with hard Lewis bases, and soft Lewis acids prefer soft Lewis bases.

Therefore, hard Lewis bases such as NH_3 and OR_2 tend to react with hard Lewis acids such as H^+, $AlCl_3$ and early transition metals such as Zr(IV) and Ti(IV). Softer Lewis bases, such as PR_3 and SR_2, prefer softer Lewis acidic groups such as Br_2 and electron-rich late transition metals such as Pt(II) and Au(I). In designing new ligands for transition metals, careful consideration of these concepts is necessary.

1.2 Conventional η^1- Bonding Interactions Between Transition Metals and Ligands

The majority of η^1-interactions between a ligand and a metal can be described based on three (or combinations thereof) bonding motifs.

1) sigma donation from ligand to metal

2) pi donation from ligand to metal

3) pi donation from metal to ligand (back-bonding)

Stable complexes involving sigma donation from metal to ligand are much less common although examples have been reported and will be discussed in section 1.3.

1.2.1 Ligand To Metal Sigma and Pi Donation

The vast majority of transition metal complexes in the literature involve sigma interactions with electrons donated from the ligand to the transition metal. A sigma-bonding interaction involves the donation of a high lying electron lone pair from a

ligand atom. In these cases then, the ligand acts as the Lewis base, the metal as the Lewis acid. Such interactions are commonly observed for elements in groups 14 through 17, and include examples from neutral ligands such as NH_3 and CO and also from anionic ligands such as H^-, CH_3^- and Cl^-.

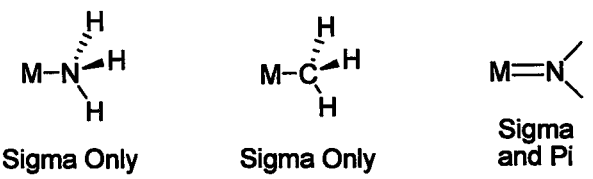

Figure 1.3: Sigma and Pi Donation From Ligand to Metal

In addition to sigma bonding, pi-bonding interactions are also commonly seen, where two (or more) lobes of one involved element overlap with two (or more) lobes of the other involved element. Pi bonds are usually weaker than sigma bonds, and are only found in conjunction with anchoring sigma bonds. Examples of this type of bonding are found in Hal^-, OR^-, and NR_2^- ligands which possess a second lone pair in addition to that used to form the stronger sigma bond. Alkyl ligands such as CH_3^- can only coordinate through a single sigma bond since a second lone pair of electrons is not present on the carbon atom as with oxygen or nitrogen. Halide, alkoxide and amide ligands do not always participate in pi bonding; a second suitable accepting orbital must be present on the metal.

1.2.2 Metal To Ligand Pi Donation

A variety of different interactions between a metal and a ligand are possible since the metal can behave not only as a Lewis acid, as described in the previous section, but

also as a Lewis base. Typically, a ligand is complexed via a strong sigma bond from ligand to metal with the pi bond being formed by transfer of electron density from the metal back to the ligand. Examples of pi acceptors include carbonyl (CO) and alkyne ligands, where there is concerted and synergic donation and backdonation of electron density between the metal to the ligand. The bonding in alkyne complexes is described by the Dewar-Chatt-Duncanson model, Figure 1.4.

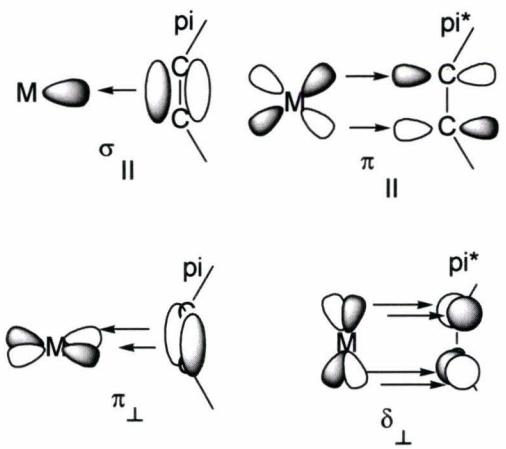

Figure 1.4: Dewar-Chatt-Duncanson Bonding Diagram for Alkyne Ligands

This type of bonding is synergistic in nature; the greater the sigma donation to the metal, the greater the backbonding to the ligand. A very similar model is used to describe backbonding to CO where a C-O pi antibonding orbital is available. CO groups, therefore, typically act as electron-withdrawing ligands depleting electron density at the metal, in turn making it more Lewis acidic.

The Lewis basic tendencies in transition metals can also be unveiled through control of ligand architecture and oxidation state. This Lewis basicity can facilitate complexation of ligands, such as in Figure 1.5,[10] where the metal transfers electron density to the incoming ligand. Thus, complexes which may not be isolable merely based on

unidirectional electron transfer from ligand to metal are stabilized. In the case of alkyne complexes, the oxidation state at the metal would be viewed as 0, II or something in between depending on the extent of electron transfer from metal to ligand (oxidative addition). This of course is dependent on the metal in question and the nature of the co-ligands; in general, the more electron rich the metal centre, the more metal to ligand backbonding occurs. X-ray crystallography is often used to gauge the extent of backbonding by comparison of M-L and intra-ligand bond distances and angles. Spectroscopic and analytical techniques can also be used; for example, IR spectroscopy (C-C stretch) and redox potentials for M-alkyne complexes can be highly informative.

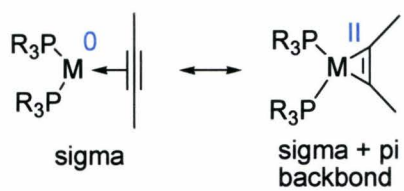

Figure 1.5: Pi Backbonding Leading to Oxidation State Change

Backbonding interactions are important not just as a means of forming new complexes but also for many catalytic transformations which involve coupling two or more molecules in the coordination sphere of a metal. As was pointed out, in the majority of cases, these bonding interactions from the metal to an incoming molecule are accompanied by a donation of electron density from the incoming molecule into low-lying empty orbitals on the metal fragment. It is rare indeed that complex formation occurs via solely σ-donation from a transition metal to another entity, and the few that exist will be discussed in the following section.

1.3 Transition Metals as Sigma Donors

As mentioned, there are relatively few stable complexes which involve donation of electron density from metal to ligand via a sigma interaction. Probably the most familiar examples are metal hydride complexes such as $[H_2Fe(CO)_4]$ and $[HCo(CO)_4]$ which have acidities similar to acetic acid and trifluoroacetic acid respectively.

Since trivalent group 13 Lewis acids have a vacant bonding orbital and do not possess a lone pair to donate to the transition metal, their only possible role is as an electron acceptor. For E=B, only σ- acceptance can occur, but for E > B, both σ- and π-acceptance can be envisaged. Therefore, it is logical that substantially Lewis acidic ER_3 molecules should readily form a metal-group 13 Lewis acid bond with a basic transition metal ($TM \rightarrow ER_3$, where E = B, Al, Ga, In). There are, however, only a relatively small number of stable complexes of this type. Examples involving B-based ligands will be discussed first, followed by those of the heavier Al, Ga and In Lewis acidic ligands.

An additional reason that there are so few authenticated transition metal-Lewis acid complexes is the difficulty in describing such complexes as unquestionably involving sigma-donation from metal to ligand. Ambiguity exists in the classification or identification of $M\text{-}ER_3$ complexes due to alternative ways to view an $M\text{-}ER_3$ interaction. Examples of this will be discussed later in this section, and will illustrate that it is not always simple to determine if a Group 13 element is acting as a Lewis acidic ligand. This is especially true in the absence of X-ray crystallographic data, and indeed, many judgment errors have been made in the past.

Within the context of metal-borane Lewis acid complexes, boryl metallocenes will also be discussed. These complexes contain TM-BR_3 interactions, and although the interactions are weak, existence of such bonds is useful to illustrate the conditions necessary for these interactions to occur.

1.3.1 Transition Metal-Borane Complexes

Since the early 1960s, reactions of complexes containing basic metal centres with various boranes have been studied,[11] but very few have been verified to contain a discrete metal-boron bond. Several of these complexes were believed to contain M-B bonds, based primarily on IR spectra. In fact, the complex $[(C_5H_5)_2WH_2(BF_3)]$ (**I**) was published in textbooks as a model borane-transition metal complex (Figure 1.6)[12]

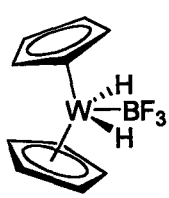

I

Figure 1.6: Classic Text-Book Example of a Transition Metal Borane Complex

With the development of improved spectral characterization, however, investigation of this complex three decades later by NMR spectroscopy and X-ray structure analysis showed that no tungsten-boron bond was actually present and that the complex is in fact salt-like $[(C_5H_5)_2WH_2][BF_4]$.[13]

The first fully characterized and structurally verified metal-borane was recently published by A. Hill *et al.* In 1999, they presented an unusually stable metal-borane complex $[Ru(CO)(PPh_3)\{B(mt)_3\}]$ (mt = 2-sulfanyl-1-methyl-imidazole) (**II**, Figure 1.7).[14]

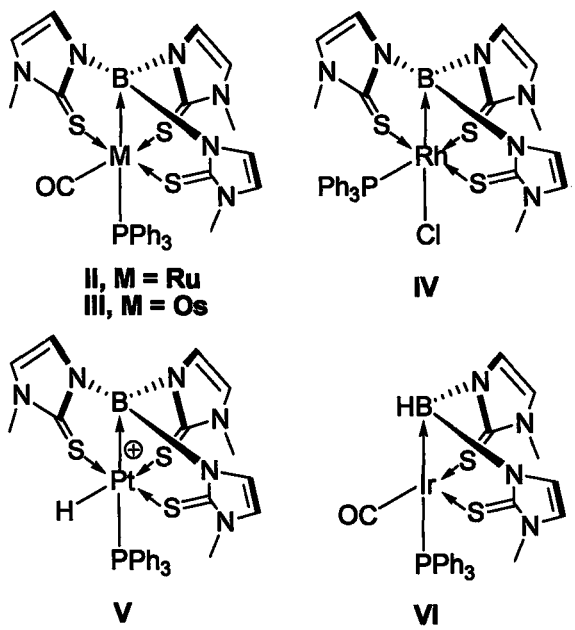

Figure 1.7: Recent Examples of Metal Borane Complexes

This complex was formed from the reaction $[Ru(CH{=}CHCPh_2OH)Cl(CO)(PPh_3)_2]$ with $Na[HB(mt)_3]$. The mechanism is believed to involve intramolecular activation of the bridgehead B-H bond to form an agostic intermediate, followed by the elimination of RH to provide the metallaboratrane (Scheme 1.1).

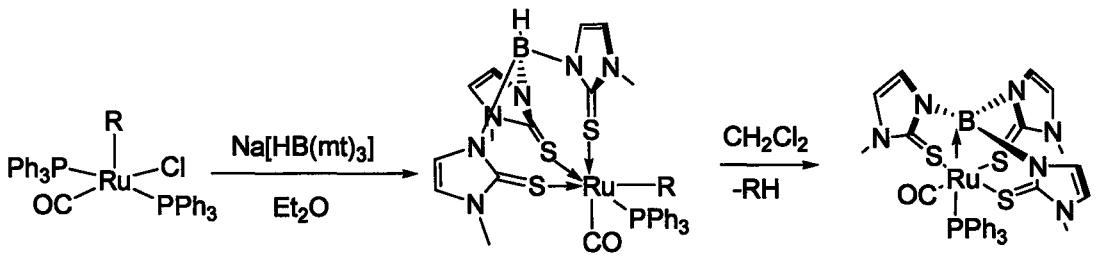

Scheme 1.1: Formation of a Metal Borane Complex via Hydrotris(methimazolyl)borate complex

The reason for the unusual stability of this compound is that the borane is tethered in the proximity of the Ru by three chelating 2-sulfanyl-1-methylimidazole arms. This serves to first allow the B-H activation reaction to occur and subsequently to place the B in a favorable location for interaction with the Ru. Hill *et al.* later obtained the Os and Rh metallaboratrane analogues through similar reactions: hydrotris(methimazolyl)borate salt $Na[HB(mt)_3]$ with d^6 transition-metal organyls $[M(R)Cl(L)(PPh_3)_3]$ (ML = OsCO, RuCl; R = aryl, vinyl) to afford the d^8 metallaboratranes $[OsCO(PPh_3)\{B(mt)_3\}]$ **(III)**[15] and $[RuCl(PPh_3)\{B(mt)_3\}]$ **(IV)**[16], respectively. The reactions are thought to occur because of factors such as d occupancy, geometric constraints, and metal basicity. Hill then went on to synthesise three more metallaboranes to investigate the limitations of these features. The most recent metallaboratranes from groups 9, **(IV)**[17] and 10 **(V)**[18] have shown the metallaboratrane motif to be generally accessible for late transition metals with high d-occupancies. In addition, the isolation of a di-buttressed iridaboratrane, $[IrH(CO)(PPh_3)\{(mt)_3\}]$ **(VI)**[19], indicates that the presence of only 2 chelating mt arms is sufficient to enforce M→B bonding. The metal-borane bonds are generally quite short (Table 1.1), with the average bond lengths being around 2.2 Å. Most recently, analogous

Rh complexes have been synthesised using phosphine and isonitrile co-ligands[20] and dimetallic $[Rh_2\{B(mt)_3\}_2\{\kappa^2\text{-}S,S'\text{-}HB(mt)_3\}]Cl$[21] has also been prepared.

Table 1.1: Existing Metal Borane Complexes and Their M-B bond lengths and ^{11}B NMR Spectroscopic Shifts

Metal Borane Complex	**M→B bond length (Å)**	**δ ^{11}B NMR (ppm)**
$[Os\{B(mt)_3\}(CO)(PPh_3)]$ [15]	2.171(8)	12.4
$[Ru\{B(mt)_3\}(CO)(PPh_3)]$ [16]	2.161(5)	17.1
$[RhCl(PPh_3)\{B(mt)_3\}]$ [17]	2.122(7)	1.47
$[RhH(PPh_3)\{B(mt)_3\}]$ [17]	N/A	9.63
$[PtH(PPh_3)\{B(mt)_3\}]^+$ [18]	N/A	1.56
$[Pt\{B(mt)_3\}(PPh_3)]$ [18]	N/A	1.47
$[IrH(CO)(PPh_3)\{B(mt)_2H\}]$ [20]	2.210(5)	-4.5
$[Rh(PPh_3)(CN\textit{t}Bu)\{B(mt)_3\}]^+$ [20]	2.155(7)	9.0
$[Rh(PPh_3)(CNXyl)\{B(mt)_3\}]^+$ [20]	2.146(3)	8.7
$[Rh(PMe_3)(PPh_3)\{B(mt)_3\}]^+$ [20]	N/A	8.8
$[Rh(PMe_3)_2\{B(mt)_3\}]^+$ [20]	2.153(11)	9.5
$[Rh_2[B(mt)_3]_2\{\kappa^2\text{-}S,S^1\text{-}HB(mt)_3\}]^+$ [21]	2.098(6), 2.0915(5)	N/A
$[\{B(mt)_3\}Co(PPh_3)][BPh_4]$ [22]	2.132(4)	N/A
$[RhCl(DMAP)(PhB(C_6H_4(P\textit{i}Pr_2)\text{-}2)_2)]$ [23]	2.306(3)	43
$[CpFe(CO)_2(BPh_3)]^-$ [24]	N/A	28.8

To date, the only other metal borane complexes to have been reported are : $[\{B(mt)_3\}Co(PPh_3)][BPh_4]$[22], an analogue of Hill's Ru complex, and the most recent PBP-Rh complexes, $[\{Rh(\mu\text{-}Cl)(PhB(C_6H_4(P\textit{i}Pr_2)\text{-}2)_2)\}_2]$ and $[RhCl(DMAP)(PhB(C_6H_4(P\textit{i}Pr_2)\text{-}2)_2)]$ (**VII and VIII**, Figure 1.8).[23]

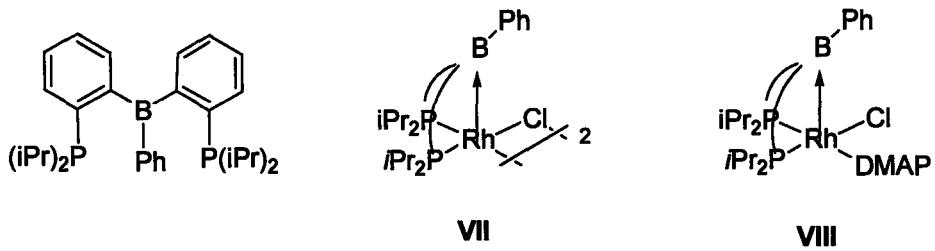

VII VIII

Figure 1.8: PBP Ligand and PBP-Rh Complexes

There are also several structures that are not so certain, but very likely contain the metal-borane interaction. One such complex is $[NEt_4][CpFe(CO)_2(BPh_3)]$,[24] which could not be characterized by X-ray crystallography due to conversion into a second product in solution. This transformation is believed to involve a metal-to-ring migration and aromatic substitution by the triphenylboron group. IR, ^1H NMR and ^{11}B NMR spectroscopies, however, corroborate the presence of an Fe-borane bond in the initial complex. Other probable complexes which can be considered to involve a TM-BR_3 interaction are the rare metal-boryl complexes: $[\eta^5\text{-}C_5Me_5)Fe(\mu\text{-}CO)_2(\mu\text{-}BCl_2)Pd(PCy_3)]$[25], $[Rh(DiPPE)(\mu\text{-}H)_2(\mu\text{-}Bcat)RhH(DiPPE)]$[26] and $[Pt_2(PPh_3)(\mu\text{-}dppm)_2(Bcat)(\mu\text{-}Bcat)]$,[27] (**XI, XII** and **XIII,** Figure 1.10). In the former complex, the borane unit is pyramidal, while in the latter two examples, the borane is approximately planar. These complexes are further discussed in section 1.3.3.

1.3.2 Transition Metal-Group 13 Lewis Acid (AlR_3, GaR_3 and InR_3) Complexes

There are currently a few more heavier group 13 M-ER_3 compounds than M-BR_3, but the number is still relatively small. Complexes which have been fully characterized are listed below: $[NEt_4][CpFe(CO)_2EPh_3]$ (E=Al, Ga, In), $[N(PPh_3)_2][CpCo(CO)_4InPh_3]$,

$[N(nPr)_4][CpMn(CO)_5InPh_3)]$[24], $[CpRh(PR_3)AlR'_3]$ (R_3=Me_3, R' = Me, Et; R_3 = Me_3, R' = Me; R_3 = Me_2Ph, R'= Me), $[CpCo(PMe_3)(AlMe_3)]$, $[CpRh(PMe_3)(C_2H_4)(AlMe_3)]$ $[CpRh(PMe_3)(Al_2Me_4Cl_2)]$,[28] $[Cp^*Rh(\mu^2\text{-}Cl)_2(InC(SiMe_3)_3)_3]$, $[Cp^*Rh(InCp^*)_2(InCl_2Cp^*)]$,[29] $[K][GaCl\{Co_2(CO)_6\}(\mu\text{-}CO)\{Co(CO_4)\}]$, $[(Na(OEt_2))_2][Fe(CO)_4(GaCl_3)_2]$,[30] $[Na(THF)_2][InCl_3\{Mo(CO)_3(\eta\text{-}C_5H_5)\}_2]$,[31] $[Cp^*Ir(PMe_3)H_2AlPh_3]$,[32] $[CpFe(C_7H_8)][Cp(CO)_2FeGaI_3]$,[33] $[Cp_3Mo_3(CO)_6(\mu_3\text{-}O)][Cp(CO)_3Mo(InCl_3)]$,[34] $[K][(CO)_4CoGaCl_3]$.[35]

1.3.3 M-ER_3 (E = B, Al, Ga, In) Complex Ambiguity

In addition to those listed in the previous section, there are several other compounds that appear to be M-ER_3 complexes, but upon closer inspection of the literature, their possession of a metal-Group 13 Lewis acid interaction becomes doubtful. Examining the published complexes, it appears that there are two types of ambiguity: one in which the complex is just not crystallographically or sufficiently characterized; the other occurs when the structure is well characterized, but the bonding situation is more complex and leads to ambiguity. Compounds published by Burlitch *et al*,[24] are examples of the first type of uncertainty, as many have not been fully validated. For example, $[NBu_4][Cp(CO)_3WAlPh_3]$ is purported to contain a metal-Al adduct, but no crystallographic or IR spectroscopic evidence is given. In the complex $[NBu_4][Cp(CO)_3WInPh_3]$, In is considered to be bound to the W rather than CO, based solely on the IR absorptions being at higher frequency than those in $[CpW(CO)_3]^-$, but

again, no crystallographic data is produced to support this. Two other complexes were also alleged to contain a metal-borane interaction, $[IrCl(CO)(PR_3)_2\{B(C_6F_5)_3\}]$,[36] $[Rh(PCy_2)\{\kappa^3\text{-}^tBuP\{(CH_2)_3PPh_2)_2\}(BPh_3)\}]$,[37] but these also suffer from lack of spectroscopic data and full characterization.

IX, R = Me, Et

X, R = *i*Pr, Et

Figure 1.9: Examples Highlighting Ambiguities in TM-ER$_3$ Complexes

The second difficulty occurs when complexes have been structurally characterized, but they are not simple adducts and the interaction between the metal and group 13 atom can be viewed in different ways. The complexes $[Ir(AlMe_2)CMe{=}CH_2(N(SiMe_2CH_2PPh_2)_2)]$[38] (**IX**) and $[\{Cp'(\mu\text{-}\eta^1\text{:}\eta^5\text{-}C_5H_3Me)Mo(\mu\text{-}AlRH)\}_2]$ (Cp' = C_5H_4Me, R = *i*Bu, Et),[39] (**X**) in Figure 1.9 are examples of this second type of ambiguity. Looking at the published X-ray crystal structures of these complexes, it is evident that the bonding around the group 13 atom in these molecules is close to trigonal planar, including the metal, rather than tetrahedral as is more common for discrete R_3Al complexes. In these cases, the molecules are better viewed as M-AlR_2 complexes with partial donation to E by a 4th, non-metal substituent. Another example would be the tantalum $CH_2B(C_6F_5)_2$ borataalkene complexes investigated by Piers *et al.*[40] In these complexes, M→B interactions contribute to the bonding, and the ligand could be viewed either as a tethered borane or a monoanionic borataalkene. Spectroscopic and

crystallographic data point to the predominance of the latter. In addition, under some circumstances, ER_3 could in fact be more akin to a dianion, making it a conventional sigma donor. In such cases, the compound could be viewed as an anionic base stabilized metal boryl complex, related to $[(\eta^5\text{-}C_5H_5)Fe(CO)_2BCl_2{\cdot}NC_5H_4\text{-}4\text{-}CH_3]$,[41] where X-ray spectroscopy reveals the metal boryl to be coordinated to a neutral base. This ambiguity is also discussed by Hill in his description of his Ru-boratrane complex.[42] The dative coordination of the borane is one extreme view of the metal-boron interaction, with an internally base-stabilised σ-boryl interaction at the other extreme, and it is possible that the nature of such interactions lies somewhere in between.

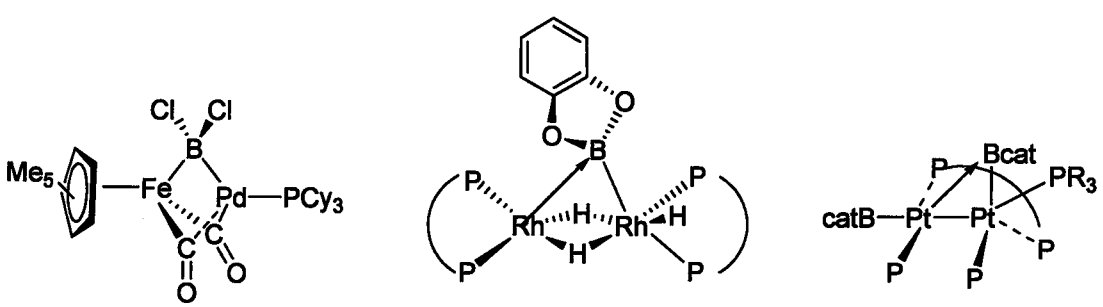

XI **XII** **XIII**

Figure 1.10: Bridging Boryl Complexes Involving M→B Interactions

An additional complication is the issue of whether or not bridging boryl complexes can be considered to be true metal-borane complexes. The bridging complex, $[\eta^5\text{-}CpFe(CO)_2BCl_2Pd(PCy_3)_2]$[25] (**XI**, Figure 1.10) was previously listed in section 1.3.1 as most likely containing a metal-borane interaction. The bridging interaction between the two metals makes it difficult to unequivocally describe it as a purely σ interaction, as the Fe-B is clearly a boryl interaction. Viewing the metal interaction from the Pd side, however, the borane behaves as a Lewis acidic BR_3 group, due to the Pd being in the 0

oxidation state. The interaction between Rh and bridging B in the [Rh(DiPPE)(μ-H)$_2$(μ-Bcat)RhH(DiPPE)][26] **(XII)** boryl complex also potentially houses a Lewis acidic borane. In this case, the Rh and B form a bridging boryl that is approximately trigonal planar, but calculations suggest that despite planarity, the Rh-B interaction can be viewed as σ-donation from Rh to the vacant p-orbital of the boron. A similar bonding situation may also be involved in [Pt$_2$(PPh$_3$)(μ-dppm)$_2$(Bcat)(μ-Bcat)] (**XIII**).[27]

1.3.4 Boryl Metallocenes: Weak TM-BR$_3$ Interactions

A special class of metal borane interactions not discussed in section 1.3.1 is observed in boryl metallocenes. α-Metallocenyl carbocations have been extensively studied, and their stability has been ascribed to a metal-C interaction where electron density is transferred from the metal to the carbocation. This interaction is indicated by the angle between the plane of the cyclopentadienyl ring and the direction of the C(Cp)-C(C$^+$) bond (**XIV** in Figure 1.11).[43] Carbocations and boranes are isoelectronic and possess analogous structures in most cases. Certain boryl-substituted metallocenes have also been found to contain bonding interactions between the metal and boron Lewis acid. This influence of the boryl group on the structure of the sandwich complex has been demonstrated by X-ray structure analysis, where it is shown that weak metal-B bonding interactions are present. The synthesis and structural characterization of 1,1'-bis(dibromoboryl) ferrocene (**XV**) is an example. It is notable that this particular

structural feature is not observed in the more electron rich 1,1'-bis-[bis(diisopropylamino)boryl]ferrocene (**XVI**).[44]

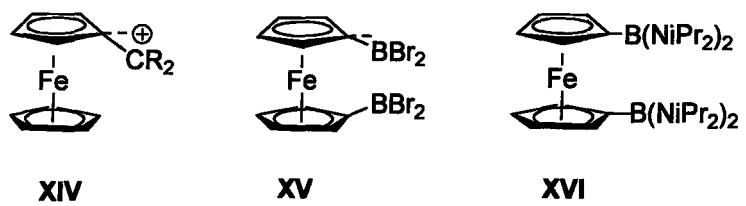

XIV **XV** **XVI**

Figure 1.11: Isolectronic Ferrocenyl Carbocations and Boranes

The Cp-BBr_2 bending was found to be a consequence of an electronic interaction between boron and iron rather than a result of crystal lattice effects. Fe-B bonding stems from a direct electronic interaction between a d orbital at iron and the empty p orbital at boron. When the Lewis acid is placed in close vicinity of the metal, there is distortion of the boryl moiety toward the metal. The distances are relatively long, with TM-BR_3 interactions ranging from 2.856(6) Å in $Fe(Cp(BBr_2))_2$ to 2.924 Å in $[Fe(Cp(B(C_6F_5)_2)]$.[45] Even longer interactions were observed in the Ru and Os boryl metallocenes studied by Nöth et al.[46] The $[Ru\{C_5H_3(BBr_2)_2\}_2]$ complex was found to contain a Ru-B interaction with a distance of 3.19 Å, and the Os-B for interaction in the $[Os\{C_5H_3(BBr_2)_2\}_2]$ analog was found to be even longer at 3.21 Å. That an interaction was present between the boron and the metal, even at such long distance, was determined by the degree of tilt of the boron atoms out of the plane of the Cp ring towards the metal. In the Ru complex, a tilt of 7.4 degrees was observed, with 6.9 degrees for the Os analog. By comparison, TM-BR_3 distances in Hill's metallaboratrane complexes average closer to 2.2 Å. This signifies the importance Lewis acidity has on the potential of bond forming: if a metal is held in

proximity to a borane moiety, even when positioned at a substantial distance from a transition metal, metal-borane bond formation can be favourable, provided that the borane is sufficiently acidic.

1.4 Other Hybrid Lewis Acid/Base Compounds

The previously mentioned poly(*N*-methylthioimidazolyl)boranes and boryl metallocenes also are forms of Lewis acid/Lewis base ligands that have been generated in the coordination sphere of a metal. Attempts to create stable hybrid Lewis base/Lewis acid complexes which can then be directly coordinated to metals have been largely unsuccessful. Some reasons for this are discussed below, and consideration of these factors will be used in the design of our own hybrid ligands. As shown in Section 1.3, many of the examples of metal borane complexes that do exist are possible through first tethering the Lewis acidic borane to the metal center by coordination of a Lewis basic group (*e.g.* the sulfur atoms from Hill's mt-based ligand and Cp's in the ferrocene complexes). Other molecules possessing both a Lewis base and a Lewis acid component not necessarily designed as ligands exist and will be discussed in the following section.

1.4.1 Molecules Designed for Bifunctional Activation and Catalysis

Bifunctional catalysis, especially the combination of a Lewis acid working cooperatively with a Lewis base, has been an intriguing area of research in organic

chemistry for many years. Activation of substrates and nucleophiles occurs concurrently at the Lewis acid and the base moieties in the catalyst, affording high chemo-and enantio-selectivities in a variety of reaction. There are a variety of molecules which specifically contain both a group 13 Lewis acid and a Lewis base, representative structures of which are shown below in Figure 1.12.[47]

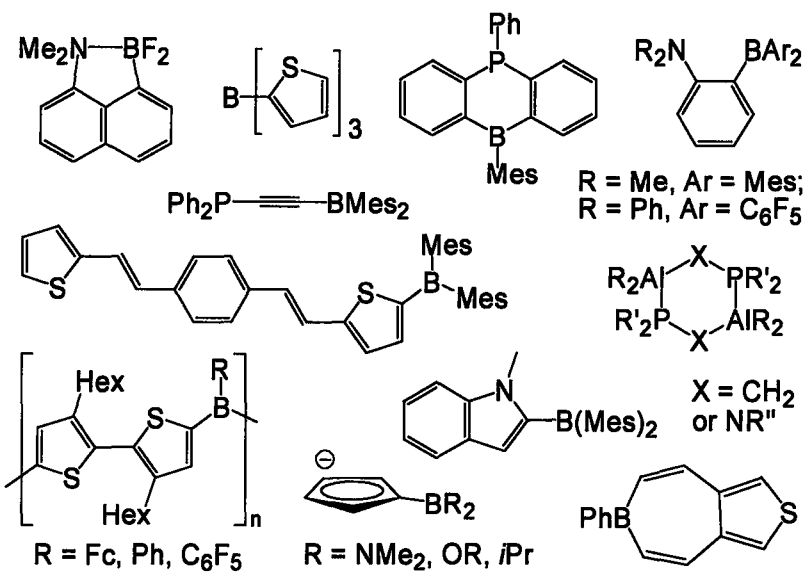

Figure 1.12: Literature Examples of Bifunctional Ligands Containing Both LA and LB Groups

The LA/LB molecules can be distinguished by the steric accessibility of the LA and LB groups in the monomer. The very bulky molecules are generally of interest because of their interesting optical properties: donor-pi-acceptor compounds used in dyes, for 2-photon absorption and as fluorescent compounds, as small molecule fluorescent sensors and as nonlinear optical materials (NLO).[48] Less hindered molecules have typically been investigated with a view to cooperative catalysis or small molecule sensors. Examples of such ligands actually being of catalytic use are: R_2AlPPh_2 (R = Me, Et, CH_2SiMe_3),

which has been shown to cleave common organic solvents (*e.g.* reducing acetonitrile),[49] $Ph_2PN(R)AlR'_2$ (R = *t*Bu, R'= Et; R = *t*Bu, R = Me; R = *t*Bu, R'= Ph; R = *i*Pr, R'= Et; R = *i*Pr, R' = Me; R = Ph, R' = Me), which has found use in catalysed migration reactions with alkylmetal carbonyls,[50] and $(Me_2AlCH_2PMe_2)_2$, which has been used as a co-catalyst for the Ni(II)-catalyzed oligomerization of $PhSiH_3$.[51]

1.4.2 Bifunctional Molecules Designed for Other Applications

Systems such as the aminoboranes, in Figure 1.13, often suffer from the interference of a self-quenching reaction, and consequentially are not good candidates for binding metals. In such situations, the Lewis base and Lewis acid combine, forming *e.g.* a dative boron-nitrogen bond, resulting in a catalytically inactive adduct.

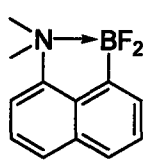

Figure 1.13: Example of an Intramolecular LA/LB Adduct Formation

One of the key concerns in designing a Lewis acid-Lewis base catalyst is the prevention of such internal complexation. One route to addressing this problem is to use bulky Lewis acids, such as mesityl and duryl substituents on boron.[52] Another strategy is to use a weak Lewis acid or a weak base, *e.g.* NPh_2 (Figure 1.14).[40] A third approach is to use a rigid backbone, such as the one proposed in dibenzo-1,4-phosphoborine (Figure 1.14),[53] where the physical separation of the two functionalities should prevent (strong) intramolecular adduct formation.

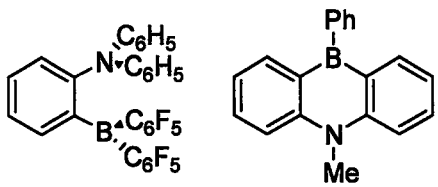

Figure 1.14: Strategies to Avoid Internal Complexation, Weak LA/LB (left), and Physical Separation (right).

All these derivatives, however, do not provide an ideal solution to the problem. Relatively strong Lewis acids and bases are needed for the bifunctional activation process to be useful, and very bulky substitutes are poor candidates for coordination studies because of their reduced Lewis basicity due to high steric hindrance. In order to make monomeric bifunctional molecules, they should be designed such that a strong Lewis acid and Lewis base are tethered using a framework which prevents them from interacting with each other, but in a geometry such that they can both interact with incoming substrates. This is the strategy employed for the synthesis of the LA/LB ligands discussed in this thesis.

1.5 A Brief Overview of Some Boron Lewis Acid Chemistry

Boron and its compounds are used extensively in organic synthesis to mediate a number of useful C-C bond forming reactions. In general terms, a Lewis base (*e.g.*, aldehyde, ketone, enone, epoxide *etc.*) coordinates to the electronically and coordinatively unsaturated boron center which initiates reaction with a second nucleophilic reagent (*e.g.* silane, allylsilane *etc.*). The classical boron Lewis acids, BX_3,

such as BF_3 are the most commonly used compounds for this purpose; however, organoboranes such as RBX_2, and R_2BX (X= F, Cl, Br, OTf) have also been shown to be effective for many transformations. This opens up the possibility for using chiral boranes to mediate/catalyse enantioselective reactions.[54]

$BF_3(OEt_2)$ has historically been the most commonly used Lewis catalyst for reactions such as Diels-Alder cycloadditions, but its relative Lewis acidity is lower than many other commonly used Lewis acids, such as $AlCl_3$ and $TiCl_4$ due to competing ether coordination.[55] Furthermore, the susceptibility of the B-F bonds to cleavage often prevents it from being used in truly catalytic amounts for many reactions. In recent years, tris(pentafluorophenyl)borane, $B(C_6F_5)_3$ (Figure 1.15), has been shown to be a convenient, commercially available Lewis acid of comparable strength to BF_3, but without the problems associated with reactive B-F bonds.[56] $B(C_6F_5)_3$ also provides increased steric protection and the opportunity to modify the aryl substituents on boron. Its primary commercial application has been as a co-catalyst in metallocene-mediated olefin polymerization since it has both strong Lewis acidity and is resistant to ligand transfer deactivation pathways[57]; its effectiveness has spawned a number of perfluoroarylboron derivatives being synthesized in various groups (see Figure 1.15).[58] Furthermore, its potential as a Lewis acid catalyst for organic transformations is now recognized as being much more extensive, allowing for true catalysis of many important organic transformations much more effectively than BF_3.[56] For example, $B(C_6F_5)_3$ catalyzes the hydrosilation of imines, aromatic aldehydes and ketones, and esters,[59] as

well as the allylation of secondary benzyl acetates[60] and the allylstannation of aldehydes.[61]

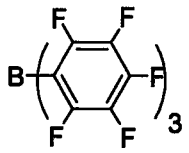

$B(C_6F_5)_3$

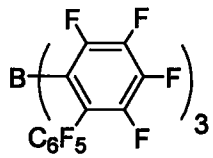

PBB

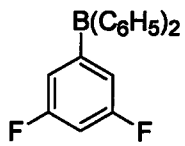

$(3,5\text{-}F_2C_6H_3)B(C_6H_5)_2$

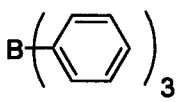

$B(C_6H_5)_3$

Figure 1.15: Examples of Aryl Boranes Used in Catalysis

The presence of perfluoroaryl groups certainly imparts Lewis acidity to the boron rivaling that of BF_3, without the inherent problems mentioned above. However, other less-fluorinated arylborane derivatives have also been synthesized and shown to be of synthetic utility. For example, the encumbered fluoroaryl borane $(3,5\text{-}F_2C_6H_3)B(C_6H_5)_2$ has been used as a catalyst in ethylene polymerisation[62] and triphenylborane ($B(C_6H_5)_3$), although generally less effective than related perfluoro derivatives, has been used successfully as a co-catalyst in olefin polymerization as well as hydrometallation reactions, alkylations and catalyzed aldol-type reactions.[63] In choosing a borane Lewis acid, clearly, a variety of options exists which allows tuning of sterics, electronics and stability. This structural diversity makes boranes strong candidates for the challenging goal of designing and synthesizing new hybrid compounds possessing both a Lewis acid and a Lewis base in close proximity but which do not react with each other (irreversibly).

1.5.1 ^{11}Boron NMR Spectroscopy

^{11}Boron is an NMR-active nucleus but yields relatively broad signals, being quadrupolar with a spin of 3/2. It has, however, a natural abundance of 80.42% and a wide chemical shift range, so very useful chemical shift information can be obtained and used for analysis, especially to gauge coordination number at the boron. Tri-coordinate boron in a trigonal planar configuration gives rise to an asymmetric electric field gradient and a characteristic NMR line shape, which is significantly different from that observed for tetrahedral four-coordinate B. The addition of a ligand or base to the empty p-orbital on boron results in an upfield shift as compared to the tricoordinate borane. This effect is also seen with coordinating solvents such as THF. The chemical shift is dependent on the strength of the coordination complex, with the stronger complexes shifted further upfield.

Borane dimers such as B_2H_6 are also found upfield from the free monomer and may show more complex coupled spectra due to the presence of both terminal and bridging hydrogens coupling to the boron. The addition complex with solvent or a basic ligand is generally found at higher field than the dimer. The trialkylboranes are found in a narrow low field region, 83-93 ppm. These chemical shifts are largely independent of the structure of the alkyl group. Some representative boranes and their chemical shifts are provided in Table 1.2, in addition to the borane transition metal complexes listed previously in Table 1.1.

Table 1.2: Examples of ^{11}B chemical NMR shifts

Compound	δ ^{11}B shift (ppm)
BPh_3	+60.2 [64]
$BPh_3 \cdot NH_3$	-2.7 [65]
BCl_3	+41.9 [66]
$BCl_3 \cdot THF$	+10.2 [67]
$B(C_6F_5)_3$	+58 [68]
$CH_3B(C_6H_5)_2$	+70.6 [69]
$B(CH_2C_6H_5)_3$	+82.0 [65]

1.6 A Brief Overview of Organoplatinum Chemistry

Platinum occupies a position of paramount importance in transition metal-complex chemistry. The versatility of platinum chemistry is related to the fact that coordination compounds of platinum are known in many oxidation states, namely, 0, I, II, III, IV and higher. The most common oxidation states for the organometallic compounds are 0, II, and IV which are often shuttled between via reductive elimination or oxidative addition reactions. This ability to shift back and forth between 0, II and IV oxidation states is of course what makes platinum complexes such effective catalysts for a number of reactions. Although the number of catalytic reactions discovered for platinum is not as large as for Pd, there are cases where platinum can behave differently than palladium leading to unique reactivity.[70]

The first Platinum(0) complexes remained unknown for a relatively long time, in contrast with other d^{10} metals which make compounds such as $[Ni(CO)_4]$. It was not until

1957 when the triphenylphosphine adduct [$Pt(PPh_3)_4$] was first prepared.[71] This discovery was followed by extensive development in the chemistry of Pt(0) complexes which have proven of interest due to their catalytic effectiveness. There are currently many different types of Pt(0) complexes in the literature: [$Pt(COD)_2$] (**XVII,** Figure 1.6), which was the first purely olefin complex of Pt(0), as well as many other alkene complexes, such as [$(PPh_3)_2Pt(CH_2{=}CH_2)$][72], [$Pt_2(nbe)_3$], and alkyne complexes such as [(COD)Pt(PhC≡CPh)][73] (**XVIII**). In contrast, there are very few stable Pd(0) alkene starting materials in the literature[74] because the lower radial extension of the 4d orbitals (versus 5d) leads to increased alkene lability and facile decomposition to palladium metal.

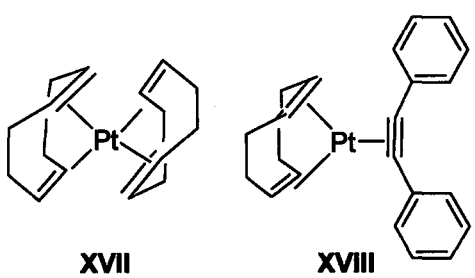

XVII **XVIII**

Figure 1.16: Examples of Pt(0) Complexes

The most common oxidation state of Pt is Pt(II), and there are many examples of 4-coordinate Pt(II) in the literature. Pt(II) forms stable mononuclear complexes with anionic monodentate ligands (halides, carboxylates, etc.) and also with neutral donor ligands (group IV, V and VI donor atoms). As a d^8 metal complex system, it has unique features such as a coordinatively unsaturated character and ease of formation of pi-complexes, hydrido- and Pt-C σ-bonded complexes. These properties result in its being a good catalyst in a wide range of reactions: [$PtCl_2(COD)$] is a common catalyst, used in

reactions such as the cyclisation of enynes[75]; $[Pt(NO_3)_2]$ is a cocatalyst in the hydrogenation of alkylphenols[76]; $[Pt(acac)_2]$ (acac = acetylacetonate) has been used in the dehalogenation of chloromethanes and chlorobenzene.[77] In recent years, researchers have demonstrated that Pt(II) complexes ligated by phosphine and other neutral donors can be important catalysts as well. Examples include $[PtCl_2(PPh_3)_2]$, which is used in the nucleophilic addition of methanol to nonactivated alkynes[78] and the allylation and propargylation of arylepoxides,[79] and $[Pt(nbe)_3]$ is used in the hydrosilation of styrene.[80]

Platinum has another useful advantage over metals such as Pd in that it is NMR active (^{195}Pt, 34% abundance, I = 1/2; all other naturally abundant isotopes of Pt have I = 0) and couples with phosphorus in ^{31}P NMR, (^{31}P, 100% abundance, I = ½). Since both ^{31}P and ^{195}Pt have spins of 1/2, each nucleus will interact with the other in two possible orientations, and each will therefore absorb at two different energies resulting in a doublet of equal intensity. Indeed, many studies have used ^{31}P NMR spectroscopy to a) show the presence and stability of phosphine ligands directly bound to Pt and b) to also ascertain the coordination environment at Pt (such as *cis* vs. *trans* phosphine donors, since ^{31}P-^{31}P coupling constants are much larger for trans complexes). Several examples of Pt-P complexes are shown in Table 1.3 with the corresponding ^{31}P NMR spectral shift(s) and coupling constants to platinum. It is apparent that a wealth of information can be collected from ^{31}P NMR especially when more than one phosphine donor is coordinated to the metal.

Table 1.3: Examples of ^{31}P chemical shifts, ^{31}P-^{195}Pt and ^{31}P-^{31}P Coupling Constants

Compound	δ ^{31}P NMR		^{31}P-^{195}Pt coupling constants (Hz)		^{31}P-^{31}P coupling constant (Hz)	
Cis-$PtCl_2(PPh_3)_2$[81]	20.5		3671			
Trans-$PtCl_2(PPh_3)_2$ [82]	20.5		2627			
Cis-$[PtCl_3(PPh_3)_3][NO_3]$[83]	7.81		2054			
Trans- $[PtCl_3(PPh_3)_3][NO_3]$[70]	8.08		1454			
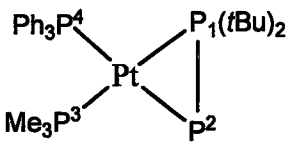 [84]	P^1	79.9	P^1	1866.8	P^1-P^2	-605.0
	P^2	-54.2	P^2	-104.6	P^2-P^3	-4.4
	P^3	-24.6	P^3	3306.8	P^3-P^4	-10.7
	P^4	21.6	P^4	3302.6	P^1-P^3	210.0
					P^1-P^4	-34.2
					P^2-P^4	24.0

Chapter 2: Ligand Design and the Platinum Chemistry of Phosphine/Thioether/Borane Ligand, TXPB

2.1 Design of Hybrid Phosphine/Borane-Ligands Based on the Thioxanthene Backbone

The goal of this research is to investigate hybrid Lewis acid/Lewis base ligands, with the intention of forming rare transition metal borane bonds ($TM \rightarrow BR_3$). This investigation requires judicious selection of an appropriate ligand in order to maximise the likelihood of forming a stable complex with such an interaction. The general strategy to be used will be to design a ligand with a Lewis basic group which anchors the metal and in the process, place a tethered Lewis acid near the metal such that bonding can occur.

Since there are so few fully-characterized transition metal borane complexes, it is necessary to study the reasons behind the failure of forming these types of complexes, and more importantly, the reasons for success in the few that exist. In order to accommodate both a functioning Lewis acid and Lewis base in the same molecule, the two groups must be physically separated to prevent adduct formation, or coordination must be reversible in the presence of other molecules. For the synthesis of Hill's metal-borane complexes discussed in Section 1.3.1, a protection strategy was used; the Lewis acidic borane center is created from a borohydride *after* coordination of the anionic ligand to the metal. Separating the Lewis basic groups from the boron prior to complexation is therefore not required. It is important to note that the borane-transition

metal bond is strengthened by the rigidity of the methylimidazole buttressing arms, which due to structural rigidity, also precludes intramolecular coordination of the arms of the ligand to boron. Rigidity is therefore an important feature that should be designed into new Lewis acid-Lewis base hybrid ligands.

An alternative strategy towards borane complexes is the preparation of a ligand containing both a functioning Lewis acid and Lewis base in the same molecule. These two groups must be physically separated and the ligand must be of sufficient rigidity and steric presence to prevent inter- and intramolecular adduct formation. However, if adduct formation does occur, the Lewis acid and Lewis base groups may still be accessible if coordination is reversible in the presence of other molecules.[85] We have chosen to focus on the use of free Lewis acid containing ligands to prepare borane-transition metal complexes since this strategy is more likely to allow the rational synthesis of a broad range of metal complexes. In our search for a suitable ligand framework, we turned to rigid multidentate phosphine ligands, the coordination chemistry of which is very well developed, for inspiration.

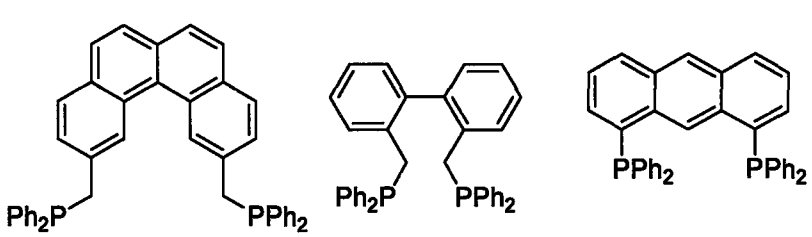

Transphos **BISBI** **Anthraphos**

Figure 2.1: Examples of Chelating Ligands Based on Aromatic Backbones

One group of potential candidates that possess a rigid backbone are polycyclic aromatic compounds, which have two or more single or fused aromatic rings. Phosphine ligands based on this class of backbone include **transphos**, 2,2'-bis((diphenylphosphino)methyl)-1,1'-biphenyl (**BISBI**), and **anthraphos**, (Figure 2.1). One problem with many ligands such as **transphos** is that they possess too much flexibility: a mixed Lewis acid/Lewis base derivative of **transphos** is likely to suffer from intramolecular complexation.[86] In contrast, anthracene–based ligands like **anthraphos** are much less flexible. Since the phosphorus atoms are directly bound to the rigid aromatic backbone, the donor atoms of the anthracene-type ligands are well oriented to form complexes with many transition metals, such as Ni, or Pd (Scheme 2.1), having bite angles much larger than 90°.[86]

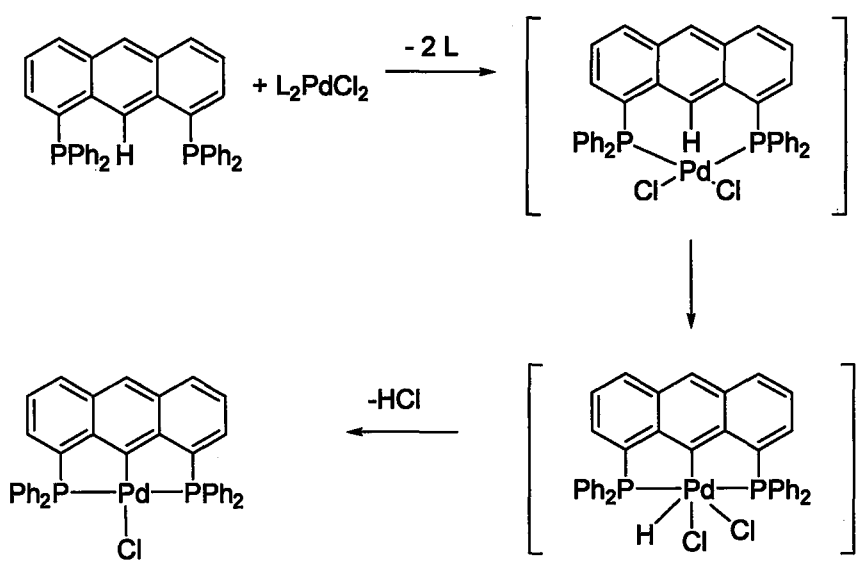

Scheme 2.1: Cyclometallation of 4,5-bis(diphenylphosphino)anthracene

Through a metallation reaction (C-H activation), these anthracene derived complexes are covalently bound to the central ring carbon anchoring the metal between

the two phosphines.[87] When designing hybrid ligands, zero valent metals will be targeted to enhance the likelihood of a metal Lewis acid interaction; this covalent attachment strategy will therefore not be appropriate. We have opted to use the three-fused ring anthracene motif as a starting point for preparing mixed phosphorus, boron ligands but have targeted heteroaromatic derivatives based on oxygen, nitrogen and sulphur (xanthene (**XPB**), acridine (**APB**) and thioxanthene (**TXPB**) backbones respectively, Figure 2.2) to enhance likelihood of both the phosphorus and boron participating in bonding to metal. By analogy with the coordination chemistry of Anthraphos, these backbones should allow for trans-chelation via both phosphorus and boron if a suitable metal can be found which will both accept electron density from the phosphorus and donate electron density to the boron. With another basic group (oxygen, nitrogen or sulphur) also present, coordination in the pocket formed between the phosphine and borane groups should be further encouraged, especially for **TXPB and APB**.

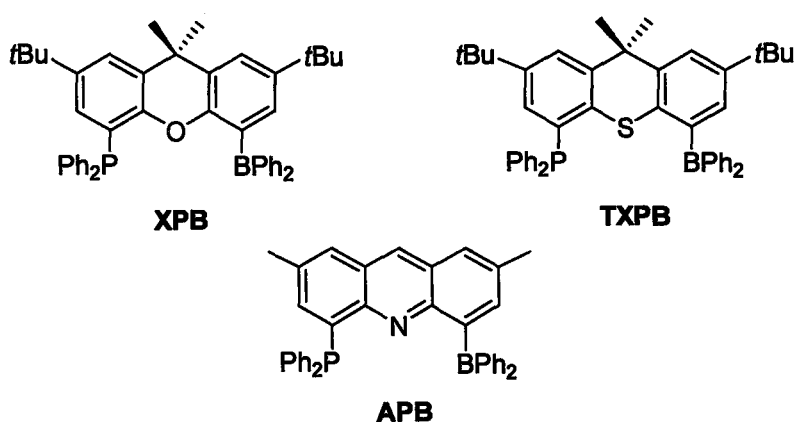

Figure 2.2 Target Borane-Containing Ligands

This second donor group (nitrogen or sulphur) in these target molecules is viewed as an essential design element to enhance the likelihood of the borane group being near

the metal. Even in cases where electron donation from metal to boron is not strong, a bonding interaction could be encouraged to occur. Without this anchor, it is likely that the P atom will coordinate to the metal center external to the phosphorus, rendering the formation of a $M \rightarrow BR_3$ interaction far less likely. Of the three target ligands in Figure 2.2, TXPB and APB derivatives should be best suited to lure a late transition metal within the vicinity of the boron, due to greater ligative properties of nitrogen and sulphur relative to oxygen. Again, zero valent metals are most likely to engage in bonding to the B atom since they are electron rich. However, chemistry of these ligands in conjunction with higher valent metals is likely to be interesting in its own right in order to assess whether the boron center can interact with or activate different ligands at the metal.

In summary, ligands have been designed with the following three key features to encourage formation of a metal-borane interaction:

1) A rigid polyaromatic backbone to separate boron and phosphorus atoms from each other and create a pocket for coordination of the metal.
2) Two donor atoms positioned such that chelation will place a metal close to the boron atom.
3) Soft, neutral donor atoms to allow for complexation of electron-rich low valent late transition metals.

2.1.1 Platinum Complexes From a Thioxanthene-based Ligand TXPB

Thioxanthene is the sulfur analogue of xanthene (see Section 2.3), where a sulfur atom exists in the ring system in place of an oxygen atom. Thioxanthene compounds are primarily used in pharmaceutical synthesis, from which antipsychotic agents are derived, including: chlorprothixene, flupenthixol, chlopenthixol and thiothixene.[88] Few examples of its use as a backbone for creating new ligands have been documented, and those that have been documented are only briefly mentioned, a synthetic procedure has never been reported, and their existence is not entirely credible.[89] The new thioxanthene hybrid ligand, (2,7-di-(*tert*-butyl)-4-diphenylboryl-5-diphenylphosphino-9,9-dimethyl-thioxanthene, **TXPB)** is a promising candidate for forming the desired metal borane complexes.

2.1.2 Synthesis of a Phosphine/Thioether/Borane Ligand TXPB

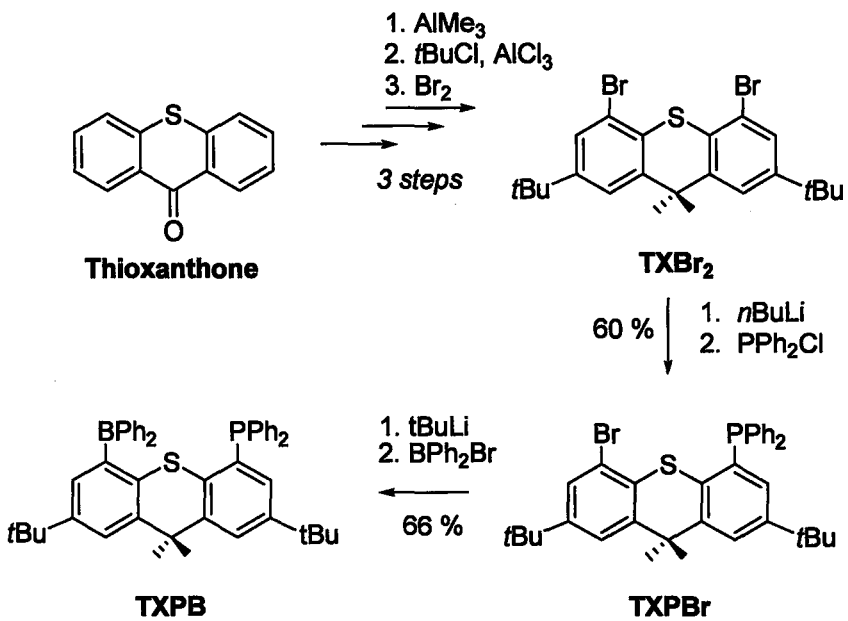

Scheme 2.2: Synthesis of the TXPB Ligand

Using a procedure developed previously in the Emslie lab,[90] TXPB, can be prepared as a solid, moisture sensitive compound in gram quantities (Scheme 2.2). The synthesis involves sequential lithiation of the two bromine atoms of 2,7-di-(*tert*-butyl)-4,5-dibromo-9,9-dimethylthioxanthene, $TXBr_2$. The phosphine group is installed first since it is tolerant of alkyl lithium reagents needed to react the second bromide group, whereas a borane would not be. In order to isolate TXPB, the acetonitrile adduct (TXPB-CH_3CN) is precipitated from solution, isolated and then dried *in vacuo* to remove acetonitrile loosely bound to boron. The TXPB ligand is a bifunctional compound, possessesing a non-protected Lewis basic and Lewis acidic group, a phosphine and a borane, which do not interact with each other. As anticipated, the TXPB ligand has been

shown to be successful as a means to position a borane in close proximity to late transition metals such Fe, Rh and Pd.[91]

2.1.3 Reaction of TXPB With [$PtCl_2$(COD)]

[$PtCl_2$(COD)] can be used as a soluble monomeric source of $PtCl_2$ with a labile 1,5-cyclooctadiene (COD) ligand which can be easily displaced by other Lewis basic ligands such as phosphines. A wide range of complexes containing bridging chloride ligands exists in the literature, including bimetallic platinum compounds, and also between boron fragments (*e.g.* in 1,8-napthalenediylbis(dichloroborane)(μ-chloride)[92]). Therefore, it was expected that if a complex between TXPB and $PtCl_2$ could be formed, a chlorine anion might bridge between the platinum and boron, since the borane is electron poor, and the chlorides are a readily available source of electron density. The TXPB ligand and [$PtCl_2$(COD)] were mixed together in a 1:1 ratio in dichloromethane at room temperature, resulting in formation of the 1:1 complex [PtCl(μ-Cl)(TXPB)] **(1)** . The ^{31}P NMR spectrum shows a characteristic 1/4/1 pattern consisting of a singlet (δ 32.4 ppm), due to phosphorus bound to I = 0 platinum nuclei, (Figure 2.4) and two satellites, $^1J_{P,Pt}$ = 3880 Hz, assigned to phosphorus coupled with ^{195}Pt (I=1/2, natural abundance 33.8%).

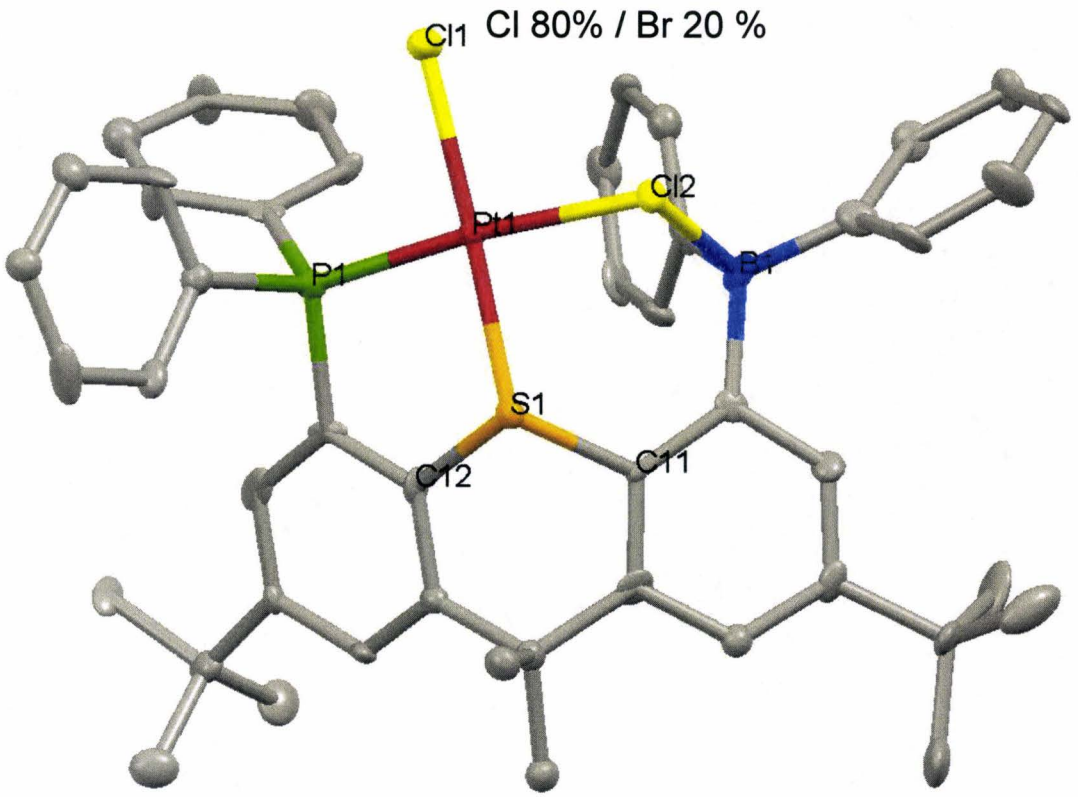

Figure 2.4: X-ray Structure of [Pt(x)(μ-Cl)(TXPB)]•DCE, [x = Cl (80%), Br (20 %)]

A second attempt at recrystallisation of pure [PtCl(μ-Cl)(TXPB)] yielded crystals, but these have not been analysed using X-ray crystallography. The ^{1}H NMR spectrum of pure **1** indicates two separate methyl peaks, at 1.17 ppm and 1.24 ppm, and two separate *t*-butyl peaks at 1.54 ppm and 2.17 ppm. The peaks in the aryl region overlap considerably, and it was not possible to identify all of the proton peaks in this range. As expected, no significant change was seen in the ^{1}H NMR spectra between 20 to -80 °C. NMR spectroscopy cannot be used to determine whether the terminal and bridging Cl atoms exchange positions.

Although it was expected that the boron would be bridged to the platinum by a chloride, and that no direct borane-platinum interaction would be formed, this product is still of interest as it shows that the phosphorus and sulphur atoms of TXPB can chelate a late transition metal and thereby lure the metal in the vicinity of the boron. The structure of **1** further emphasizes the necessity to carefully consider properties of co-ligands; in order to achieve a direct Pt→B interaction, co-ligands should not be capable of bridging platinum and boron. Another strategy, discussed in Section 2.1.8, is to use metals in low oxidation states where more electron density resides at the metal center. Nonetheless, the complex **1** clearly illustrates that the TXPB ligand can accommodate metals such as platinum in the phosphorus, sulphur, boron coordination environment where all three of the heteroelements of TXPB contribute to binding.

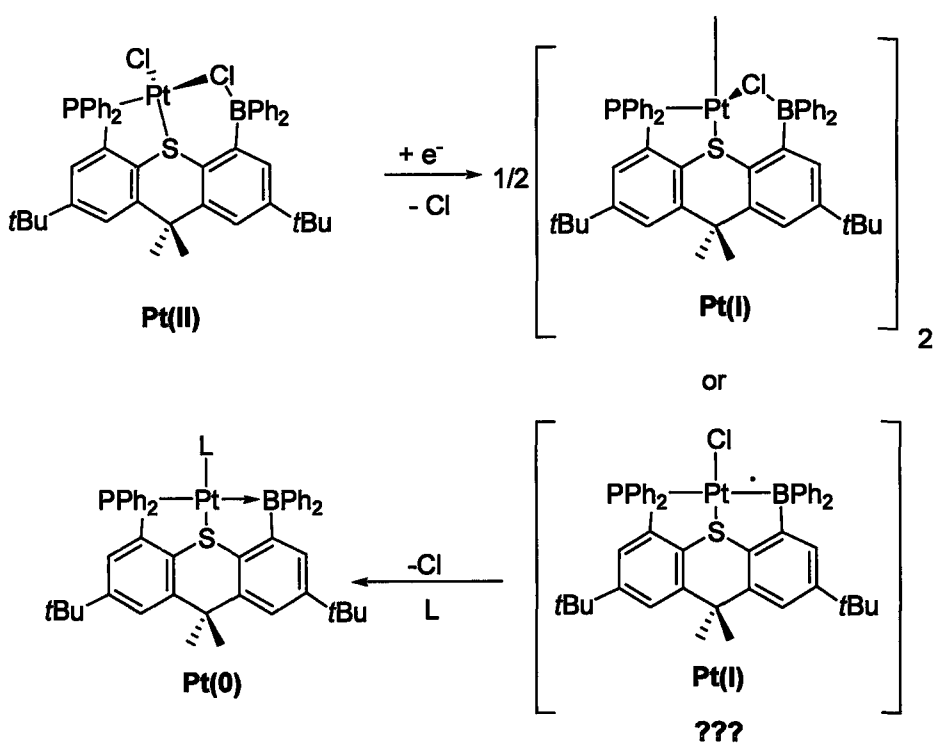

Scheme 2.3: Possible Reduction Pathway of 1

1 could also be used as a well-defined precursor to make lower valent Pt complexes of TXPB through reduction to remove one or both of the Pt-Cl bonds, Scheme 2.3. Reductions carried out with the ligand already complexed to platinum could lead to products different than those accessible by direct reaction of TXPB with Pt(0) starting materials, possibly even Pt(I) complexes. Potential reductants include Zn and $PbCl_2$. The role of the boron group in stabilizing either Pt(I) or Pt(0) products will be of particular interest as they both could involve Pt/B interactions. Often, Pt(I) complexes when formed, will dimerize through a single M-M bond. The presence of the electron-poor boron atom may circumvent this pathway.

Applications of $PtCl_2$ as a Lewis acid to mediate various transformations are well-known (*e.g.* in hydroformylations,[93] hydrosilylations,[94] and vinylations[95]). Although coordination of a phosphine will weaken its Lewis acidity, the presence of the borane substituent could offset this problem. Partial abstraction of one of the chlorine atoms by the borane could be expected to increase the Lewis acidity at platinum which could result in enhanced activity, see Scheme 2.4. In the presence of a suitable Lewis base which favors coordination to platinum over boron, full abstraction could result, leading to a cationic platinum center. It should be emphasized that **1** is an example of a bifunctional Lewis acid possessing two discrete Lewis acidic centers, one a transition metal and one a main group element. Future work will explore coordination of bases preferentially to the platinum and/or the boron. Bifunctional bases or other bases known for bridging could lead to coordination to both elements.

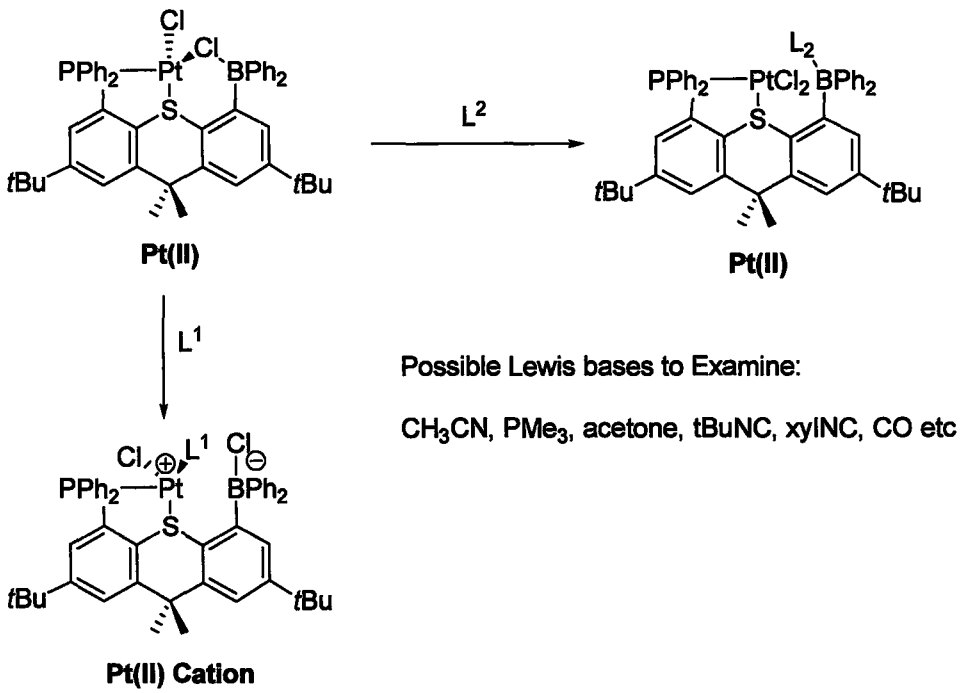

Scheme 2.4 Possible Binding of Lewis Bases to the Bifunctional Lewis Acid 1

2.1.4 Introduction to Cyclic Voltammetry

Cyclic voltammetry is an important and widely used electrochemical technique. In addition to providing a measure of the redox potential, it can provide information about the rate of electron transfer between the electrode and the analyte, as well as the stability of the analyte after reduction or oxidation.

An external source of energy is supplied to drive an electrochemical reaction which would not normally occur. The externally applied driving force is an applied potential, and the resulting (faradaic) current in the cell is measured as a function of this potential. In cyclic voltammetry, the potential of the working electrode is linearly cycled from a starting potential to a final (or switching) potential and then back to the starting potential. At the start of the experiment (zero current), the solution at the electrode contains only the unchanged analyte, but at critical potential during the forward scan, the electroactive species will begin to be reduced (if scanning towards more negative potential) or oxidised (if scanning towards more positive potential). In a reversible reaction, the redox product is not removed from the equilibrium reaction, so its concentration at the surface is controlled by the potential and the rate of diffusion of the test compound to the electrode. Irreversibility occurs when the redox reaction is slow or coupled with a chemical reaction or when adsorption of either reactants or products occurs. Quasireversibility (electrochemical irreversibility, chemical reversibility) typically occurs as a result of a large structural change which accompanies a redox process; for example, oxidation of square planar copper(II) complex to a tetrahedral

copper(I) complex, or oxidation of [(κ^2-Tp')Rh(CO)(PPh_3)] to [(κ^3-Tp')Rh(CO)(PPh_3)]$^+$.[96] A wave is typically described as partially reversible at scan rates where it is not completely chemically reversible. In this case, the faster the scan rate, the more reversible the wave will become. The diagnostic power of cyclic voltammetry is most useful for irreversible reactions, and information is usually obtained by comparing two or more experimental voltammograms.[97]

2.1.5 CV of [PtCl(μ-Cl)(TXPB)] *vs.* [$PtCl_2$(TXPH)]

In this project, solution cyclic voltammetry was used to probe the effect of the borane-chloride interaction on the amount of electron density at the metal centre in complex **1** (for complexes with comparable coordination geometries, redox potentials should vary linearly with the amount of electron density on the metal). In order to gauge the effect of the M-Cl-B interaction, a borane-free analogue of TXPB, **TXP*H***, was used to synthesise [$PtCl_2$(TXPH)] as a comparison with [PtCl(μ-Cl)(TXPB) (Figure 2.6).

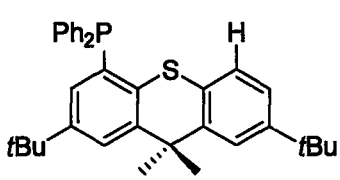

Figure 2.5: The TXPH Ligand

The bridging chlorine facilitates electron withdrawal from the metal to the Lewis acidic boron, and so the metal should be more easily reduced. When the borane is not

present, this bridging interaction is not possible and so the metal should be less easily reduced, resulting in a more negative reduction potential.

The cyclic voltammogram measurements were taken in CH_2Cl_2,, with $[NBu_4][PF_6]$ as the base electrolyte, and $FeCp^*_2$ as the reference compound.[98] Cyclic voltammetry runs for **1** and $[PtCl_2(TXPH)]$ are shown in Figure 2.6.

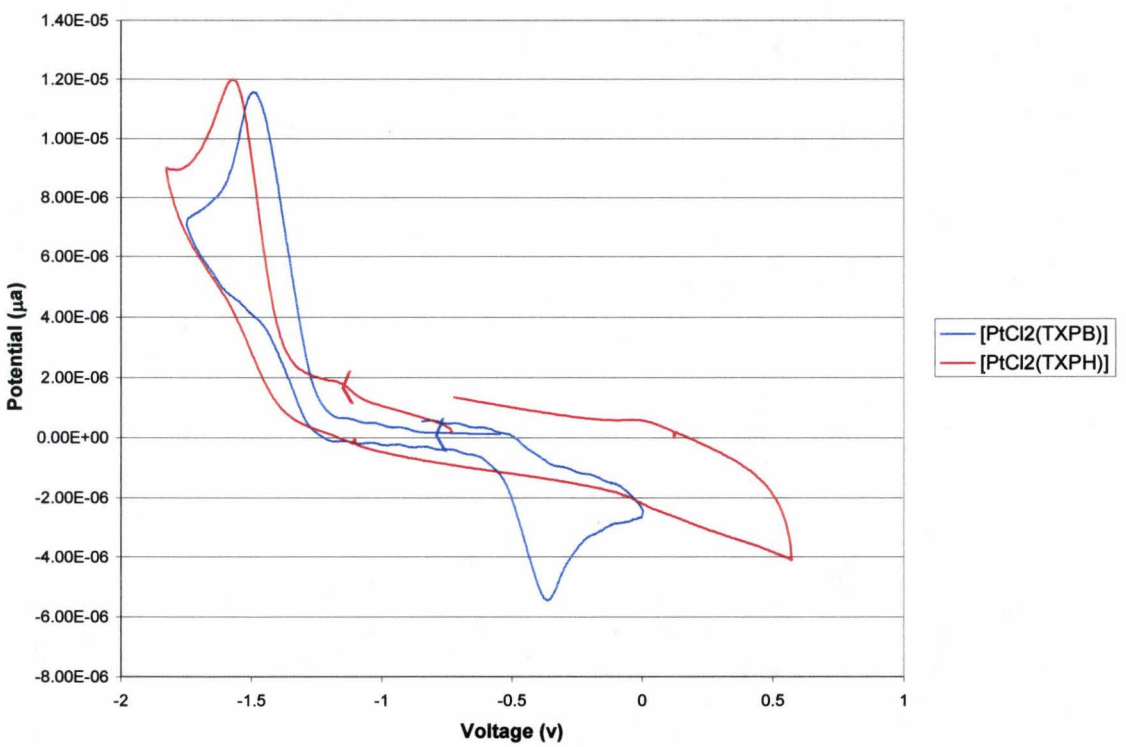

Figure 2.6: Cyclic Voltammograms for* [PtCl(μ-Cl)(TXPB)] *and [$PtCl_2$(TXPH)] at 200 mV/s

The graph shows that both complexes undergo irreversible reduction, presumably to give a Pt(I) dimer such as that shown in Scheme 2.3. **1** shows a reduction potential of -1.50 V (ν = 200mV/s), compared to -1.58 (ν = 200mV/s) for $[PtCl_2(TXPH)]$. This gives a difference of 0.08V(ν = 200mV/s). As expected, a more negative value for $Ep_{(red)}$ is

observed with the borane present, since the bridging interaction facilitates reduction at the metal center.

Further information about these complexes could be gathered by comparison to the reduction peak potentials of similar complexes. Thus, the $PtCl_2$ complexes were compared to the reduction peak potentials of both $PdCl_2$ and PtI_2 complexes of TXPB and TXPH, (Emslie group, unpublished results). In comparison to the Pt-Cl-B or Pd-Cl-B interactions, which are quite strong (B-Cl bond distances similar to those found in chloroborate anions), the Pt-I-B distance is 2.760(24) Å (~0.5 Å longer than in any crystallographically characterized iodoborate), indicative of only a weak I--B interaction.

Table 2.1: Comparison of the irreversible reduction potentials of PtI_2, $PdCl_2$ and $PtCl_2$ TXPH/TXPB complexes at 200 mV/s

Compound	**Irreversible Reduction Potential, $Ep_{(red)}$ (V)**	**$\Delta Ep_{(red)}$ (V)**
PtI_2(TXPB)	-1.38	0.19
PtI_2(TXPH)	-1.57	
$PdCl_2$(TXPB)	-0.88	0.18
$PdCl_2$(TXPH)	-1.06	
$PtCl_2$(TXPB) (**1**)	-1.50	0.08
$PtCl_2$(TXPH)	-1.58	

As in the $PtCl_2$ case, it is evident that the borane group has a definite effect on the reduction potential of the complexes, resulting in less negative values for $Ep_{(red)}$. Also of interest is the comparison of the differences in $Ep_{(red)}$ ($\Delta Ep_{(red)}$) between each set of complexes. A much larger $\Delta Ep_{(red)}$ of the TXPH and TXPB analogues was anticipated for the chloride bridged complexes since X-ray crystallography has shown a much stronger X-B in teraction for X = Cl *versus* X = I. Surprisingly, the $\Delta Ep_{(red)}$ for the $PtCl_2$

complexes is lower than that observed for the PtI_2 complexes, and the difference between the $PdCl_2$ pairs and the PtI_2 pairs is almost identical. Therefore, whether a chloride or an iodide is coordinated to the metal does not appear to a make difference to the size of $\Delta Ep_{(red)}$. With the available data it is difficult to make any definite conclusions on the reasons for this observation. Perhaps this is an electronic effect, or it could be due to ligand rigidity forcing the chloride closer to metal, or due to steric hindrance in the PtI_2 complex resulting in longer Pt-S or Pt-P bond distances. It certainly seems reasonable that B-X interaction strength will influence platinum reduction peak potentials. However, these data suggest that other factors are also of major influence in controlling the amount of electron density at platinum.

Although the data cannot be as easily explained as had been expected, it is still valuable. More information is needed to better interpret the results, such as the X-ray structure of the complexes studied. This would allow the investigation of the relationship between the amount of electron density that a chloride can donate and B-Cl interaction strength by comparing physical characteristics such as bond lengths and angles. It would also allow investigation of variations in Pt-P or P-S bond lengths, which could occur as a result of steric constraints imposed by the rigidity of the thioxanthene backbone in response to varying B-X bond lengths.

2.1.6 Reaction of TXPB with [$PtMe_2$(COD)]

In a continuation of the coordination studies of TXPB with Pt(II) compounds, the reaction with [$PtMe_2$(COD)] was investigated. This compound, which must be synthesized,[99] contains a labile 1,5-cyclooctadiene (COD) group, which should allow facile addition of the ligand through displacement reaction analogous to that observed for **1**. In this case, the platinum metal contains two methyl groups which are less likely to form a bridge between platinum and the TXPB borane group as observed for the dichloride adduct. A methyl group can bridge between two aluminum (III) centers through 3-center-2-electron bonding or between an aluminum atom and a transition metal or lanthanide ion,[100] and similar bridged complexes exist for boranes as well. Linked diboron compounds have recently been reported as methide abstracting agents for use in single-site olefin polymerization catalysis.[101] Although they are known to exist, bridging methyl groups are still uncommon, and are not expected in the case of TXPB.

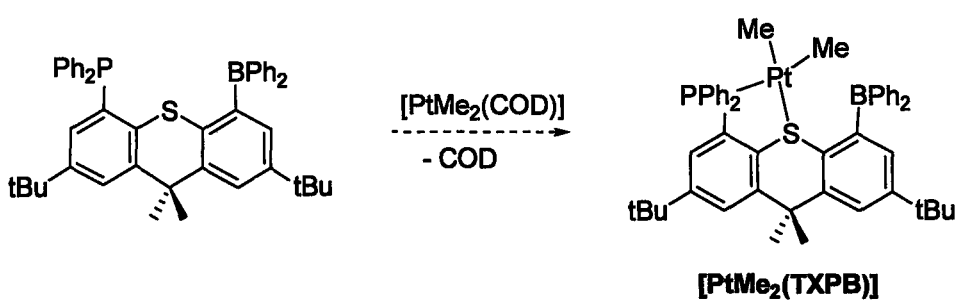

Scheme 2.5: Expected Product From the Reaction of TXPB With [$PtMe_2$(COD)]

It was thought that for Pt(II) a square planar complex would result with Pt coordinated by both the phosphorus and sulphur donors of TXPB. Another possible product however could be the zwitterionic complex [PtMe(TXPBMe)] formed by abstraction of a methide group from platinum, although this would lead to a three coordinate platinum center,

Figure 2.7. Again, an isomer with a bridging methyl group seems less likely than complete abstraction by boron or no interaction at all.

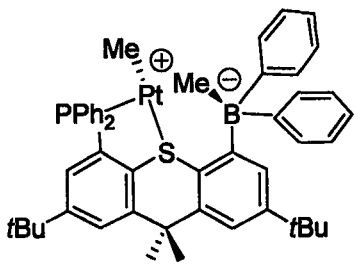

Figure 2.7: Zwitterionic [PtMe(TXPB-Me)]

[$PtMe_2$(COD)] may also be a better candidate than [$PtCl_2$(COD)] as a reagent leading to a complex with the desired Pt-B bond as the platinum center in $PtMe_2$ is more electron rich than for $PtCl_2$, which possesses two electron-withdrawing chloride atoms. The Lewis acidic borane could thus accept electron density directly from platinum rather than through interaction with the co-ligands as observed for the platinum dichloride. This could be particularly important if formation of the zwitterion in Figure 2.7 is precluded on steric grounds or if a coordinatively unsaturated platinum cation is disfavoured.

2,7-di-(*t*-butyl)-4-diphenylborano-5-diphenylphosphino-9,9-dimethylxanthene thioxanthene (TXPB) was reacted with [$PtMe_2$(COD)] in dichloromethane in a 1:1 ratio at room temperature, and then the solvent was removed in *vacuo*. The product was washed with hexanes to remove liberated COD, and recrystallised from dichloroethane/hexanes at -30°C giving an 82% yield of white crystals. The ^{31}P NMR spectrum (Figure 2.9) for this purified compound again shows a peak with satellites: δ = 45.3 (d, $^1J_{31P\text{-}195Pt}$ = 2285 Hz) showing that a Pt-phosphine complex had indeed formed.

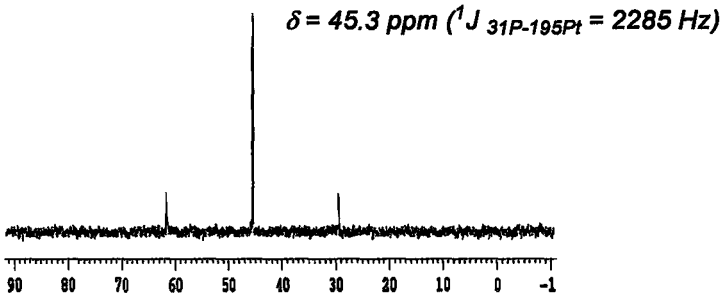

Figure 2.8: ^{31}P NMR Spectrum of 2

X-ray quality crystals of the complex were grown by slow diffusion of hexanes into a CH_2Cl_2 solution at -30°C. X-ray analysis revealed that an intriguing ligand redistribution reaction had occurred between the boron and platinum, (Figure 2.9). The resulting complex contains one Me and one Ph group on both boron and platinum, with the Pt-Me group *trans* to sulphur and the Pt-Ph group *trans* to phosphorus. Some flexibility in the backbone twisting platinum and boron away from each other enables this sterically congested complex, [PtPhMe($TXB^{Me,Ph}$] (**2**) to form.

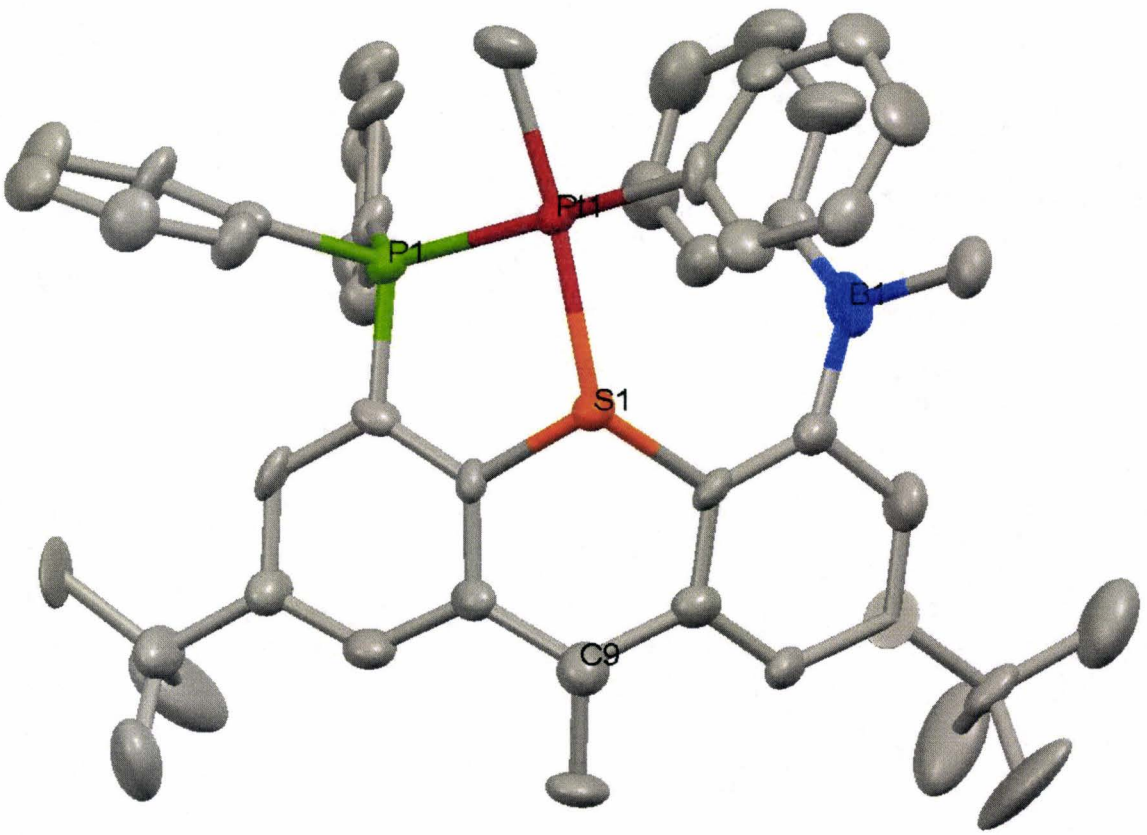

Figure 2.9: X-Ray Structure of 2 with 50% Probability

Ellipsoids, H-atoms Omitted for Clarity

Table 2.2 Selected Angles [°] and Bond Lengths [Å] with Estimated Standard Deviation in Parentheses for 2

Bond	Angle [°]	Bond Length [Å]
C(36)-B(1)-C(5)	120.2(9)	
C(36)-B(1)-C(48	120.4(9)	
C(5)-B(1)-C(48)	117.6(10)	
C(11)-S(1)-C(12)	98.2(4)	
C(9)-S(1)-Pt(1)	163.73	
C(12)-S(1)-Pt(1)	127.9(3)	
C(24)-P(1)-C(4)	102.0(4)	
C(24)-P(1)-C(30)	103.1(4)	
C(4)-P(1)-C(30)	104.7(4)	
C(4)-P(1)-Pt(1)	107.6(3)	
C(49)-Pt(1)-P(1)	91.4(3)	
C(42)-Pt(1)-S(1)	94.1(3)	
C(42)-Pt(1)-C(49)	87.6(4)	
P(1)-Pt(1)-S(1)	86.23(8)	
Pt(1)-P(1)		2.266(2)
Pt(1)-S(1)		2.322(2)
Pt(1)--B(1)		3.650(16)
Pt(1)-C(42)		2.035(9)
Pt(1)-C(49)		2.050(9)
B(1)-C(36)		1.530(15)
B(1)-C(5)		1.562(14)
B(1)-C(48)		1.595(14)

The C_{ipso}-B-C_{ipso} angles around boron are 120.2(9)°, 120.4(9)° and 117.6(10)° (358.2 total) and the distance from boron to the C_{ipso}-C_{ipso}-C_{ipso} plane is 0.120 Å (*cf.* 0.000 Å in **3** and 0.365 Å in **1** with 20% Br impurity), which indicates near trigonal planar geometry around the borane, and that the borane is not involved in any coordination to platinum (either directly or through a bridging phenyl). The substantial distance of 3.650(16) Å

between platinum and boron suggests a lack of any Pt-B interaction. Even the weak interactions observed in $[Os\{C_5H_3(BBr_2)_2\}_2]$ (3.21 Å),[102] (previously discussed in section 1.3.3) result in a considerably shorter M-B bond length. The tilting of the platinum *away* from the borane, and lack of pyramidalisation at boron, however, illustrates the lack of any interaction. There is clearly puckering along the vertical plane of the ligand, with the angle of the ring around the sulphur, C11-S-C12, being 98.2 (4)°, rather than the 120° it should be if the ring was planar. This puckering moves the phosphine and borane closer to one another. However, platinum is positioned much closer to the phosphine than the borane, with the C(9)-S-Pt angle being 163.73° The geometry around phosphorus is tetrahedral, with angles of 102.0(4)°, 103.1(4)°, 104.7(4)°, and 107.6(3)°, which is what is expected for a 4-coordinate phosphine. The P-Pt bond length of 2.266(2)Å is typical for neutral platinum (II) phosphine complexes.[103] The platinum is held in a square planar coordination, with angles of C(49)-Pt-P 91.4(3)°, C(42)-Pt-S 86.23(8)°, P-Pt-S 94.1(3)° and C(42)-Pt(1)-C(49) 87.6(4) around it.

Although a Pt-B bond is not observed, nor Pt-Me-B bridging interactions, clearly the borane has not been an innocent spectator ligand. One possible mechanism accounting for formation of this ligand-scrambled complex is shown in Scheme 2.6, where abstraction of a methyl group by the boron in the expected complex $[PtMe_2(TXPB)]$ leads to the zwitterion [PtMe(TXPB-Me)] followed by migration of one of the phenyl groups from boron to the cationic platinum center. It seems unlikely that such a process could occur in a concerted sense (*i.e.* both the methyl and phenyl abstracted simultaneously) based on steric arguments. It also seems likely that steric

effects could lead to collapse of the zwitterion to the new neutral complex, **2**. The migration of Ph to platinum would also be favoured due to coordinative unsaturation at the platinum. A second scrambling is not observed, possibly because the second Pt-Me group is oriented away from the boron. In addition to scrambling of the groups on platinum, a new phosphinoborane ligand $TXPB^{Me,Ph}$ has been made, in the coordination sphere of the metal. This scrambling reaction suggests a new means of constructing other phosphorus, boron-based ligands from TXPB itself and other Pt(II) compounds which might not be readily accessible by conventional routes.

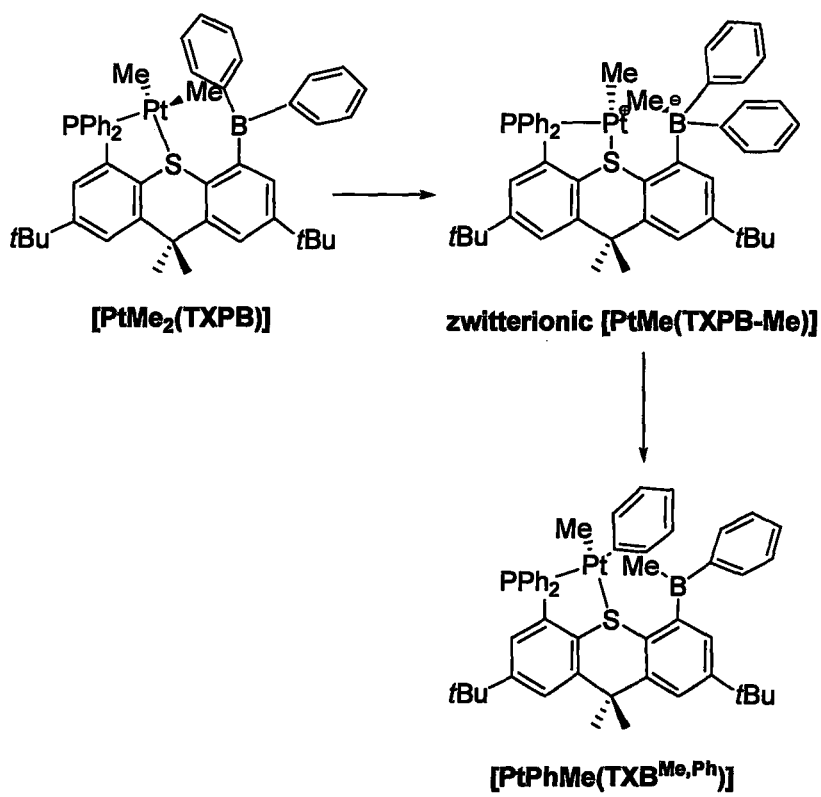

Scheme 2.6: Possible Reaction Pathway to 2

In order to compare the solution structure of this complex to that in the solid state, ^{1}H NMR spectroscopy has been used. Figure 2.11 shows the expanded alkyl region of the ^{1}H NMR spectrum of this complex, which indicates that only one of the methyl groups couples to platinum. The Pt-C coupling shows that one methyl group remains coordinated to platinum, ruling out exchange of Pt-*Me* with the B-*Me* on the NMR time scale. The observation of a single product by ^{1}H, ^{13}C and ^{31}P NMR spectroscopy, shows that [$PtPh_2(TXBMe_2)$] is not formed to any appreciable extent in solution. Attempts to observe [$PtMe_2(TXPB)$] at room temperature prior to scrambling were unsuccessful, Me for Ph exchange being very fast.

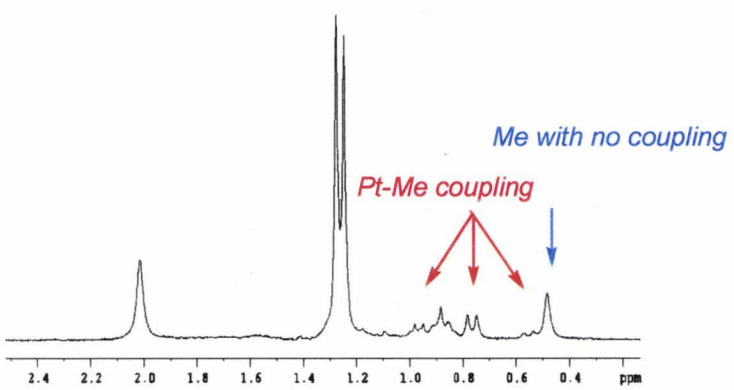

Figure 2.10: Expanded Alkyl Section of ^{1}H NMR Spectrum of 2

Despite the simple NMR spectra observed at room temperature, the ^{1}H NMR spectra of this compound at 25° C, -10° C, -30° C and -50° C clearly show that fluxional processes do occur in solution, Figure 2.12. This is supported by the ^{13}C NMR spectra. The broadness of some of the phenyl peaks in the ^{13}C NMR spectrum at 25° C may also suggest that the Pt-Ph and the B-Ph groups are exchanging.

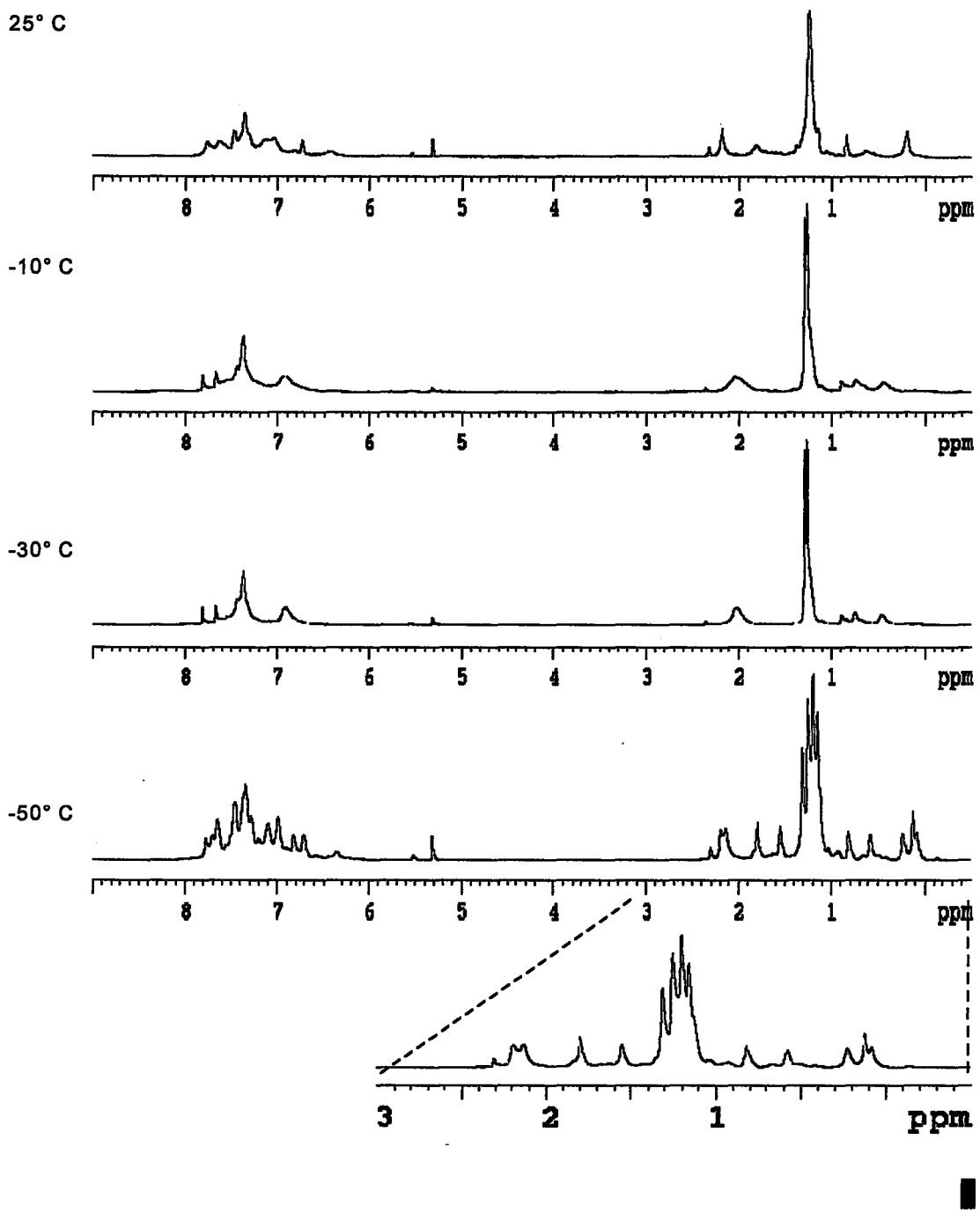

Figure 2.11: Variable Temperature ^{1}H NMR Spectra of 2 With Enlarged Alkyl Region at -50° C

The low temperature spectra indicate that there are 2 main isomers present (~1:1 ratio). This is revealed by the four distinct *t*-butyl peaks, and 2 sets of 4 methyl peaks, both those on the thioxanthene backbone and on the platinum/boron (Figure 2.12). There are several options which could account for the observation of isomeric pairs.

Option 1: The two sets of signals observed could be from isomers at platinum (Ph trans to phosphorus or sulphur), as in Scheme 2.7. These isomers could be interconverted through the intermediacy of the zwitterionic [PtMe(TXP^{B,Me})] described earlier involving a T-shaped MePt cation center where the phenyl group is abstracted by boron and then returned to the other position (trans to sulphur). This option is unlikely as the position trans to the sulphur would not be readily accessible for back-transfer of the phenyl group to complete the isomerization process.

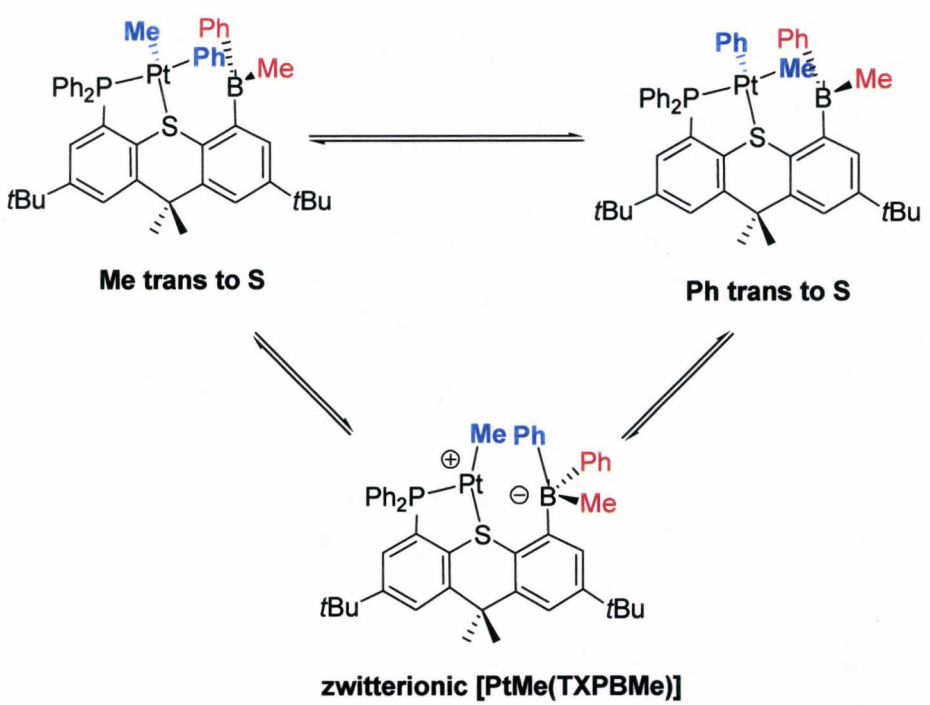

Scheme 2.7: Cis and Trans Geometric Isomers of Square Planar Pt(II)

Option 2: Isomerization at platinum could also occur via sulphur dissociation from platinum, conversion to a T-shaped complex followed by re-coordination of sulphur trans to the Ph. This mechanism seems unlikely for a Pt(II) centre, especially as it requires disruption of a stable five-membered chelate.

Option 3: A related exchange mechanism could involve partial reductive elimination of the Me and Ph bonds as illustrated in Scheme 2.8. In this pathway, reductive elimination of toluene would initiate leading to coordination of toluene which would then rotate at the Ph-Me sigma bond coordinated to platinum. Rather than being expelled from the platinum and thereby completing the reductive elimination process, oxidative addition (C-C activation) of the same Ph-Me bond occurs resulting in *cis-trans* isomerization. Although reductive elimination of *cis*-oriented Me and Ph groups at Pt(II) center would not be unusual, this option is not likely to be occurring. If it were occurring, one would expect the coordinated toluene group to escape for the platinum coordination sphere occasionally leading to decomposition of the complex; oxidative addition (C-C activation) at the Me-Ph bond to go back to product would not be feasible. This option does emphasize a possible decomposition pathway for this complex which should be considered for higher temperature applications. This possibility will be discussed at the end of this section as a possible means for making coordinatively unsaturated Pt(0) complexes of TXPB.

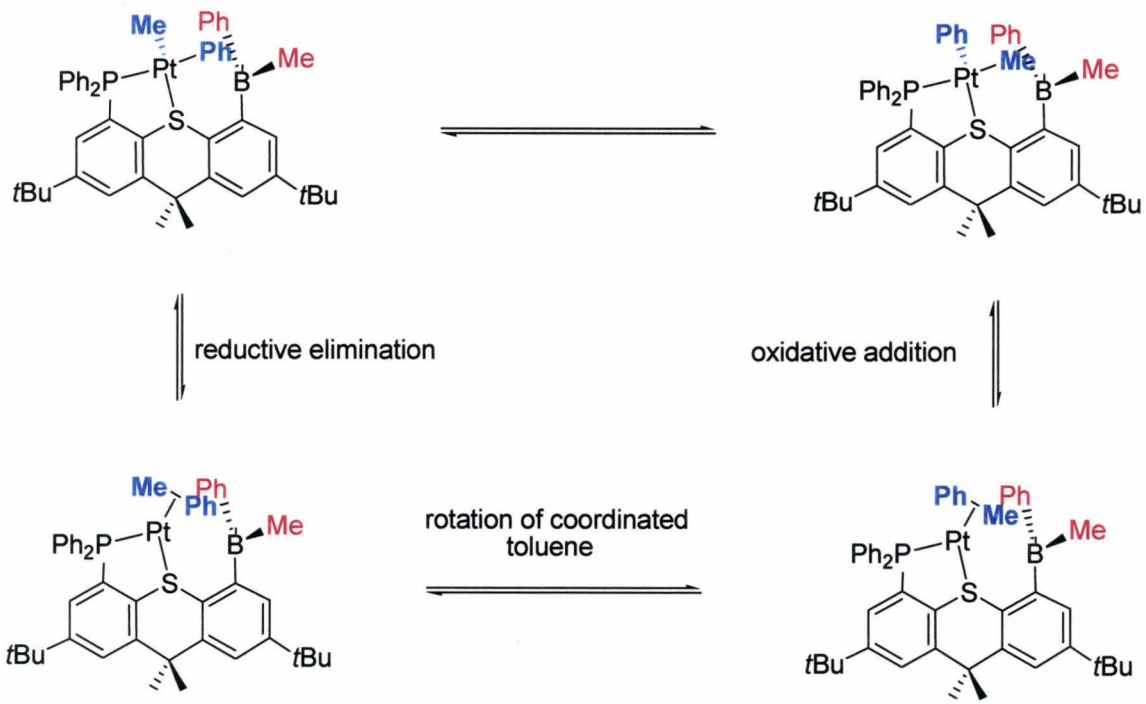

Scheme 2.8: Site Exchange of Pt-Ph and Pt- Me by Partial Reductive Elimination

Option 4: This option considers whether isomeric TXPB ligands could be interconverting. The two products could potentially be **2** and the [$PtMe_2$(TXPB)] complex, but given the much greater Pt-Ph bond strength relative to Pt-Me, and the lower Lewis acidity of the Me-substituted borane, it seems unlikely that these would exist as a 1:1 mixture. Also, an equilibrium involving [$PtPh_2(TXPB^{Me2})$] can be ruled out, since one methyl group shows ^{195}Pt coupling even at 25°C where exchange would be rapid.

Option 5: The next possibility involves interchange of the Ph and Me groups on boron rather than those on Pt. If the Ph is always trans to phosphorus and Me is always trans to sulphur and the borane always lies flat above the square plane, the two isomers observed at low temperature could be one with the B-Ph group pointing over the square plane and one with the B-Me group pointing over the square plane, Scheme 2.9. These isomers

could form through rotation at the B-thioxanthene bond although this would clearly require some type of distortion at both platinum and boron centers to accommodate this sterically demanding process. The intermediacy of zwitterionic [PtMe(TXPB-Me)] could again play a role here, where a phenyl group is abstracted, followed by partial rotation at boron-thioxanthene bond then re-addition of the other phenyl group to the platinum to reform the neutral complex. This exchange process is certainly a possibility for explaining why two isomers are observed at low temperature.

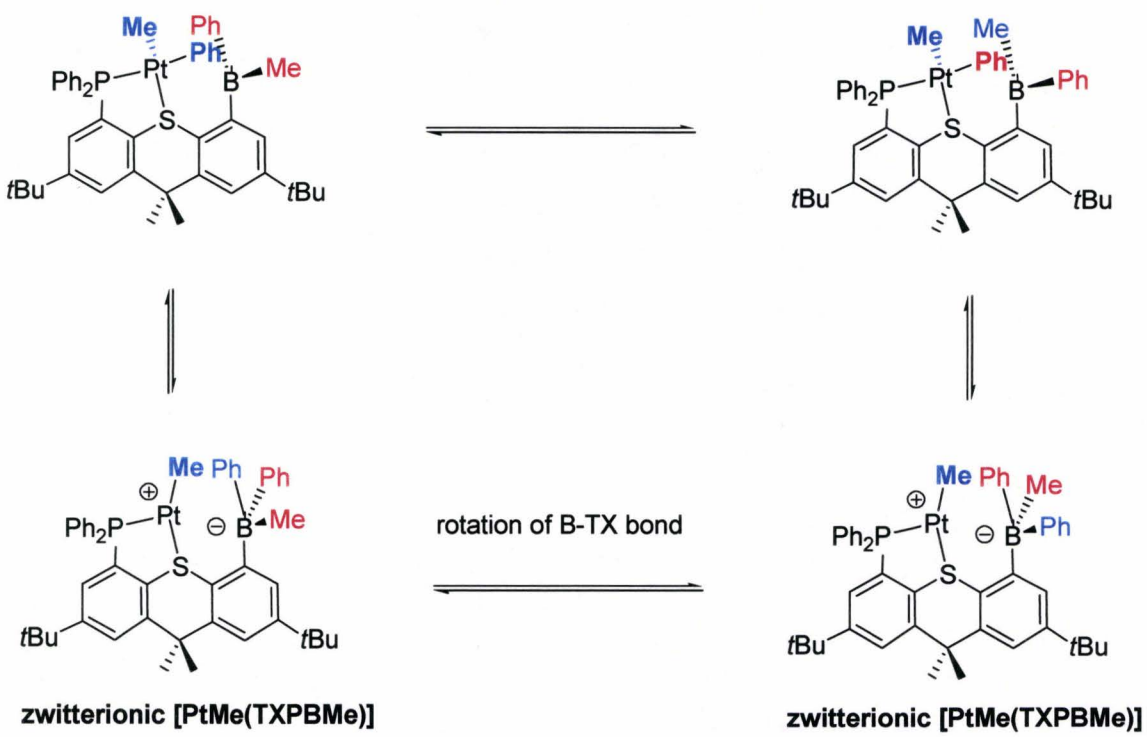

zwitterionic [PtMe(TXPBMe)] **zwitterionic [PtMe(TXPBMe)]**

Scheme 2.9: Position Exchange of B-Ph and B-Me

Option 6: Another potential set of isomers would be formed *via* puckering of the thioxanthene backbone, which would exchange backbone methyl groups from equatorial to axial and vice versa. In doing so, the Me groups on platinum and boron would be

placed in new environments and therefore under conditions where puckering was slow, the isomers would each possess 2 *tert*-butyl groups and 4 Me groups (2 from backbone, one Pt-Me and one B-Me). These isomers should not be significantly different from a steric standpoint and hence the observed 1:1 ratio is reasonable.

From the NMR data available, it is not possible to choose between these options as more advanced NMR experiments would be needed, but Options 5 and 6 are the favoured models. It is not readily obvious which additional methods, if any, will identify the isomers observed. Measuring the activation energy required for this exchange through careful low temperature studies will be informative. Presumably, NOE experiments can help as well particularly in determining whether the observed B-Me groups are in the vicinity of Pt-Me groups which might indicate that isomerization at platinum has occurred. In addition, activation parameters could be calculated to compare Me exchange with Ph exchange. Also, use of d_{10} PPh_2 would lead to a much less cluttered aryl region in the ^1H NMR spectrum, perhaps allowing distinct B-Ph signals to be observed and their exchange to be monitored.

To summarize, the reaction of TXPB with [$PtMe_2$(COD)] leads to displacement of COD and formation of the PtMePh complex of a new ligand [PtPhMe($TXB^{Me,Ph}$)] (**2**). This product exists as two rapidly converting isomers in solution which have not yet been identified. Although this complex itself does not involve direct interaction of platinum with boron, the borane clearly plays a role in its formation, which involves swapping of one B-Ph group for one Pt-Me group. This potential for a strong Lewis acid positioned in the vicinity of a Pt(II) to encourage deviations from typical Pt(II) chemistry needs to be

further explored. This complex can also be viewed as a bifunctional Lewis acid, possessing electron-poor Pt(II) and boron atoms positioned very closely together. Co-activation of appropriate Lewis bases could certainly be possible. The proximal B center could also enhance Lewis acidity of the Pt(II) center by abstracting the Ph group (or possibly the Me group) from the platinum to create a transient zwitterionic species. Again, the impact to typical Pt(II) mediated transformations needs to be explored further.

This stable Pt(II) complex also can be envisioned to be a starting point for investigation of Pt(0) chemistry at TXPB ligands. As will be discussed in the next section, direct routes involving coordination of TXPB to Pt(0) sources lead to unstable complexes. This Pt(II) complex could potentially be induced to reductively eliminate Ph-CH_3 in the presence of stabilizing bases allowing Pt(0) chemistry to be studied from a well-defined precursor. By tuning the properties of these bases, chemistry at the boron including Pt→B bonding may be revealed.

2.1.7 Reaction of TXPB + $Pt(nbe)_3$

$Pt(nbe)_3$ (nbe = norbornene) is not commercially available but can be readily synthesized from $[PtCl_2(COD)]$, nbe and $Li_2(cot)$.[104] $[Pt(nbe)_3]$ was viewed to be a promising reagent for making Pt→B complexes for a variety of reasons. First, it is a source of Pt(0) which has a greater likelihood of interacting with boron than do Pt(II) compounds due to a greater radius of the metal and increased electron density at platinum. Secondly, the nbe ligands are labile and can be readily displaced by phosphines allowing the anchoring interaction to proceed. Also, any remaining norbornene ligands are unlikely to bridge between platinum and boron as observed for halides. Finally, the nbe ligand is not strongly electron-withdrawing so the platinum center will remain electron-rich as required for a Pt→B interaction to occur.

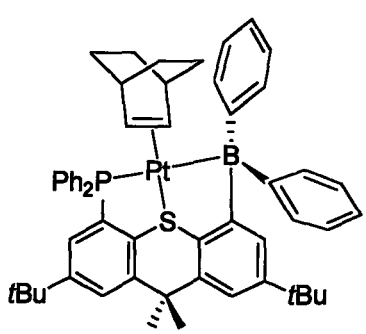

Figure 2.12: Potential Structure of [Pt(nbe)(TXPB)]

The ligand, 2,7-di-(*tert*-butyl)-4-diphenylboryl-5-diphenylphosphino-9,9-dimethylthioxanthene (TXPB), was reacted with $[Pt(nbe)_3]$ in dichloromethane at room temperature. The expected structure is shown in Figure 2.12, where one unbridged nbe ligand remains on the platinum which is also bound by both the phosphorus and sulphur

atoms of TXPB. This is based on the assumption that the borane occupies one coordination site of the platinum atom and there is not room for binding a second nbe. The platinum in this molecule is not electronically saturated however, so regardless of whether or not a Pt-B interaction forms, if there is sufficient room at the metal center, a second nbe ligand could be coordinated.

The ^{1}H NMR spectrum of the initial crude product is shown in Figure 2.13. This spectrum shows clearly that unreacted [$Pt(nbe)_3$] remains and that there are more than one set of signals now attributable to nbe. Although it is not possible to pick out all the signals for free and coordinated nbe from this complicated spectrum, it is clear that considerable free nbe is present as exemplified by the peak at 6 ppm, associated with the vinylic protons. The most notable peaks for coordinated nbe are those below 0.6 ppm. Three distinct signals are present, two broad peaks (likely to be ^{195}Pt satellites) flanking one sharp peak at 0.1 ppm. Integration of these peaks relative to the methyl signals at 3 ppm indicate that one nbe ligand remains on the metal.

The ^{1}H NMR spectrum also shows clearly that free TXPB is no longer present and that complexation must have occurred. This is firmly supported by ^{31}P NMR spectroscopy where a new peak at 39.9 ppm has appeared and that for TXPB at -8.65 ppm is no longer present. Furthermore, Pt-P satellites are observed showing that TXPB has indeed displaced at least one nbe ligand from $Pt(nbe)_3$. A Pt-P coupling constant of 3265 Hz is observed (Figure 2.14).

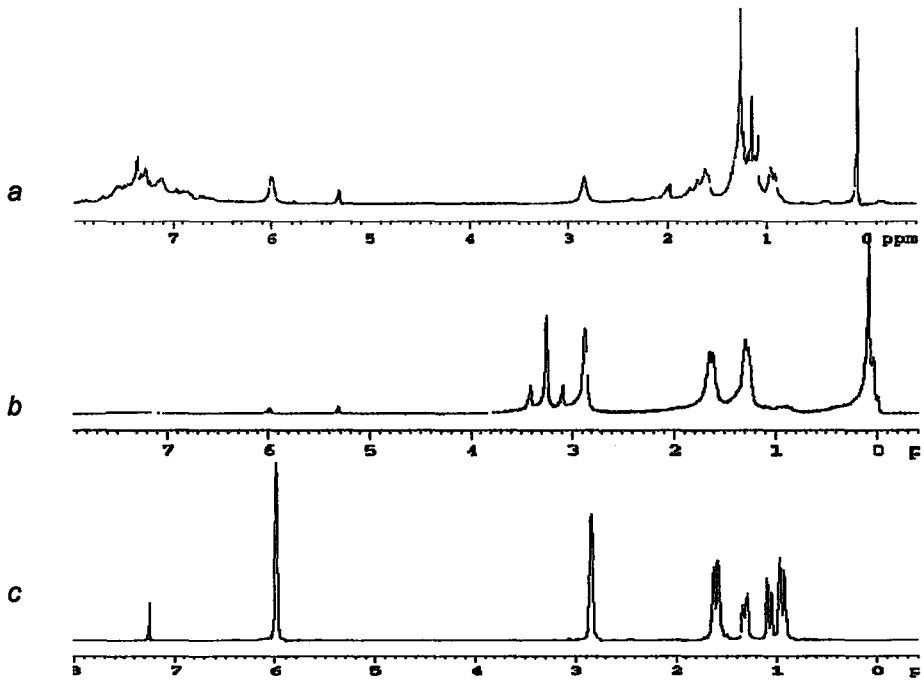

Figure 2.13: ^{1}H NMR Spectra in CD_2Cl_2 of (a) Reaction Mixture of ([Pt(nbe)$_3$] With (TXPB)) (b) Pt(nbe)$_3$ and (c) Free nbe

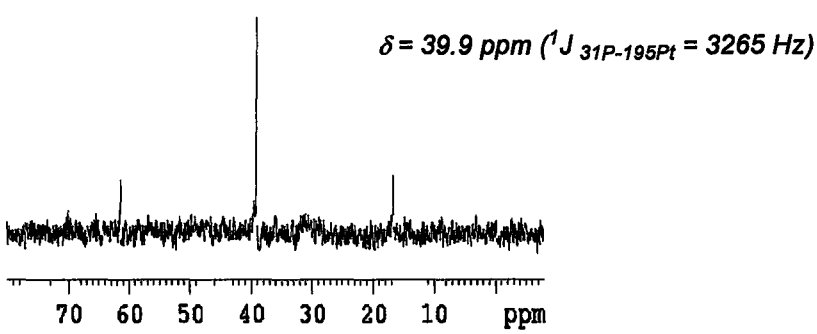

Figure 2.14: ^{31}P NMR Spectrum of [Pt(nbe)(TXPB)]

Unfortunately, the product could not be purified from the uncoordinated nbe by selective crystallization or simply washing away the free nbe with solvent. When washed with hexane to remove the displaced nbe, the product turns from dark brown to an orange solid. ^{1}H NMR spectroscopy indicates that the complex has "decomposed" to one major new compound. The ^{31}P NMR spectrum now shows a major peak at 67 ppm. It is not

clear what this new compound is, although it does possess a TXPB-Pt fragment as indicated by Pt-P satellites which show a significantly larger coupling, ($J_{31P-195Pt}$ = 6016 Hz, Figure 2.15). A large coupling constant can be attributed to an increased s-character on platinum, and this could be due to the borane or due to geometric constraints leading to a shorter Pt-P bond distance or a geometry favouring increased Pt-P s-character.[105] Further work needs to be carried out to try to unequivocally identify both the first substitution product and this new product formed upon attempted isolation. In summary, ^{1}H and ^{31}P NMR spectra have been used to tentatively assign the first product as [Pt(nbe)(TXPB)]. The second compound could be a product resulting from loss of the last nbe ligand proceeding through an activated "TXPB-Pt" species which would be expected to be reactive at the coordinatively and electronically unsaturated Pt center.

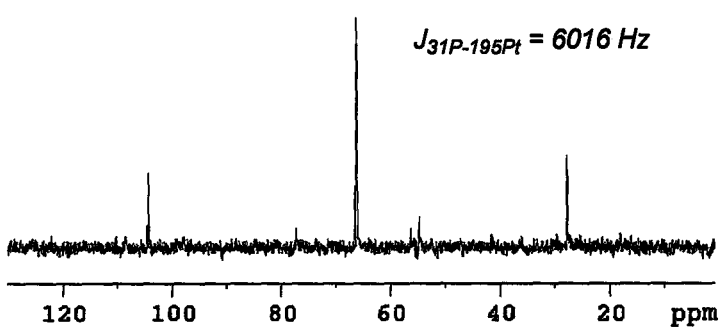

Figure 2.15 ^{31}P NMR Spectrum of "Decomposed" [Pt(nbe)(TXPB)]

It was thought that since the nbe is a labile ligand, the complex may be more stable if the nbe ligand is replaced with a second phosphine ligand which should be more tightly coordinating. One such complex targeted was [Pt(PPh_3)(TXPB)]. The crude

initial product containing uncoordinated nbe was mixed with PPh_3. The ^{31}P NMR spectrum (Figure 2.16), however, indicates that rather than substitution of the nbe for PPh_3, the PPh_3 had in fact abstracted the Pt(nbe) fragment leaving free TXPB. The ^{31}P spectrum shows the peaks corresponding to the [Pt(nbe)TXPB)] starting material, a new peak with satellites at 36.2 ppm ($^1J_{31P\text{-}195Pt}$= 3328 Hz) and also a peak at -8.65 ppm, which corresponds to the free TXPB ligand . If the reaction had worked as intended, the resulting [Pt(PPh_3)TXPB] would presumably show two separate doublets with ^{195}Pt satellites in the ^{31}P NMR spectrum. With the presence of just one ^{31}P peak in conjunction with the TXPB free ligand peak, it can be concluded that the reaction did not work as planned.

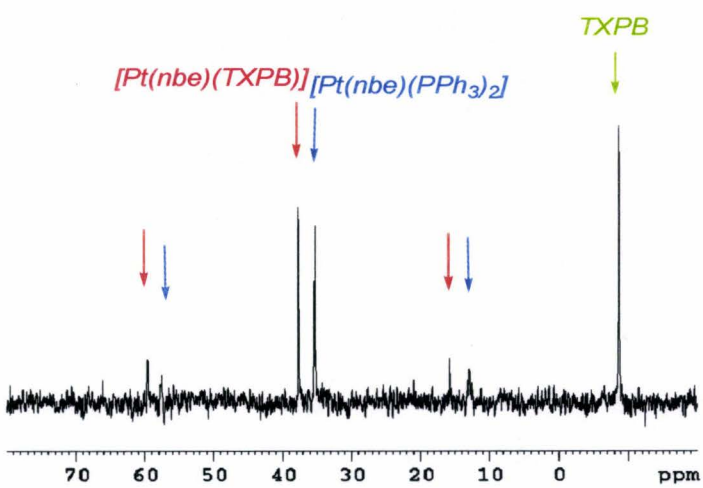

Figure 2.16 ^{31}P NMR of [Pt(nbe)(TXPB)] + PPh_3

However, when the more electron rich and sterically hindered phosphine, [P(tBu)$_3$] was added to the crude [Pt(nbe)(TXPB)] mixture, the ^{31}P NMR spectrum indicated two doublets flanked by ^{195}Pt satellites. This ^{31}P NMR spectrum is as would be

expected for a product such as [Pt(P*t*Bu$_3$)(TXPB)], (Figure 2.17, red and green arrows correspond to bis(phosphine) Pt complex).

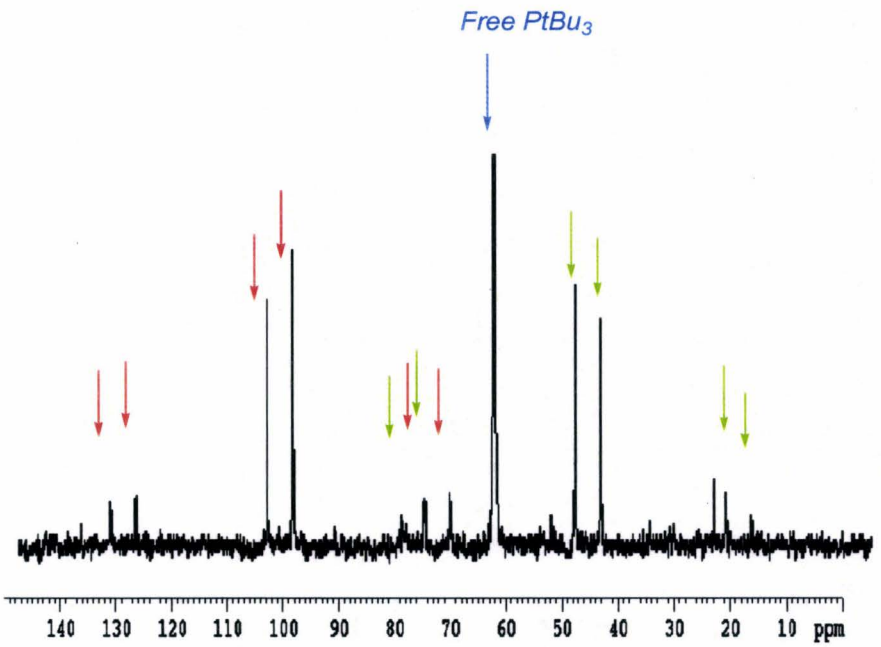

Figure 2.17: ^{31}P NMR of [Pt(nbe)(TXPB)] + P(tBu)$_3$

Purification of this product was attempted, but it was found to decompose in solution over several hours, and removing the solvent also initiated decomposition. Because of the instability of this complex, pure material could not be isolated. It is thought that this complex could well contain the desired M-B bond, but since it is so unstable, it is not possible to say for certain.

It should be noted that an activated Pt-B moiety could certainly participate in other reactions, intermolecularly or intramolecularly. If such a species is being formed in these substitution reactions, attempts at isolation may be thwarted by further reaction. Further ligand design may be necessary to shut down any further reactions (decomposition) and identify whether a Pt-B bond actually does form, and then to

systematically investigate any chemistry associated with this type of linkage. However, the strategy to make a [Pt(PR$_3$)(TXPB)] complex does show promise, further demonstrating the utility of [Pt(nbe)$_3$] as a valuable starting material since the nbe ligands can be substituted sequentially. Another option which could be investigated as a cleaner method is to pre-form a [Pt(nbe)$_2$PR$_3$] complex which can then be reacted with TXPB to give [Pt(PR$_3$)(TXPB)]. Other Lewis bases such as nitriles or isonitriles could be used instead of phosphines to displace the last nbe ligand after coordination of TXPB.

2.1.8 Reaction of TXPB + [Pt$_2$(dba)$_3$]

Mixtures of TXPB with Pt(dba)$_2$ (dba = dibenzylideneacetone) in dichloromethane or toluene fail to react, even after several days or heating. Previous work done by the Emslie group has shown that Pd$_2$(dba)$_3$ reacts readily with TXPB, to give a product containing one remaining dba molecule. The dba ligand is coordinated to the palladium via one of its double bonds and to the boron by the oxygen (Figure 2.18).[90] From the X-ray crystal structure, it appears more appropriate to consider this a palladium(II) η^3-boratoxypentadienyl complex, but in solution at room temperature, the palladium(0) resonance structure must also be accessible, since coordinated dba and free d$_2$-dba undergo facile exchange. To form this complex, the TXPB ligand is able to isolate and complex one "Pd(dba)" unit. Apparently, the corresponding "Pt(dba)" unit is not

accessible via an analogous route, perhaps due to inherent differences in the reactivity of platinum and palladium or due to the extremely low solubility of $Pt(dba)_2$ in suitable solvents.

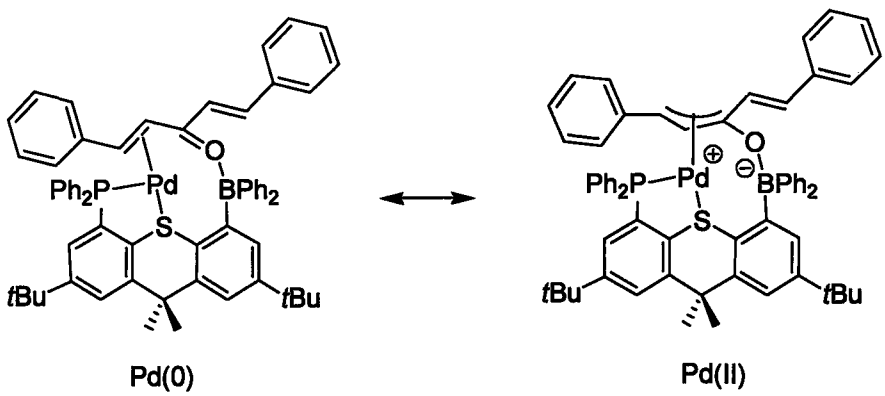

Figure 2.18: Resonance Forms of [Pd(dba)(TXPB)]

2.2 Summary of TXPB Coordination Chemistry

By employing the TXPB ligand previously developed in the Emslie lab, [PtCl(μ-Cl)(TXPB)] (**1**) and [PtPh,Me($TXB^{Me,Ph}$)] (**2**) were synthesized and characterized. **1** is structurally similar to the complex [$PdCl_2$(TXPB)], and the observed bridging interaction of the chlorine atom is not unexpected. Complex **2** was not the product that had been anticipated, and is a result of an interesting ligand redistribution between the hydrocarbyl groups on platinum and boron. Although this complex does not contain the metal-borane bond which had been the aim of this project, it is of interest nonetheless. The ligand scrambling reveals the possibility of a new means of constructing other phosphorus, boron-based ligands from TXPB itself, in addition to synthesizing Pt(II) compounds which might not be readily accessible by conventional routes.

The reaction of TXPB with [$Pt(nbe)_3$] was considered the most promising route to the desired metal-borane bond, since [$Pt(nbe)_3$] is a source of Pt(0). However, while the TXPB ligand did react with the Pt compound, and a product was observed by ^1H NMR spectroscopy, the product was found to be too unstable to allow isolation. Attempts to substitute nbe with different phosphine ligands were also unsuccessful due to persistent instability.

Although no complex with a metal-borane interaction was formed in this research project, a new ligand was synthesized in addition to several interesting complexes. This work has suggested potential routes to the synthesis of the M→BR_3 complexes and has produced the first TXPB complex in which free borane is held in close proximity to the metal; an intriguing situation with considerable potential in bifunctional catalysis.

Chapter 3: Ligand Design, Synthesis and the Platinum Chemistry of Phosphine/Ether/Borane Ligand XPB

3.1 Applications of the Versatile Xanthene Backbone

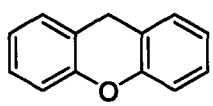

Figure 3.1 Xanthene

Xanthene is a polycyclic diaryl ether compound in which two benzene rings are fused to tetrahydropyran which is a six membered cyclic ether with five carbons and one oxygen. Its derivatives are widely used in biological stains, light and temperature sensitizers, as photoinitiators of polymerization processes, and as photochromic and thermochromic agents. Xanthene dyes include fluorones, fluoresceins, rosamines, rhodamines, fluorenes, pyronins, succineins, sacchareins and rhodols, (Figure 3.2).[105]

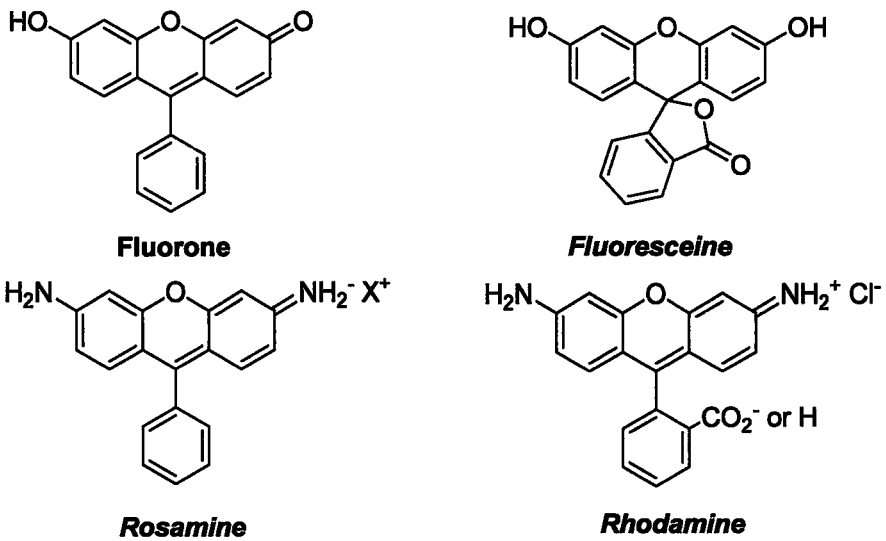

Figure 3.2: Examples of Useful Compounds Based on the Xanthene Skeleton

The great utility of xanthene derivatives is possible due to simple and selective methods for functionalizing xanthene at positions 4 and 5.[106] Another valuable quality, the rigidity of the xanthene backbone, makes it a useful scaffold for larger molecules. As a result, the potential for xanthene derivatives for housing convergent functional groups with cleft-like shapes makes them useful receptors for other molecules such as quinine and quinidine,[107] and even sizable ones like porphyrin subunits.[108]

The rigid skeletons of xanthene-based molecules have also been employed in the construction of new chiral and achiral bidentate phosphine ligands with potential applications in various catalytic processes. The diphosphine, Xantphos with diphenylphosphino groups in the 4 and 5 positions of the backbone, is one derivative that has found widespread interest (Figure 3.3). It was first developed by van Leeuwen, where it was used with Ru for the hydroformylation of long chain alkenes.[109]

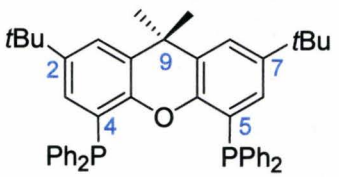

Figure 3.3: Xantphos

Xanthphos has gone on to be widely studied, and has been shown to be a remarkable ligand in late transition metal catalysis, especially in combination with palladium, platinum and ruthenium. For example, [Xanthphos-Pd(dba)$_2$] gives exceptionally high selectivity in the synthesis of industrially useful linear aldehydes.[110] Xantphos has also been found to be one of the most powerful ligands in the coupling of electronically neutral or electron-deficient *N*-alkylanilines with electron-deficient aryl bromides when used in conjunction with palladium.[111] Furthermore, xanthene ligands have been used with palladium in the development of convenient and efficient methods for C-N bond formation under rather mild conditions that tolerate various functional groups.[112] It has also been used with palladium in intermolecular hydroamination of vinylarenes where the catalyst system is substantially more active for this process than catalysts published previously.[113] It has found use with ruthenium as an efficient catalyst system for the asymmetric transfer hydrogenation of ketones, with a remarkably broad substrate scope. Even notoriously difficult ketones such as isopropyl methyl ketone are reduced with extraordinarily high enantioselectivity (ee's up to 99%) with BINOL-derived diphosphonites, Figure 3.4.[114] Recently, Pt(II) complexes have been shown to be effective in the hydroformylation of styrene.[115]

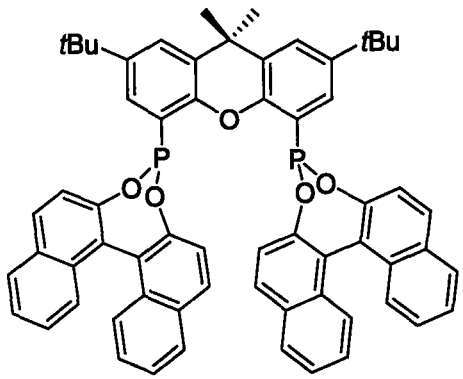

BINOL-based diphosphinite

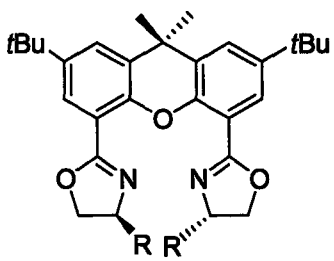

XABOX

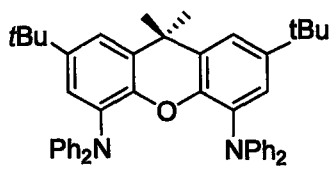

Xantamine

Fig. 3.4: Bidentate Ligands Based on the Xanthene Backbone

These xanthene-based ligands, give very efficient catalysts for several reactions, and are not limited to the xantphos derivatives. Although the xanthene backbone itself is not chiral, chiral elements can be introduced as part of the Lewis basic substituents. For example, C_2-symmetric diphosphines have met great success, but high ee levels have also been reached with mixed-phosphorus, nitrogen and nitrogen-based donor bidentate ligands, such as 4,5-bis(2-oxazolinyl)-(2,7-di-tert-butyl-9,9-dimethyl)-xanthene (**XABOX**, R = *i*Pr, Ph, Bn)[116] and van Leeuwen has also investigated ligands with amine and arsine groups (with rhodium and platinum) for hydroformylation chemistry. The diamine analogue, **xantamine** however was shown to lead to poor catalysts, since the NAr_3 moiety is hard, and the soft ruthenium metal does not bind to it.[8]

3.1.1 Expected Coordination Behaviour for Xanthene-Based Hybrid Phosphine/Borane Ligands

The xanthene-based backbone is similar to that in thioxanthene-based ligands described in Section 2.2 in that it is rigid, but not necessarily planar; it can also adopt a butterfly structure, where the two aromatic rings of the backbone move closer to each other. However, there are two particularly significant differences between the xanthene and thioxanthene ligand backbones: (1) The substituents in the 4- and 5-positions of the xanthene backbone are positioned closer to one another as a result of the smaller atomic radius of oxygen compared with sulfur. (2) In contrast to thioethers, SR_2, the OR_2 moiety is a hard donor group, and so platinum, a soft late transition metal, would not be expected to bind strongly to it. Indeed, in the chemistry of xantphos ligands, only two examples of oxygen-coordination have been observed (Figure 3.5): 2,7-bis(SO_3Na)-xantphospalladium chloride[117] (**XIX**) and xantphos(4-cyanophenylpalladium)[118] (**XX**). These complexes are unusual in that the metal center is both cationic and coordinatively unsaturated, resulting in an unusual trans-coordination mode of the xantphos phosphine groups and a planar configuration of the xanthene backbone.

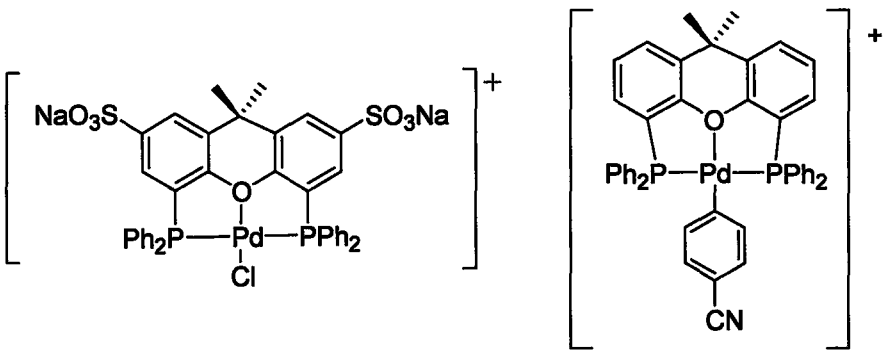

XIX XX

Fig. 3.5: Cationic Examples of O-M Coordination in a Xantphos Complex

As a result of two-point-binding via phosphorus and sulphur, the thioxanthene based TXPB ligand is effective in positioning a pendant borane in close proximity to a coordinated metal. By contrast, metal coordination in the XPB ligand will likely occur via phosphorus alone. As a result of free rotation around the C4-P bond, the borane may be located close or distant to a coordinated metal center depending on steric factors and the favourability of Lewis acid-Lewis base adduct formation (Figure 3.6). There are certainly advantages that can be considered where a poorer donor atom such as oxygen is present in the backbone. For example, in cases where two or more organic molecules need to coordinate to platinum during catalysis (as in hydroformylation), the sulphur atom could interfere by occupying a coordination site. An oxygen atom will be less likely to do so, but still may stabilize uncoordinated species formed during a catalytic process through a weak donation.

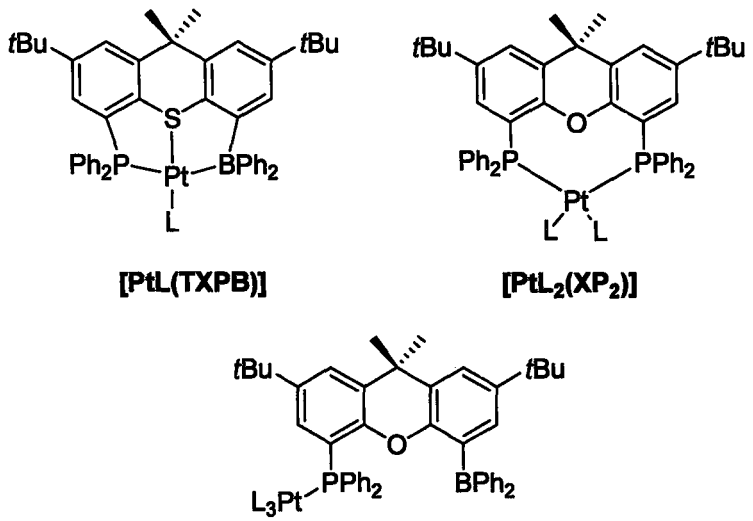

Fig. 3.6: Comparison of Metal Coordination Possibilities Due to Lewis Basic Groups on TXPB, XP_2 and XPB Backbones

In addition, as a monodentate hybrid ligand, XPB would provide a valuable comparison with the bidentate thioxanthene, in terms of metal-ligand bonding, and the metal-borane distances that result. Given the greater range of M--B distances available to XPB, long M-B bonds, similar to those seen for borylmetallocenes (as discussed in 1.3.3) may still be accessible, and XPB is expected to show quite different behaviour with respect to co-ligand coordination and abstraction.

3.1.2 Synthesis of 2,7-di(*tert*-butyl)-9,9-dimethyl-5-diphenylboryl-4-diphenylphosphinoxanthene (XPB)

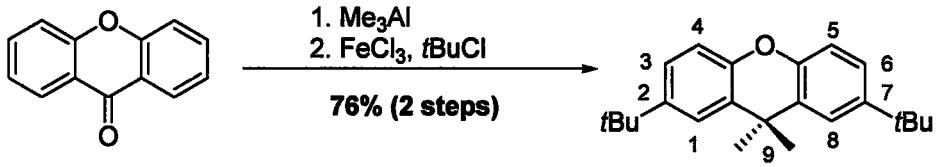

xanthone **2,7-bis-(*tert*-butyl)-9,9-dimethylxanthene**

Scheme 3.1: Synthesis of 2,7,-bis-(tert-butyl)-9,9-dimethylxanthene

Initial work used xanthone as a starting material since this is readily available and can be converted to the known complex 2,7-bis-(*tert*-butyl)-9,9-dimethylxanthene in high yields and on large scale (Scheme 3.1).[107] From this molecule, two strategies were considered for installing a phosphine and then a borane in the 4- and 5- positions. The first strategy involves direct lithiation of these positions sequentially with *n*BuLi followed by an appropriate electrophile. Alternatively, the positions can be brominated first to give the dibromo derivative where the bromines can then be sequentially lithiated and functionalized. This second strategy was employed by van Leeuwen *et al.* who sequentially monolithiated the backbone, substituted with a phosphine, and then lithiated the second position to install a second Lewis base (*e.g.* an arsine or a different phosphine).[119] Their reported yield, at 50% seemed quite low, due to a mixture of mono and diphosphine products after the first step, and it was reasoned that the presence of two reactive bromine groups was the origin of this problem. Direct ortho-directed lithiation of aryl-H bonds in 2,7-bis-(*tert*-butyl)-9,9-dimethylxanthene would be expected to be less

favourable than lithiation of aryl-Br bonds, and as such, monolithiation might be favoured. This strategy was explored first.

Indeed, direct lithiation of 2,7-bis-(*tert*-butyl)-9,9-dimethylxanthene followed by quenching with $ClPh_2P$ produced the mono-phosphine ligand 2,7-bis-(*tert*-butyl)-9,9-dimethylxanthene-4-phosphinoxanthene (XPH), which was isolated by filtration to remove LiCl, (Scheme 3.2). Concentration of the filtrate resulted in a white powder with a yield of 70%. A small amount of the diphosphine product is also produced, as seen in the ^{31}P NMR, but this product is soluble in hexanes and so is easily removed.

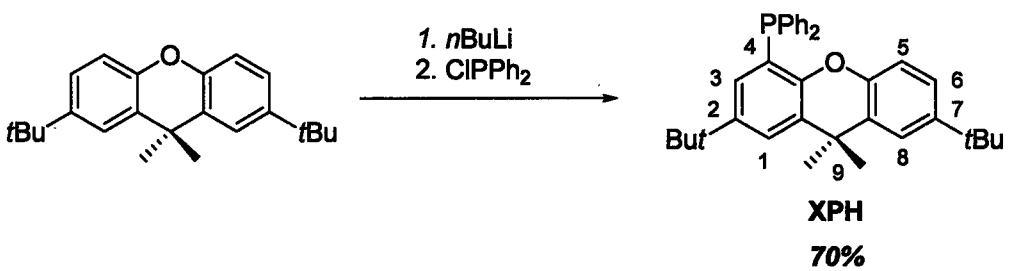

Scheme 3.2 Synthesis of the XPH Ligand

Further attempts at a second lithiation (at position 5) using various solvents, temperatures and lithiating agents (THF, Et_2O, -60° C to 25 °C, *n*BuLi, *t*BuLi, TMEDA), were not successful. In order to ensure that both the 4- and 5-positions could be activated sequentially, readily prepared 2,7-bis-(*tert*-butyl)-4,5-dibromo-9,9-dimethylxanthene (XBr_2) was next investigated. This compound is prepared from reaction of XH with bromine as documented by Nowick *et al*[107](3 equivalents of Br_2 is first added, stirred for 24 hours, then a catalytic amount of Fe is added, followed by another equivalent of Br_2. The dibromide was subsequently lithiated and attempts at selectively installing a

diphenylphosphine group were made according to the literature procedure of van Leeuwen (Scheme 3.3).[119]

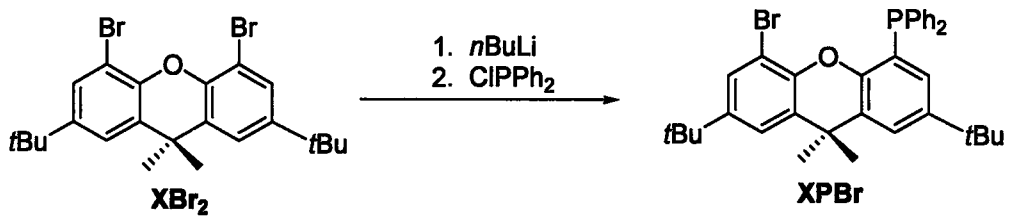

Scheme 3.3 Synthesis of the XPBr Ligand Precursor

After several attempts following this procedure, none of the desired product could be isolated. It was found that the initial lithiation required several hours to reach completion, rather than the hour stated in the literature. Another problem was encountered during the attempted workup of the product. It was found that the monophosphine product (XPBr) is substantially air sensitive, and so the documented HCl/H_2O washing step lead to the formation of the corresponding monophosphine oxide. The same problem occurred even when degassing of the solvents was attempted. It was found that pure phosphine oxide could be isolated after column chromatography, but was not useful in the direct preparation of XPB, so was not characterized further. However, the desired oxide-free product, XPBr, could be obtained in high purity and free of the oxide when lithiated using a 1.1% excess of the lithiating agent, followed by washing with hexanes under Ar. The ^{1}H NMR and ^{31}P NMR of XPBr are shown in Figure 3.7. The yield of this product was 60 %.

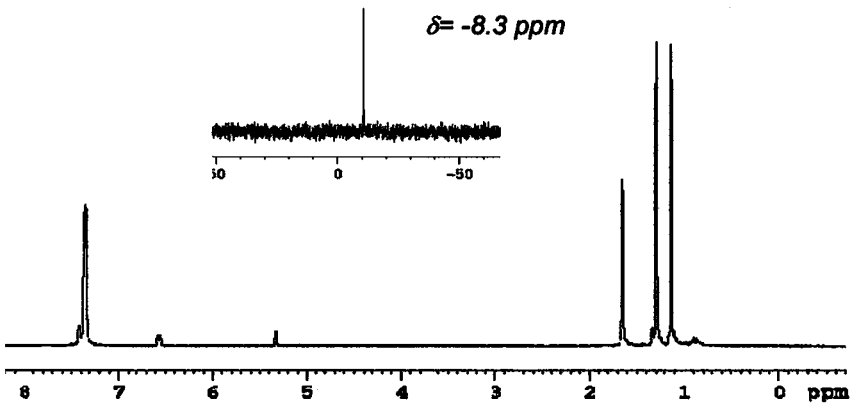

Figure 3.7: ^{1}H NMR Spectrum of XPBr, With ^{31}P NMR Spectrum in Inset

It was found that at this level of purity, the starting material is sufficiently clean for further reactions. It was observed, however, that when the purity falls to lower than approximately 90%, by ^{1}H NMR spectroscopy, subsequent lithiation and reaction with Ph_2BCl to form XPB results in a complex mixture from which pure product cannot be isolated.

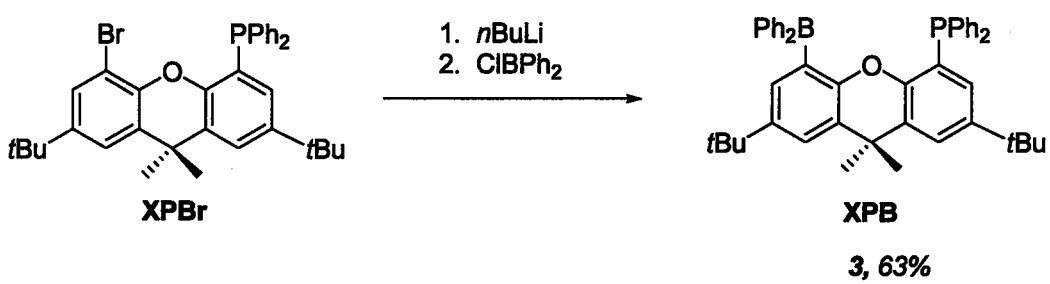

Scheme 3.4: Synthesis of XPB from XPBr

The second lithiation step was found to occur most successfully in ether (scheme 3.4). In THF, there appeared to be an adduct forming with the added Ph_2BCl, observed by ^{1}H NMR spectroscopy, hindering substitution onto the xanthene backbone. It was also found that a by-product was formed when Ph_2BBr was used instead of Ph_2BCl, seen in

the ^{31}P NMR spectrum as a multiplet at around 60 ppm, but this product was never isolated. In contrast, when Ph_2BCl was used as the source of diphenylboron, the resulting ^{31}P NMR spectrum showed only one main peak before workup (11 ppm). The product was then washed with hexanes to remove excess Ph_2BCl, followed by sonication in CH_3CN to form an adduct (**XPB-MeCN**, Scheme 3.5). As had been observed in the synthesis of TXPB, this adduct precipitated out of solution, and was then isolated by filtration and dried *in vacuo*. Under high vacuum, the CH_3CN was removed, leaving base-free 2,7-di(*tert*-butyl)-9,9-dimethyl-5-diphenylboryl-4-diphenylphosphinoxanthene (**XPB, 3**) as a pure white powder, with a yield of 63%.

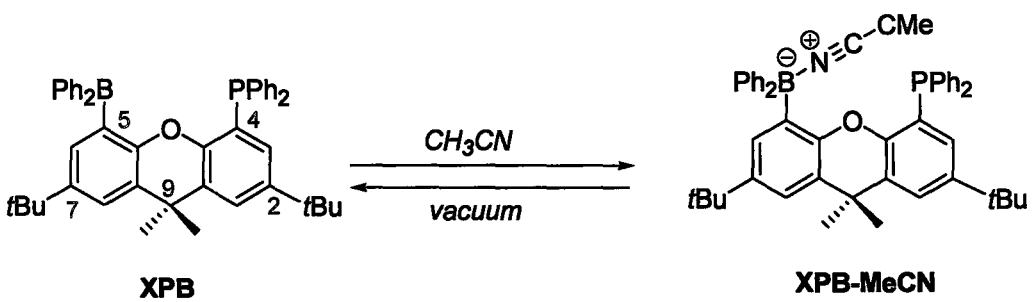

XPB **XPB-MeCN**

Scheme 3.5: Synthesis/Decomposition of the MeCN - XPB Adduct

Figure 3.8 shows the ^{1}H NMR and ^{31}P NMR spectra of **3**. The ^{31}P NMR spectrum shows a single peak at 11 ppm, compared to the peak at 10 ppm seen in the spectrum of XPBr. In the ^{1}H NMR spectrum, the doublet of doublets at 6.8 ppm corresponds to the proton at position 3 on the backbone, adjacent to the phosphine group. Another difference between this ligand and the TXPB ligand is that the three sets of peaks corresponding to the aryl protons on the phosphine are well defined, while those corresponding to the aryl protons on the borane are less well defined.

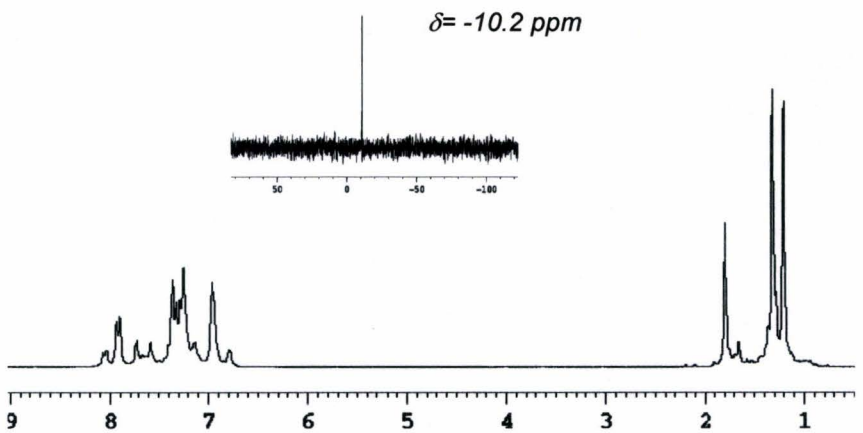

Figure 3.8: ^{1}H NMR Spectrum of 3, With ^{31}P NMR Spectrum in Inset

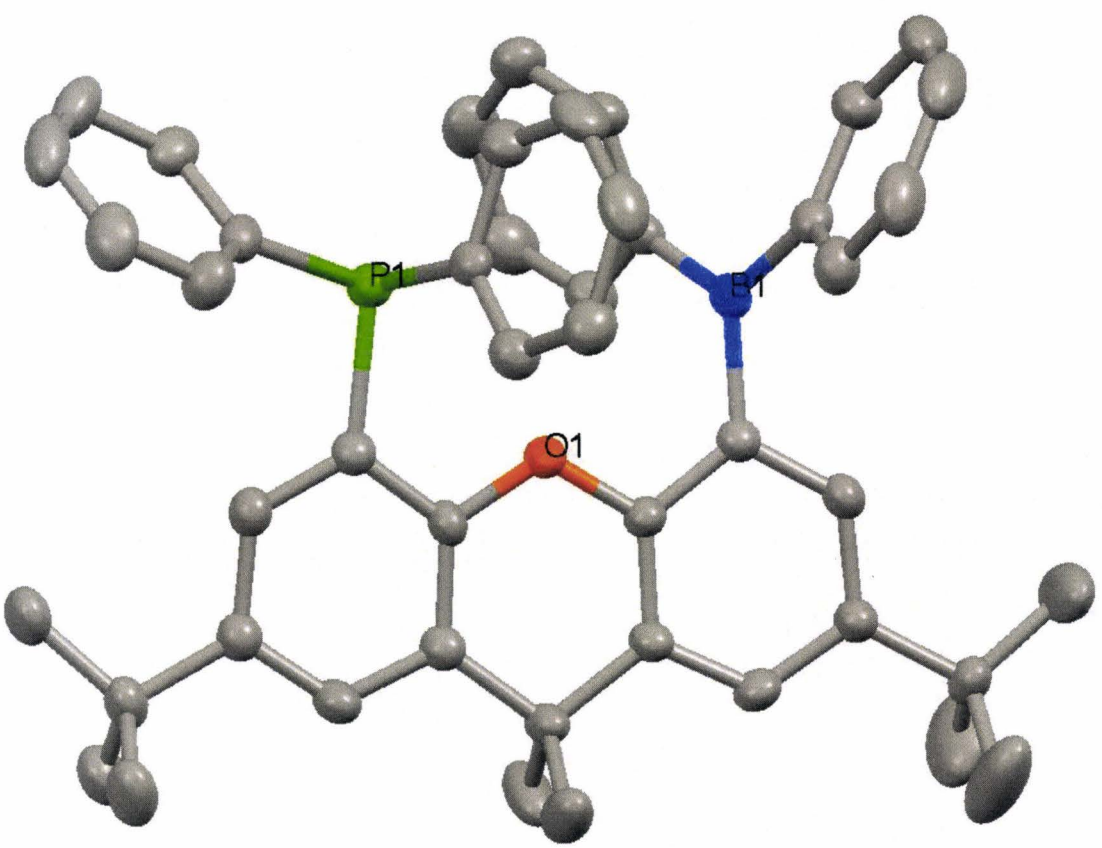

Fig. 3.9 X-ray Crystal Structure of 3, at 50% Probability Level Ellipsoids (Hydrogen Atoms Omitted For Clarity)

Table 3.1: Selected Bond Angles [°] and Bond Lengths [Å] for 3 with Estimated Standard Deviation in Parentheses

C(30)-P(1)-C(24)	98.75(11)
C(30)-P(1)-C(4)	103.40(12)
C(24)-P(1)-C(4)	102.11(12)
C(11)-O(1)-C(12)	119.5(2)
O(1)-C(11)-C(10)	123.0(2)
O(1)-C(12)-C(13)	122.5(2)
C(42)-B(1)-C(36)	121.9(2)
C(42)-B(1)-C(5)	119.3(2)
C(36)-B(1)-C(5)	118.7(3)
P(1)-C(4)	1.839(3)
B(1)-C(5)	1.576(4)

Crystals of **3** were grown by cooling a concentrated solution of XPB in hexanes to -30° C, and the X-ray structure is shown in Figure 3.9. It is not possible to directly compare this free ligand to the TXPB analogue, since suitable crystals of it could not be grown due to extremely high solubility and low crystallinity. However, in comparison to the puckered, butterfly-shaped, TXPB complexes, the pyran backbone in XPB is planar, with the C(11)-O-C(12) angle of the ring around oxygen being 119.5(2)°. The borane adopts a trigonal planar geometry, with angles of 121.9(2)°, 119.3(2)°, 118.7(3)°, which is as expected for a three-coordinate borane.

In summary, the new mixed phosphine/ether/borane complex **3** was synthesized in 5 steps from xanthone. The compound is purified by precipitation of its acetonitrile

adduct where the acetonitrile can then be removed following filtration and drying. As with TXPB, reactions of XPB with a number of platinum complexes were explored.

3.1.3 Metal Complexation With XPB Ligand

Since oxygen is a much harder Lewis base than sulphur, the chemistry of the ether-based XPB ligand is expected to differ significantly from that of thioether-containing TXPB. Perhaps the most important difference is likely to be in ligand hapticity; while TPXB coordinates through both the phosphine and thioether group, XPB is expected to coordinate via the phosphine alone (as discussed previously in Section 3.1.1). In order to investigate the effects of these differences in the coordination chemistry of XPB and TXPB, the reactivity of XPB with $[PtCl_2(COD)]$, $[PtMe_2(COD)]$ and $[Pt(nbe)_3]$ was investigated. The reactions of the XPB ligand with these Pt starting materials would serve as intriguing and informative comparisons to the complexes formed upon reaction of the same metal compounds with TXPB.

3.1.4 Reaction of XPB With $[PtCl_2(COD)]$

The first source of Pt(II) investigated was $[PtCl_2(COD)]$. As illustrated previously, TXPB reacts with this reagent to give a chelated structure with a Cl-bridge between the Pt and B via displacement of the COD ligand from platinum. A major difference is apparent for the reaction of XPB: a white precipitate immediately begins to form in CH_2Cl_2. Free COD is produced, as assessed by ^1H NMR spectroscopy, and this

precipitation reaction continues over the course of several hours. ^{1}H and ^{31}P NMR spectra of the solution (Fig. 3.10) indicate the gradual diminishment of XPB and [$PtCl_2$(COD)] without the concomitant increase in signals from a new major product (aside from COD). Over time, several new peaks are observed growing in the ^{31}P NMR spectrum, but the intensities are very low and it is not possible to ascertain whether they are representative of the precipitate formed or small amounts of decomposition products.

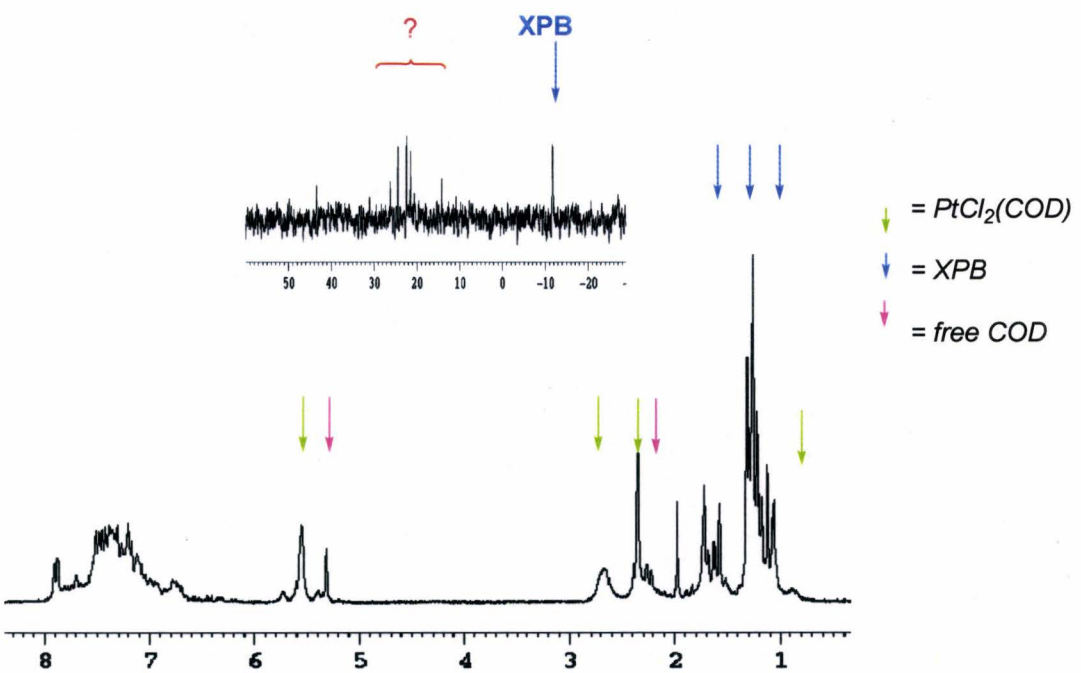

Fig. 3.10 ^{1}H NMR and ^{31}P NMR Spectra of XPB + [$PtCl_2$(COD)] Reaction

Efforts to dissolve the solid in other NMR solvents such as THF, toluene and benzene were unsuccessful due to persistent insolubility. Attempts at dissolution by heating the product in benzene appeared to lead to decomposition. Similarly, attempts to dissolve and crystallize the product were unsuccessful. Without NMR spectroscopic

data, it is impossible to unequivocally identify this product; however, there are a few reasonable possibilities.

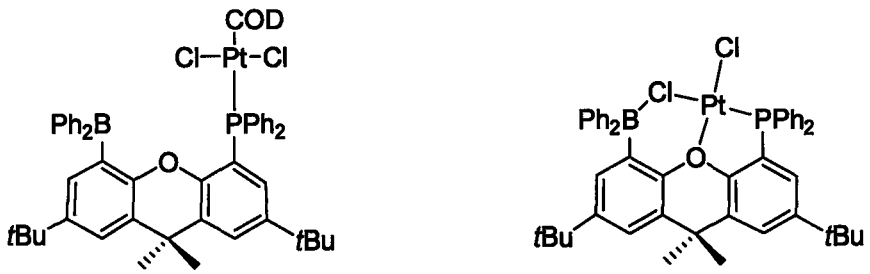

[$PtCl_2$(COD)(XPB)] (*cis* or *trans*) **[PtCl(μ-Cl)(XPB)]**

Figure 3.11: Possible Monomeric Products/Intermediate From XPB and [$PtCl_2$(COD)]

The simplest feasible product, [$PtCl_2$(COD)(XPB)], would be a direct adduct resulting from the phosphorus of XPB having displaced one of the double bonds of COD at platinum. In this case, there could be *cis* and *trans* isomers produced. Since COD is lost by platinum, as seen in the ^{1}H NMR spectrum, this is not likely to be the structure of the product, but it could be an intermediate. The final product from this initial complex would be the second proposed compound: the chelated [PtCl(μ-C)(XPB)], which is analogous to that formed with TXPB. This is, however, also unlikely based on a) vastly differing solubilities compared to TXPB complex, and b) lack of precedent for coordination of the oxygen in neutral xanthene-ligand metal complexes. If the product is in fact this proposed complex, it is not immediately obvious why such a product would be so insoluble.

The formation of insoluble metal complexes often indicates formation of a more complex structure, such as a dimer. The structures of additional possible complexes are shown in Figure 3.12.

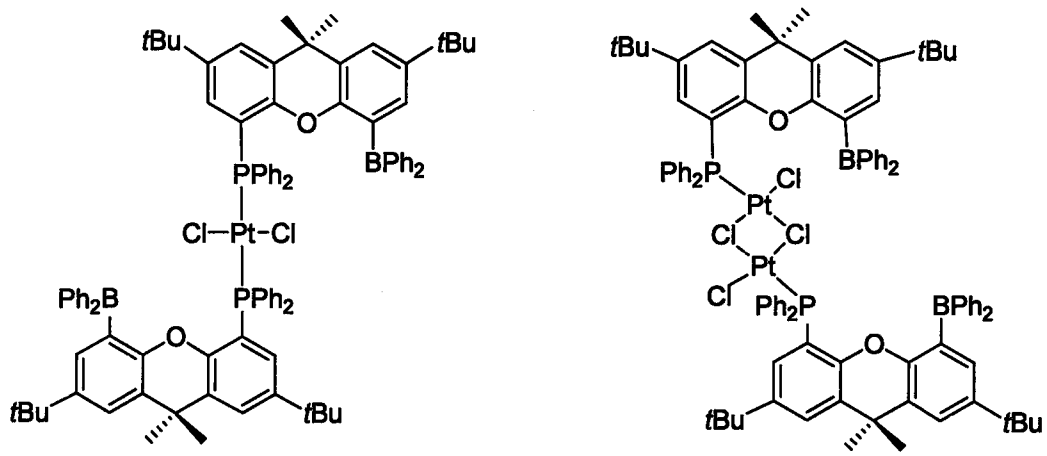

[$PtCl_2(XPB)_2$] **[{$PtCl(\mu\text{-}Cl)(XPB)\}_2$]**

Figure 3.12: Possible Bis-Phosphine Complex and Dimer Formed From XPB With [$PtCl_2$(COD)]

In the one conceivable situation, two XPB molecules would displace the cod ligand, leading to the bisphosphine complex [$PtCl_2(XPB)_2$], where chlorine ligands could potentially bridge two platinum centers though formation of a Pt_2Cl_2 core. Such a species is possible since it would achieve tetracoordination at each Pt center consistent with the displacement of a COD. However, given the 1:1 stoichiometry of this reaction and complete consumption of [$PtCl_2$(COD)], [{$PtCl(\mu\text{-}Cl)(XPB)\}_2$] is the more likely identity of the precipitate. This type of dimerisation is seen in dinuclear complexes such as [$Pt_2(PR_3)_2(\mu\text{-}Cl)_2Cl_2$], (R= Ph, Et, Me, *etc.*).[120] Such an extended coordination mode could be expected to lead to an insoluble product. While intramolecular B-Cl interactions could also occur, intermolecular B-Cl coordination would lead to further oligomerisation

and a concomitant decrease in solubility. Regardless of the exact identity, it is clear that XPB demonstrates substantially different reactivity from TXPB, suggesting an important role of the sulphur in facilitating formation of well-defined monomeric complexes. Although it is difficult to fully characterize the product of this reaction, it may be possible to functionalize it through reactions of the Pt-Cl bonds with various nucleophiles.

3.1.5 Reaction of XPB with [$PtMe_2$(COD)]

The next starting material investigated was [$PtMe_2$(COD)]. When added to the XPB ligand in stoichiometric quantities, no product was formed, as seen by ^{1}H NMR spectroscopy. It is possible that the XPB does react reversibly with [$PtMe_2$(COD)], forming the complex [$PtMe_2$(COD)(XPB)], with the cod being coordinated to the Pt by only one double bond. The cod could be dispelled completely if a second donor atom were able to form a bond as observed for TXPB through chelative assistance from the S, (Scheme 3.6). However, without participation by the oxygen in the case of XPB, the equilibrium could favour bidentate coordination of the COD ligand through the chelate effect. This lack of reactivity highlights a key difference between XPB and TXPB. Interestingly, two molecules of XPB do not displace the COD ligand either. It is also interesting to compare XPB reactivity to [$PtCl_2$(COD)] where reaction occurs readily. This difference may be due to enhanced Lewis acidity of the dichloride species and also the possibility for formation of the [Pt_2Cl_2] bridge (if this is the structure of the insoluble precipitate) allowing COD to be expelled from the coordination sphere.

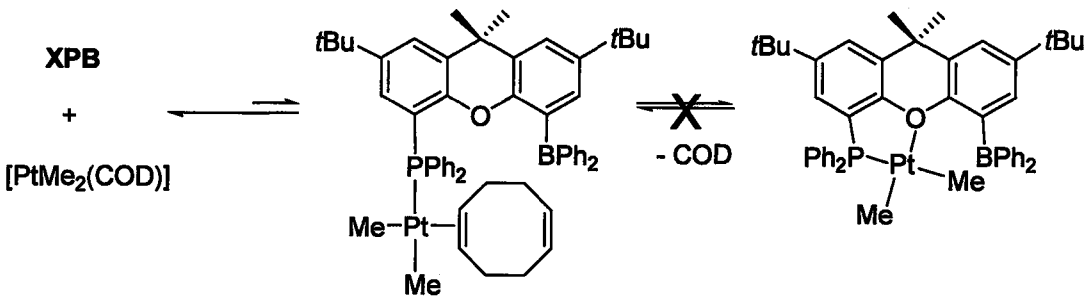

Scheme 3.6: Possible Equilibrium Reaction of XPB With [$PtMe_2$(COD)]

3.1.6 Reaction of XPB with [Pt_2(nbe)$_3$]

The XPB ligand was also reacted with [Pt(nbe)$_3$]. This reaction was observed to occur relatively cleanly, by ^{1}H NMR spectroscopy. The resulting brown solution was evaporated under high vacuum and the residue was washed with hexanes. The solid product was found to contain small amounts of nbe, as seen in the ^{1}H NMR spectrum. In contrast to the [Pt(nbe)TXPB] product, the XPB analog proved to be stable at room temperature, and also under vacuum at room temperature. The removal of nbe was attempted by evaporation under a dynamic vacuum over several days. As this had no effect, the product was held under a dynamic vacuum at 50° C over several days, but this also did not remove the remaining free nbe. Finally, the product was held under a dynamic vacuum at 70°C, but was found to decompose. Crystals of the product were grown from a solution of the complex in dichloromethane and hexanes, cooled to -30° C. Unfortunately, these crystals could not be characterized via X-ray spectroscopy due to the

crystals decomposing rapidly, presumably due to desolvation. Capillary mounting in the glove box is an option, but is not straightforward if low temperature must be maintained.

^{1}H NMR and ^{31}P NMR spectra were obtained for the purest complex synthesized, where only small amounts of free nbe were still present, (Figure 3.13).

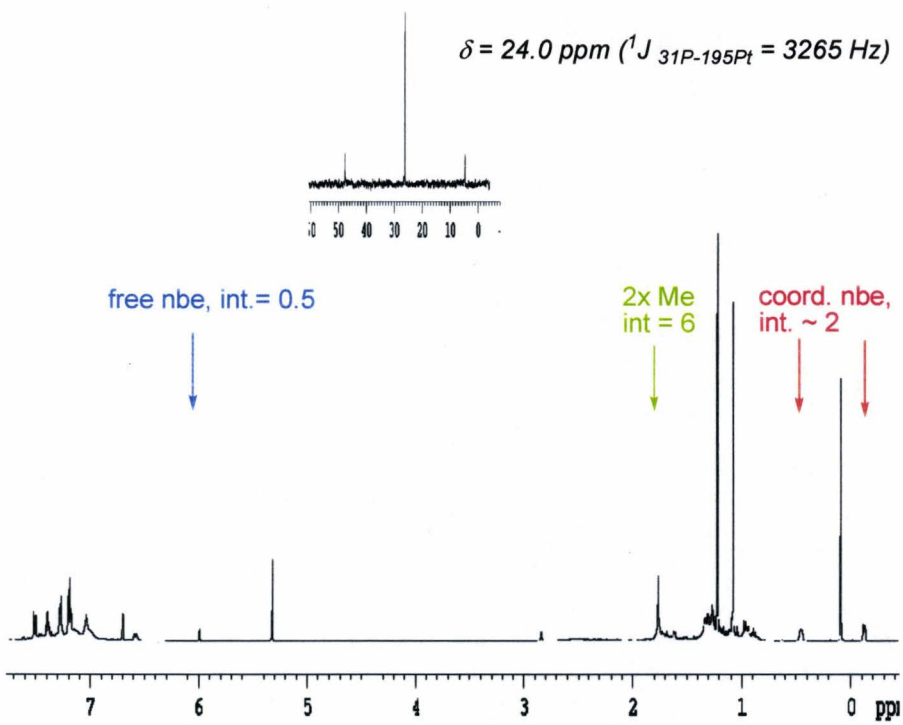

Figure 3.13: ^{1}H NMR Spectrum of [Pt(nbe)$_2$(XPB)], With ^{31}P NMR Spectrum in Inset

The ^{31}P NMR spectrum shows a peak at 24.0 ppm, with satellites of $^{1}J_{31P\text{-}195Pt}$ = 3265 Hz due to the coupling to platinum. Clearly XPB is bound directly to platinum. In order to determine how many nbe molecules remain coordinated, ^{1}H NMR can be used. Although most of the coordinated nbe signals are obscured or greatly broadened, two diagnostic peaks are readily apparent. These two peaks are both below 0.5 ppm in the spectrum and are both doublets. These protons are ascribed to those on the carbon atoms

bound directly to Pt. Relative to the backbone methyl peaks integrating to 6H, these protons each integrate to ~2H suggesting that there are two nbe and one XPB coordinated to Pt. The COSY NMR spectrum shows the two nbe signals coupling to each other, so it appears that they come from inequivalent protons on equivalent nbe molecules. The difference in the protons could arise from restricted rotation.

In summary, XPB reacts readily with [Pt(nbe)$_3$] forming [Pt(nbe)$_2$(XPB)], (Figure 3.14). Although it is possible that the oxygen atom coordinates to form square planar platinum center, it is more likely that with two nbe ligands and one bulky phosphine, platinum is sterically hindered and a 4th group cannot coordinate (as for [Pt(nbe)$_3$]).

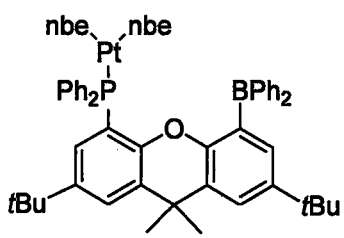

Figure 3.14: [Pt(nbe)$_2$(XPB)]

Although this Pt(0) could interact with boron since it is reasonably electron rich, it is more likely that backbonding would occur to the nbe ligands imparting some Pt(II) character to the complex. Nonetheless, this complex may turn into a valuable compound for making other XPB→Pt(0) complexes through ligand substitution reactions. More electron-rich donor ligands could conceivably promote Pt→B bond formation. It could also be used as a platform for creating XPB→Pt(II) complexes through oxidative addition reactions at the Pt(0) center facilitated by labile nbe ligands (Figure 3.15). Of course, Pt(0)→Pt(II)→Pt(0) transformations are important in a number of platinum-mediated organic reactions. The impact of the BPh$_2$ ligand in these reactions can then be assessed

relative to simpler phosphine(nbe)$_2$Pt complexes including potentially the XPH→Pt(nbe)$_2$ complex if it can be made by analogous methods. It is plausible that the Lewis acidic boron center would participate in reactivity through bridging/abstraction reactions which could not occur in the XPH derivative.

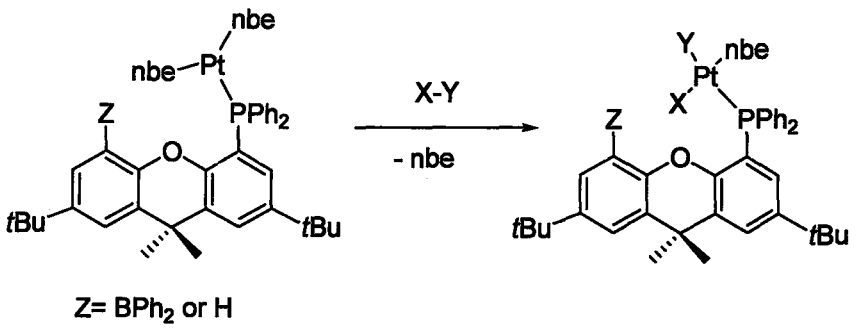

Figure 3.15: Oxidative Addition at [Pt(nbe)$_2$(XPB)] and [Pt(nbe)$_2$XPH]

3.2 Summary of XPB Coordination Chemistry

The novel XPB ligand (**3**) was synthesized as an analogue of TXPB, and reactions with $[PtCl_2(COD)]$, $[PtMe_2(COD)]$ and $[Pt(nbe)_3]$ were investigated. Although no metal-borane interaction was anticipated, the reactions would serve as an informative comparison to the TXPB complexes. Interestingly, it was found that the reaction of XPB and $[PtCl_2(COD)]$ resulted in an insoluble product, the identity of which could not be determined due to its insolubility in a variety of NMR solvents. This insolubility is a contrast to the product formed with TXPB, $[PtCl_2(TXPB)]$, which suggests the identity of this insoluble product to be a dimer or oligomer, rather than a monomer as in the TXPB situation.

Surprisingly, no reaction was observed between XPB and $[PtMe_2(COD)]$. The complex resulting from the reaction of XPB with $[Pt(nbe)_3]$, $[Pt(nbe)_2(XPB)]$ (**4**) was found to be more stable than that of the TXPB, and was isolated. The compound could not be analysed by X-ray crystallography, due to desolvation of the crystals, but was characterized using ^{1}H, ^{13}C and 2-D NMR spectroscopy and is believed to contain the XPB ligand coordinated to a $[Pt(nbe)_2]$ fragment via phosphorus.

In the characterisation of the synthesised XPB ligand and TXPB, XPB complexes, ^{11}B NMR spectroscopy was attempted to further probe the environment of the borane group in the TXPB or XPB ligand. Unfortunately, ^{11}B peaks were not observed, likely as a consequence of high molecular weights and only moderate solubility of the complexes in question, resulting in low intensity broad peaks (^{11}B I = 1). These peaks

also overlap with the broad and intense boron signal from glass in the NMR tubes and NMR probe inserts. The ^{11}B-NMR spectra of these complexes and the XPB ligand should be repeated using a boron free NMR tube and boron free probe.

Chapter 4: Towards An Extremely Rigid Phosphine/Acridine/Borane Ligand, APB

4.1 Acridines

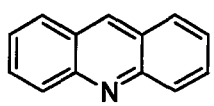

Figure 4.1: Acridine

Derivatives of acridine have long been known and investigated due to both their interesting chemical and physical properties, and because of their many useful applications. This class of compound has a variety of biological properties such as anticarcinogenic, bactericidal, antimalarial, insecticidal, antifungal and as DNA intercalating agents. Acridine derivatives are well known therapeutic agents whose mutagenic properties depend on their ability to interact with nucleic acids. Since 1888, there has been medical interest due to the discovery of antibacterial action of proflavin (Figure 4.2), and acriflavine. In 1939 the discovery of mepacrine, the first synthetic antimalarial to rival quinine in activity further accelerated the pace of investigation.[122]

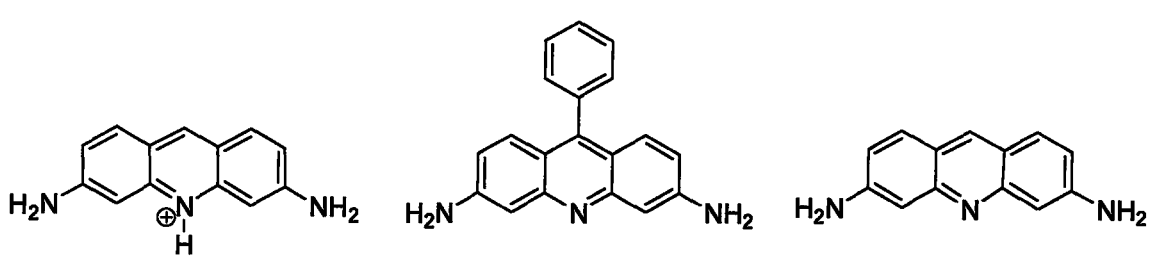

Figure 4.2 Examples of Useful Acridine-Based Compounds

Other uses for acridines include: dyes (*e.g* chrysaniline and acridine-orange, Figure 4.2), reagents for the analysis of heavy metals, fluorescent indicators for the titration of dark solutions, substances for the production of chemiluminescence, for the isolation of coenzymes, proteins, carbohydrates, and other components of interest in biochemistry, for industrial disinfection and preservation and for preventing the corrosion of metals.[122]

The study of an acridine as a ligand in catalysis was first investigated by Haenel *et al.*[123] The ligand investigated was acriphos, 4,5-bis(diphenylphosphine)acridine, the analogue of xantphos and thioxantphos (Figure 4.3).

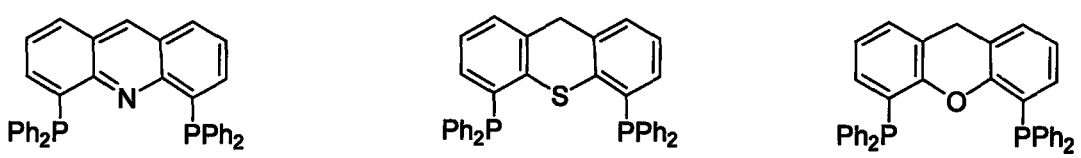

Acriphos **Thioxantphos** **Xantphos**

Figure 4.3: Structure of Acriphos and Analogues

In this system, the PNP ligand also has a rigid skeleton as seen in the oxygen and sulphur analogues, but as with thioxanthene based-ligands, it acts as a tridentate ligand. The pyridine moiety is an intermediate hard/soft group, compared to the soft thiopyran moiety, but as a very effective donor related to pyridine, it is expected to bind to late transition metals even more effectively. It also has the advantage of being much more planar than the thioxanthene backbone. By X-ray diffraction, acridine was found to have a planar skeleton, with the planes between the outer benzene rings forming an angle of 177.9°.[123]

After synthesis of the acriphos ligand, Haenel *et al.* went on to show the superior catalytic properties of this ligand with various metals such as Pd (**XVIII**), Ni (**XIX**) and Rh (**XX**) (Figure 4.4).

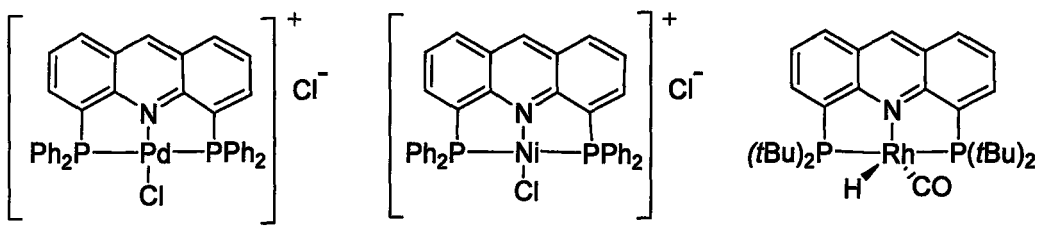

XVIII **XIX** **XX**

Figure 4.4: Examples of Acriphos Complexes

The acriphos- PdCl compound has been found to catalyze the water gas shift reaction (WGSR: $CO + H_2O \rightarrow CO_2 + H_2$) under neutral conditions. Acriphos complexes have also been reported to catalyse a wide range of other reactions such as: hydroformylation, carbonylation, carboxylation, hydrogenation, hydrocyanogenation, hydrosilylation, polymerization, isomerization, cross-couplings and metathesis.[124]

4.1.1 Established Synthetic Methods To Acridine Derivatives

Given the numerous applications of acridine derivatives, a large number of synthetic routes for forming substituted acridine compounds have been developed. There are, however, four main types of reactions which have been used to construct the acridine backbone.[122]

1) Reaction of diphenylamines with organic acids (the Bernthsen reaction)
2) Reaction of *meta*-phenylenediamines with formic acid
3) Ring-closure of diphenylamine-2-aldehydes or ketones
4) Ring-closure of diphenylamine-2-carboxylic acids

The Bernthsen reaction utilizes a Lewis acid like $ZnCl_2$ to catalyze reaction of diphenylamine with organic acids or anhydrides. In this reaction, an ortho position in each of the phenyl rings is activated sequentially to C-C bond formation *en route* to ring closure. Unfortunately, yields are not high and extended reaction times (up to 40h) and high temperatures (200-270 °C) are required.

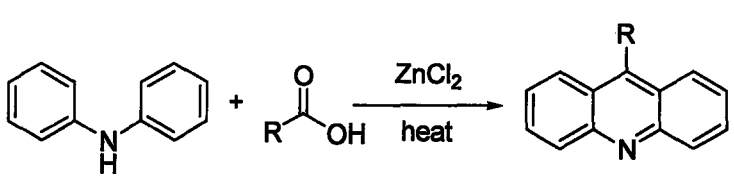

Scheme 4.1: The Bernthsen Reaction (R= Me, Et, Ph etc., route #1)

The reaction between *m*-phenylenediamine and formic acid is a useful one-step method for producing substituted acridines in good yield, and does not require oxidative or

reductive conditions. The drawback to this method is that this is a specialized type of reaction with limited application. It is mainly used in the synthesis of symmetrical acridines carrying amino groups in the 3- and 6-positions. Scheme 4.2 shows the synthesis of the symmetrically substituted compound Acridine orange.

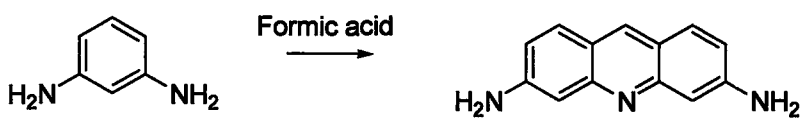

Acridine orange

Scheme 4.2: Example of Acridine Synthesis From m-phenylenediamine (Route #2)

The next two methods are facilitated by first installing carbonyl groups in the *ortho* position of one of the phenyl rings. The cyclisation of diarylamine-2-aldehydes and –ketones requires strong acids (such as trifluoroacetic acid or sulfuric acid), and/or high temperatures are used to effect ring closure,[125] (Scheme 4.3). A serious drawback to this method is the lack of a flexible synthetic route to suitably substituted precursors.[126]

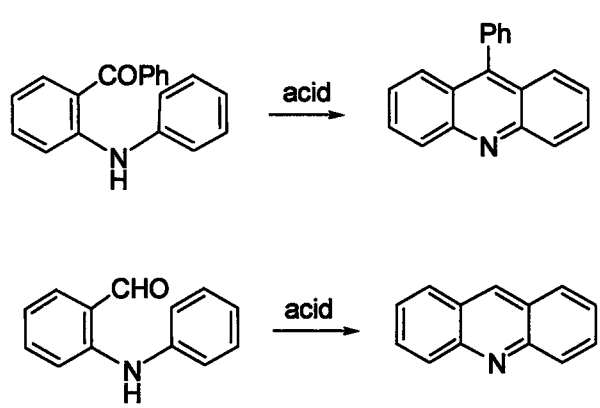

Scheme 4.3: Potential Routes for the Synthesis of Acridine from 2-keto- (top) or 2-formyl- (bottom) substituted diarylamines (Route #3)

The most common route to acridines and their derivatives is through the cyclisation of diphenylamine-2-carboxylic acids.[127] This reaction is similar to that of the diarylamine-2-aldehydes and ketones described in route #2, and also requires the use of acidic conditions for the cyclisation to the acridine. The superiority of this method, and the reason for its popularity, is the ease of formation of a wide range of diphenylamine-2-carboxylic acids. The first report for the synthesis of these types of intermediates was in 1885 by Jourdan,[128] but was later greatly improved upon by Ullmann,[129] who found that using Cu as a catalyst greatly improved coupling between compounds such as 2-chlorobenzoic acid and aniline. This allowed for the synthesis of a vast array of substituted diphenylamine-2-carboxylic acids, which in turn opened the door to the syntheses of tailor-made substituted acridines. The diphenylamine-2-carboxylic acid intermediates can be readily cyclised to the corresponding acridine using sulphuric acid or phosphoryl chloride, which is further discussed in section 4.3.2.

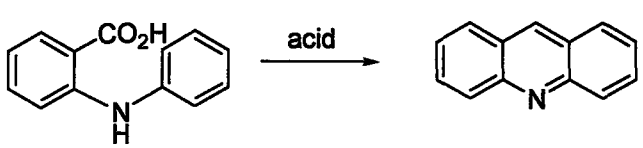

Scheme 4.4: Cyclisation of 2-anilinobenzoic acid Under Acidic Conditions, (Route #4)

4.2 Phosphine/Borane Ligands Based on Acridine

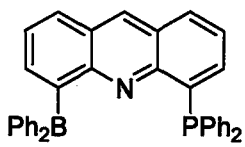

Figure 4.5: Target Ligand 4-diphenylphosphino-5-diphenylboranylacridine

The acriphos-transition metal complexes synthesized by Haenel *et al.* highlight the ability of an acridine based ligand to form extremely stable metal complexes by κ^3-coordination. In addition, the rigidity and planarity of the acridine backbone makes it a promising scaffold upon which to attach both a Lewis acid and Lewis base to synthesise the new acridine ligand 4-diphenylboryl-5-diphenylphosphinoacridine. The reactivity of this ligand with electron rich late transition metals (*e.g.* Pt(0) and Pt(II)) would then be investigated.

4.2.1 Attempted Synthesis of 4-diphenylboryl-5-diphenylphosphinoacridine

The procedure outlined below is based on the literature preparation of acriphos, but altered to allow sequential installation of phosphine and borane groups; 4-bromo-5-fluoroacridine was viewed as a more suitable precursor, since the aryl fluorides and bromides can be functionalized under different conditions.

The initial step of the synthesis is the coupling of a halogenated anthranilic acid with a halogenated iodobenzene, with the halogens being bromine and fluorine on the two starting materials .

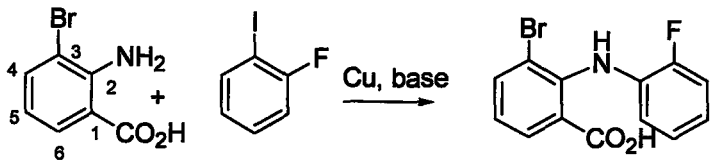

3-bromoanthranilic acid

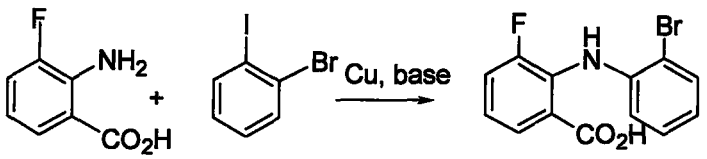

3-fluoroanthranilic acid

Scheme 4.5: Potential Synthetic Routes to 2-(2'-fluorophenylamino)-3-bromobenzoic acid

It was thought that the easiest way to synthesise this intermediate would be through the coupling of 3-bromoanthanilic acid with 1-fluoro-2-iodobenzene (Scheme 4.5). 1-Fluoro-2-iodobenzene is commercially available, but 3-bromoanthranilic acid must be synthesized. The literature preparation involves a simple bromination of anthranilic acid in acetic acid at room temperature.[130] In our hands, however, this preparation was not successful as it was found to produce 5-bromoanthranilic acid as the major product. This method was thus abandoned.

Another pair of potential starting materials is 3-fluoroanthranilic acid and 1-bromo-2-iodobenzene (Scheme 4.5). Again, the 1-bromo-2-iodobenzene is commercially available, but the 3-fluoroanthranilic acid must be synthesized.[131] The synthesis of the 3-fluoroanthranilic acid is a three step procedure as shown in Scheme 4.6.

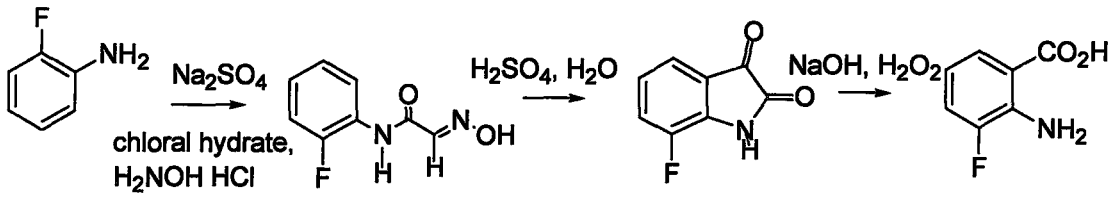

Scheme 4.6 Reported Synthesis of 3-fluoroanthranilic acid

This method was not suitable to produce the desired 3-fluoroanthranilic acid, however, due to the difficulty in obtaining the starting material chloral hydrate, a hypnotic sedative. This route was therefore also abandoned.

With the two previous routes abandoned, another path was needed. The desired product could not be made through a halogenated anthranilic acid with a halogenated iodobenzene, so the next attempt was to synthesize 2,6-dibromo-*N*-(2-fluorophenyl)benzenamine. This intermediate could then be treated with BuLi, followed by CO_2 (after N-protection, if required) to form the precursor 2-(2'-fluorophenylamino)-3-bromobenzoic acid (Scheme 4.7).

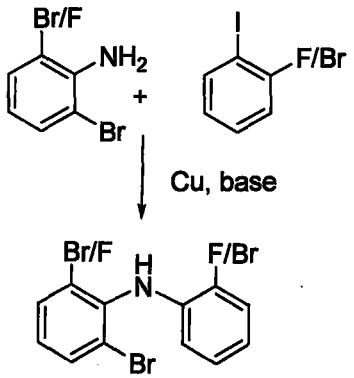

2,6-dibromo-N-(2'-fluorophenyl)benzenamine or
6-bromo-2-fluoro-N-(2'-bromophenyl)benzenamine

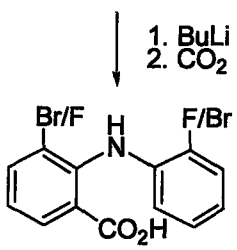

2-(2'-fluorophenylamino)-3-bromobenzoic acid or
2-(2'-bromophenylamino)-3-fluorobenzoic acid

Scheme 4.7: Potential Routes for the Synthesis of 2-(2'-fluorophenylamino)-3-bromobenzoic acid

The coupling of 2,6-dibromoaniline and 1-fluoro-2-iodobenzene, both commercially available, was first attempted. This was done via the Ullmann Cu-catalyzed coupling of amines with aryl halides.

There are a variety of different conditions available for the Ullmann condensation in the literature, each employing different solvents, catalysts and conditions.[129] For the coupling to be successful, the reaction requires a source of Cu, which can be in the form of Cu(0), Cu(I), or a mixture of the two. Secondly, a base is needed, and the two most commonly used are *N*-methyl morpholine or K_2CO_3. A suitable solvent, such as

propylene glycol or cyclohexanol must also be employed. In addition, the temperature at which the mixture is heated is important, as well as the length of duration of the reaction.

Condensation of 2,6-dibromoaniline and 1-fluoro-2-iodobenzene was first attempted using the Cu-catalyzed Ullmann reaction. Many combinations of the bases, solvents and catalysts were investigated at temperatures of 95-160°, stirred under N_2 for 3-5 days, but they were found to be ineffectual. Under most conditions, it was found that very little reaction, if at all, occurred. It was discovered that using K_2CO_3 as the base, CuI as the catalyst and cyclohexanol as the solvent produced the most reaction, but unfortunately many products formed, as seen in the ^{19}F NMR spectrum. Column chromatography was performed on the mixture of products, but the desired product could not be purified, so this method was abandoned.

Next, the same coupling was attempted using Hartwig-Buchwald palladium catalysis. Hartwig-Buchwald cross coupling is the palladium-catalyzed synthesis of aryl amines where the starting materials are aryl halides or pseudohalides (for example triflates) and primary or secondary amines.[132] Key features of this reaction include a palladium catalyst, an external base and high temperatures (Scheme 3.8, R = alkyl, CN, COR, ...; R' = alkyl, aryl).

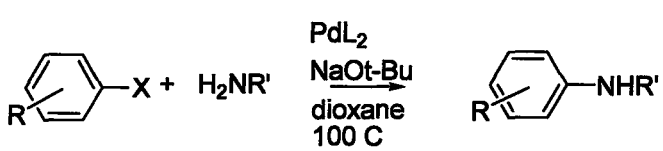

Scheme 4.8: Hartwig-Buchwald Pd Catalysed Cross-coupling for the Synthesis of Aryl Amines

The reaction is improved greatly by the use of a wide bite phosphine ligand, such as DPPF (diphenylphosphinoferrocene). A 1:3 mixture of $[Pd_2(dba)_3]$ and DPPF as the catalyst (1% mol of Pd), NaO*t*Bu was the base, and THF was used as the solvent. The mixture with 2,6-dibromoaniline and 1-fluoro-2-iodobenzene was allowed to reflux overnight at 80°C under an inert Ar atmosphere. This reaction was attempted several times, but no product was formed. It is possible that the coupling did not work due to low aniline basicity and steric hindrance as a result of the electron withdrawing bromo substituents in the 2- and 6-positions.

4.2.2 Design of a new Phosphine/Acridine/Borane ligand

The failure of the coupling of the previous starting compound resulted in a need for new starting material to be chosen. Returning to the original strategy, the coupling of 3-bromoanthanilic acid with 4-fluoro-3-iodobenzene seemed to be the most straight forward. The previously discussed synthesis of 3-bromoanthranilic acid from anthranilic acid in Section 4.2.1 was not feasible due to preferential bromination at the 5-position. To overcome this problem, the 5-position could be blocked, leaving only the 3-position available for bromination. To this end, 5-methylanthranilic acid was chosen as the precursor to the new starting material. The corresponding aryl halide would be 2-fluoro-1-iodo-4-methylbenzene, which would also need to be synthesized. These starting materials would be coupled using Ullmann condensation to produce (6-bromo-2-carboxy-4-methylphenyl)-(2-fluoro-4-methylphenyl)amine (**6**, Scheme 4.10).

4.2.3 Synthesis of the Intermediate 3-fluoro-4-iodotoluene (5)

The amine component, 2-amino-3-bromo-5-methylbenzoic acid, was synthesized according to the literature.[133] The starting material 2-fluoro-1-iodo-4-methylbenzene, had been previously reported, but with a resulting yield of only 44%.[134] Work done by Buchwald,[135] involving the use of the Finkelstein reaction to convert unrelated aryl bromides into the corresponding iodides, with yields of up to 99%, appeared to hold promise as a superior route to product.

The Finkelstein reaction is the halogen exchange between a primary *alkyl* halide or pseudohalide and an alkali metal halide, (*e.g.* NaI, KCl, KI). Halide exchange is an equilibrium reaction, but the reaction can be driven to completion by taking advantage of differential solubility of halide salts. Consequently, a suitable solvent must be chosen in which the starting salt, NaI is sufficiently soluble, and in which the final salt, NaBr, is not. The Buchwald method for the conversion of an aryl bromide into the corresponding aryl iodide uses a catalyst system of 5 mol % of CuI, 2 equiv of NaI , and 10 mol % of *trans-N,N'*-dimethyl-1,2-cyclohexanediamine, which forms the active catalyst when complexed with Cu, in dioxane. Unfortunately, this 1,2-diamine is not commercially available, and is prepared from expensive precursors. Therefore, a different amine was investigated. It was found that a ligand briefly mentioned by Buchwald, *N,N'*-dimethylethylenediamine, satisfactorily catalysed the conversion of 4-bromo-3-fluorotoluene to 3-fluoro-4-iodotoluene in good yield. A mixture of CuI, 3-bromo-4-fluorotoluene, and NaI in dioxane, heated at 110° C for 3 days produced 3-bromo-4-

iodotoluene (**5**) as a colourless liquid in 86% yield after filtration of a hexane solution though silica, (Scheme 4.9).

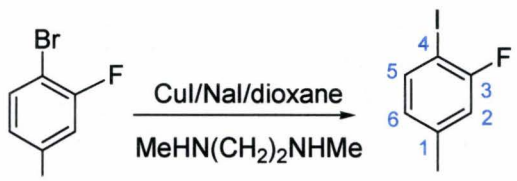

5, 86 %

Scheme 4.9: Synthesis of 5

4.2.4 Synthesis of the Intermediate 2-(2'-fluoro-4'-methylphenylamino)-3-bromo-5-methylbenzoic acid (6)

With the two starting materials synthesized, subsequent coupling via Ullmann condensation could be undertaken. It was found that that the best conditions for the coupling were using Cu-bronze as the catalyst, K_2CO_3 as the base, and cyclohexanol as the solvent, and this mixture was refluxed under N_2 for 3 days. Once the reaction was completed, the mixture was steam distilled to remove the cyclohexanol, neutralized with dilute HCl to precipitate the product which was collected by filtration, washed with H_2O, evaporated to dryness, and then sublimed. This gave 2-(2'-fluoro-4'-methylphenylamino)-3-bromo-5-methylbenzoic acid (**6**) in 48% yield as a light yellow powder (Scheme 4.10).

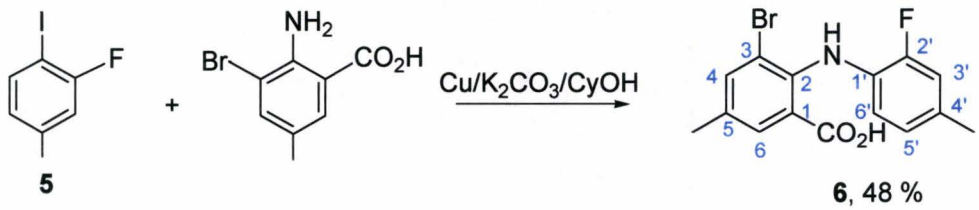

Scheme 4.10: Route for Synthesis of 6

The ^{1}H NMR and ^{19}F NMR spectra of **6** are shown in Figure 4.6. The ^{1}H spectrum is as would be expected, with two separate methyl peaks in the alkyl region, and 5 different signals in the aryl region. The ^{19}F NMR spectrum shows a single peak at -131.0 ppm, compared to -94.6 ppm for the 3-fluoro-4-iodotoluene starting material.

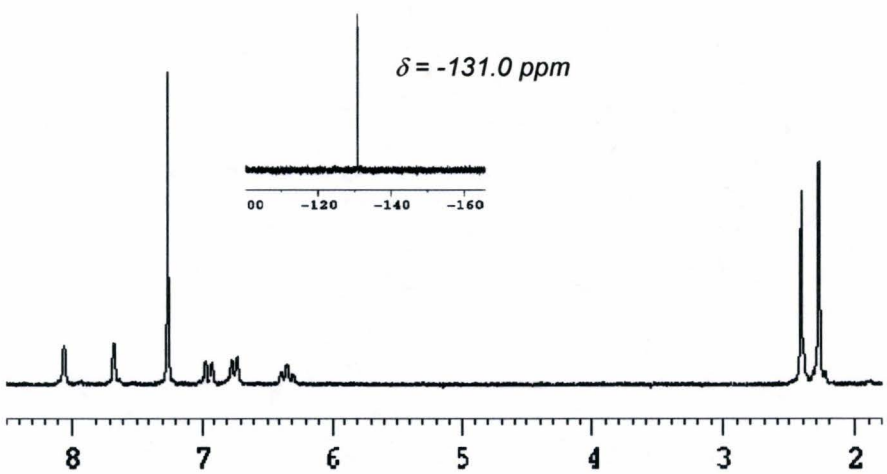

Figure 4.6: ^{1}H NMR Spectrum of 6, With ^{19}F Spectrum in Inset

4.2.5 Synthesis of the Intermediate 4-bromo-9-chloro-5-fluoro-2,7-dimethyl-Acridine (7)

The cyclisation of diphenylamine-2-carboxylic acid to an acridone was first performed by Jourdan, who used sulphuric acid, and Ullmann later demonstrated the

generality of the method.[129] Losses in yields can occur through sulphonation, particularly when electron-releasing substituents, *e.g.* amino-and hydroxyl-groups are present. It was first reported in 1922 that phosphorus oxychloride could effect ring-closure giving acridones. Several years later it was shown that the resulting acridones are readily converted to 9-chloroacridines by refluxing with $POCl_3$, and that diphenylamine-2-carboxylic acids gave quantitative yields of the corresponding 9-chloroacridines when refluxed with phosphoryl chloride for a short time. [136]

6 was cyclised to form 4-bromo-9-chloro-5-fluoro-2,7-dimethylacridine (**7**) by refluxing in excess neat $POCl_3$. It was found that the $POCl_3$ must be freshly distilled prior to use, otherwise the yield of the product is greatly reduced. After refluxing for 3 hrs, the excess $POCl_3$ is distilled away, and then the resulting viscous liquid is added drop wise to a rapidly stirred mixture of ice and NH_4OH.

The workup procedure is necessary as 9-chloroacridines undergoes relatively facile acid hydrolysis back to the corresponding acridone. The product is extracted with $CHCl_3$, evacuated to dryness, then sublimed to produce to produce **7** in 75% yield as a yellow powder (Scheme 4.11).

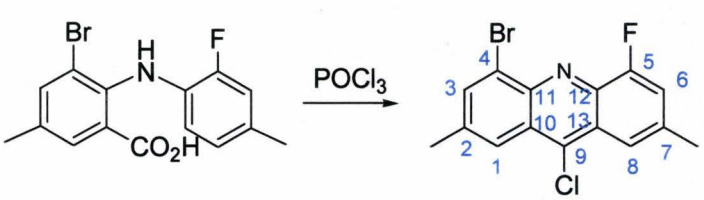

6 **7**, 75 %

Scheme 4.11 Cyclisation to Form 7

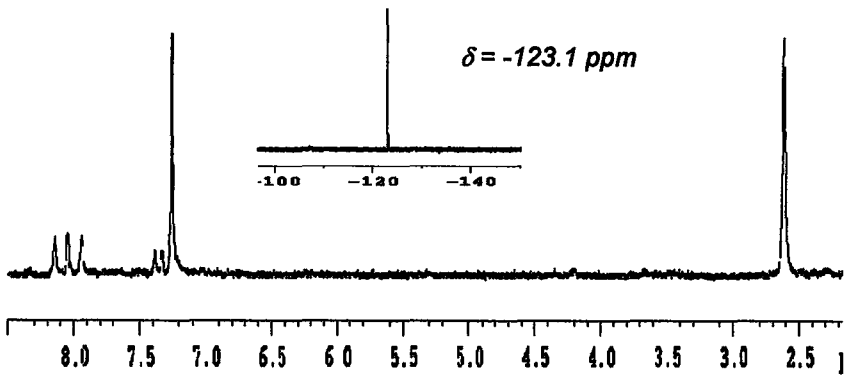

Figure 4.7: ^{1}H NMR Spectrum of 7, With ^{19}F Spectrum in Inset

The ^{1}H NMR and ^{19}F NMR spectra of 7 are shown in Figure 4.7. The ^{1}H NMR spectrum is again, as expected. There are two overlapping methyl peaks 2.6 ppm, and four signals in the aryl region corresponding to the four protons on the acridine backbone. The peak in the ^{19}F spectrum appears at -123.1 ppm.

4.2.6 Synthesis of the Intermediate 4-bromo-5-fluoro-2,7-dimethylacridine (9)

9-Chloro acridine is very susceptible to nucleophilic attack at the 9-position, so the chlorine atom at this position must be substituted. 9-Chloroacridines were discovered to be susceptible to dechlorination by hydrogenation over Raney nickel in the presence of potassium hydroxide.[137] The products of these dehalogenations are acridans, because dehalogenation occurs simultaneously with reduction, but these acridans are readily oxidized by various methods back to acridines. This kind of reductive condition, however, is not suitable for easily reducible substituents, such as bromide and fluoride.

Another method to dehalogenate of 9-chloroacridines is through the use of tosyl hydrazide and a base.[138] This method has the advantage of avoiding strongly reductive conditions. The dehalogenation reaction is based on the discovery that 1-phenyl-2-benzenesulphonylhydrazine is converted to benzene, nitrogen, and a sodium benzenesulphinate under alkali conditions. The mechanism for this reaction is likely to involve the alkali first removing a proton from the hydrazine, releasing the benzenesulphinyl anion and leaving the unstable diazene, which then proceeds to lose nitrogen, leaving benzene as the product.[139] Analogously, it was found that para-toluenesulfonic hydrazide can be used to replace the chlorine at the 9-position of acridine with a hydrazine group, which can then be cleaved using sodium hydroxide, leaving the 9-position H-substituted.[140] This method was used by Haenel [124] to prepare 4,5-dibromoacridine and 4,5-difluoroacridine, and subsequently by us in our preparation of 4-bromo-5-fluoro-2,7-dimethylacridine (**9**, Scheme 4.12).

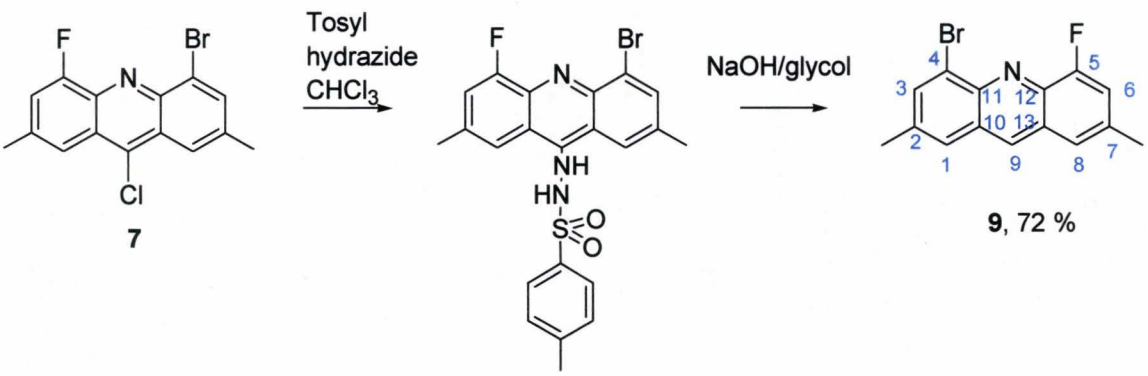

Scheme 4.12: Dehalogenation Followed by Protonation of 9-chloroacridine to Form 9

The intermediate, 9-(*p*-toluenesulfonylhydrazide)-4,5-difluoroacridinium hydrochloride (**8**), was synthesized from **7** by stirring in a suspension of *p*-toluenesulfonic hydrazide in anhydrous chloroform at 50 °C for 3 days. This produced the yellow solid **8** with a 70 % yield. This hydrazide compound was subsequently suspended in a mixture of ethylene glycol and aqueous sodium hydroxide, and the mixture was refluxed for 3 hrs. This produced a yellow solid, 4-bromo-5-fluoro-2,7-dimethylacridine (**9**) with a yield of 72 %.

The ^{1}H NMR and ^{19}F NMR spectra of **9** are shown in Figure 4.8. The ^{1}H NMR spectrum indicates a single peak for the two methyl groups, and 5 separate proton signals in the aryl region. The proton closest to the F, at position 6, is a doublet, whereas the others appear as singlets. In the ^{19}F NMR spectrum, the peak appears at – 124.7 ppm.

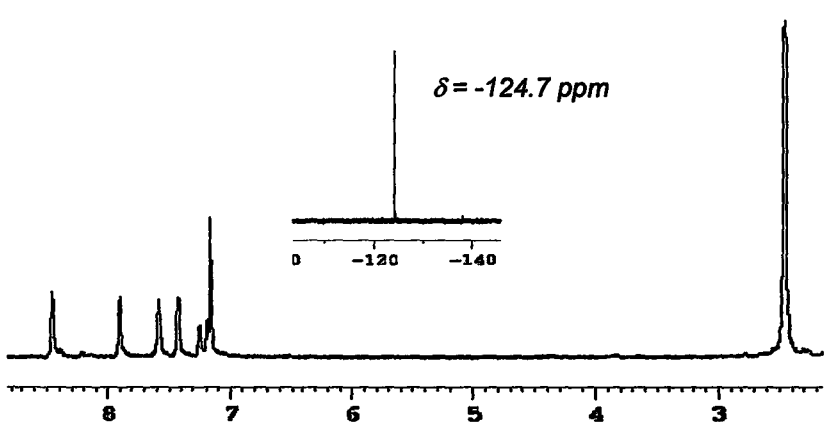

Figure 4.8: ^{1}H NMR Spectrum of 9, With ^{19}F NMR Spectrum in Inset

Attempts were made to substitute an alkyl group at the 9-position in order to synthesise a more stable acridine derivative with this sensitive position protected. The acridine was treated with isopropyl Grignard reagent in order to replace the chlorine with an isopropyl group. It was found that rather than attacking at the 9 position, the 4-bromo

substituent was substituted with a MgX unit instead, which is unusual but known to occur.[141] Another potential route to 9-alkyl acridine involves the substitution of the 9-chloro substituent using diethyl malonate followed by conversion to a methyl group by treatment with HCl.[142] This also did not produce the desired product, and by ^{1}H NMR, it is believed that the 9-chloroacridine was hydrolysed under the conditions needed for the reaction.

4.2.7 Attempted Synthesis of the Intermediate 4-diphenylphosphinyl-5-fluoro-2,7-dimethylacridine

With the ligand backbone formed, the halogen moieties are then ready to be substituted to install the Lewis base and Lewis acid groups. Substitution of the fluorine group was attempted via *ipso*-substitution using potassium diphenylphosphide. According to the Haenel procedure,[124] 4,5-difluoroacridine was converted into 4,5-bis(diphenylphosphino)acridine in 79% yield after addition of $KPPh_2$ (2 equivalents) and refluxing for one hour in THF. However, reaction of **9** with $KPPh_2$ in THF gave a bright green solution which turned brown upon heating. ^{1}H and ^{31}P NMR spectra of the reaction mixture both before and after heating showed a complex mixture of products. The reaction was also attempted at room temperature, and also at -15° C followed by warming to room temperature. It was found that even at lower temperatures, a complex mixture of products resulted.

It was decided that finding appropriate conditions for the installation of the phosphine group could require a lengthy survey of reaction conditions, reagents and perhaps the preparation an analogue of **9** bearing alternative substituents in the 7- and 9-positions. Therefore, due to the restriction of time, it was considered best to leave the ligand synthesis of the acridine ligand (APB) at this stage, and to direct the focus towards the transition metal chemistry of 2,7-di-(*tert*-butyl)-4-diphenylboryl-5-diphenylphosphino-9,9-dimethylthioxanthene (TXPB, chapter 2), which had recently been prepared by other members of the Emslie group, and synthesis of the as-yet unknown oxygen analogue of this ligand 2,7-di-(*tert*-butyl)-4-diphenylboryl-5-diphenylphosphino-9,9-dimethylxanthene (XPB, chapter 3).

4.3 Conclusions on Acridine Work

In summary, an acridine derivative with a fluoro and a bromo substituent ideally positioned for substitution by PPh_2 and BPh_2 groups has been prepared. Optimization of the steps required to make this acridine will allow larger quantities of material to be procured using the procedure described above. With larger amounts of material, attempts to selectively carry out the sensitive substitution reactions in high yield will be greatly facilitated. Hence, a phosphorus-nitrogen-boron ligand based on the acridine backbone is still a very realistic target which is expected to provide an important comparison to the phosphorus-oxygen-boron and phosphorus-sulphur-boron ligands based on xanthene and thioxanthene. The greater rigidity, larger binding pocket, and potentially decreased

lability of APB, relative to the thiopyran analogue (TXPB), may also render APB more suitable for cooperative intramolecular activation of functionalized organic substrates between a borane and a late transition metal.

Chapter 5: Experimental

General Procedures

All air-sensitive operations were performed under a purified argon or nitrogen atmosphere using glovebox or vacuum line techniques. *n*-butyl lithium solution (1.6 M in hexane), *tert*-butyllithium solution (1.7 M in pentane), TMEDA, 4-bromo-3-fluoro toluene, CuI, NaI, 1,4-dioxane, *N,N'*-dimethylethylenediamine, 5-methyl anthranilic acid, Cu (bronze), K_2CO_3, cyclohexanol, $POCl_3$, p-toluenesulfonic hydrazide, ethylene glycol, Ph_2PCl, and $[PtCl_2(COD)]$, $[Pt(acac)_2]$, COD, BCl_3, Ph_2SnMe_2, xanthone, thioxanthone, Br_2, Fe, $AlMe_3$, 2-chloro-2-methylpropane, $AlCl_3$, nbe, Li and COT were purchased from Aldrich. Ph_2PCl and Ph_2SnMe_2 were both distilled as a colourless oil and TMEDA was also distilled from sodium prior to use and stored under argon. Ph_2SnMe_2, COD and COT were dried over molecular sieves, distilled and stored under Ar. Toluene was distilled from sodium. Hexanes, DCE, CH_2Cl_2, and acetonitrile were distilled from CaH_2. Diethyl ether, THF and toluene were stored over Ph_2CO/Na and distilled prior to use. Deuterated solvents were purchased from ACP-chemicals, and CD_2Cl_2 and $CDCl_3$ were stored over molecular sieves and distilled prior to use. $[PtMe_2(COD)]$[142] and $[Pt(nbe)_3]$[143] were prepared as previously reported. Ph_2BCl was prepared as a colourless oil according to the literature procedure.[144] NMR spectra of $[PtCl_2(TXPB)]$, $[PtMe_2(TXPB)]$, XPB, $[PtCl_2(XPB)]$, $[PtMe_2(XPB)]$ and [Pt(nbe)(XPB)] were performed in dry, oxygen-free CD_2Cl_2. ^1H, $^{13}C\{1H\}$, ^{19}F, DEPT-135, ^{11}B, ^{31}P, COSY, HSQC and HMBC NMR spectroscopy experiments were performed on a Bruker AV-600 spectrometer, an AV-200

spectrometer was used for ^{19}F and ^{31}P NMR spectroscopy, and a DRX-500 spectrometer was used for VT NMR spectroscopy. Data are given in ppm relative to $SiMe_4$ for ^{1}H and ^{13}C NMR spectra, $BF_3(OEt_2)$ for ^{11}B NMR spectra, and 85 % H_3PO_4 in D_2O for ^{31}P NMR spectra. All ^{1}H and ^{13}C NMR spectra were referenced to $SiMe_4$ through the resonance of the employed deuterated solvent or protio impurity of the employed solvent; $CDCl_3$ (δ = 7.24 ppm), CD_2Cl_2 (δ = 5.32 ppm) for ^{1}H NMR and $CDCl_3$ (δ = 77.23 ppm) or CD_2Cl_2 (δ = 54.00 ppm) for ^{13}C NMR. ^{11}B and ^{31}P NMR spectra were referenced using an external standard of $BF_3(OEt_2)$ (0.0 ppm) and 85 % H_3PO_4 in D_2O (0.0 ppm) respectively. High resolution mass spectra were performed by Tadek Olech of this department on a Micromass GCT mass spectrometer in EI+ mode. X-ray crystallographic analyses were performed on suitable crystals coated in Paratone oil and mounted on a P4 diffractometer with a Bruker Mo rotating-anode generator and a SMART-1K CCD detector in the McMaster Analytical X-Ray (MAX) Diffraction Facility. Elemental analyses were not obtained for the compounds in this thesis due to problems with the elemental analyzer, which lasted for the duration of this thesis work.

2,7-di(*tert*-butyl)-9,9-dimethyl-4-diphenylboryl-5-diphenylphosphinothioxanthene dichloroplatinum(II) [PtCl(μ-Cl)(TXPB)] (1)

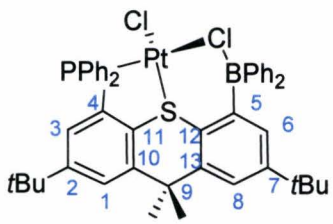

100 mg (0.15 mmol) of 2,7-di-(*tert*-butyl)-9,9-dimethyl-4-diphenylboryl-5-diphenylphosphinothioxanthene and 55 mg (0.15 mmol) of $[PtCl_2(COD)]$ were dissolved in CH_2Cl_2. The solution was then stirred at room temperature for 30 minutes. A yellow solid was produced following removal of the solvent in *vacuo*. The solid was then sonicated with 10ml hexanes, filtered and dried in *vacuo* to leave a lime green solid, yield: 78 mg, 59 %. Crystals of **$[PtCl_2(TXPB)]$•**DCE were obtained from a solution in DCE by slow diffusion of hexanes at -30° C. **^{1}H NMR (600.13 MHz, CD_2Cl_2)** : δ = 7.83 (s, 1H, C*H*^{1}), 7.77 (m, 1H, Ph), 7.63-7.59 (broad m, 1H, Ph), 7.60 (m, 1H, C*H*^{8}), 7.57-7.48 (m, 3H, Ph), 7.38-7.12 (m, 15 H, Ph), 7.25 (d, $J_{H\text{-}P}$= 11 Hz, 1H, C*H*^{3}), 7.13 (s, 1H, C*H*^{6}), 2.17, 1.55 (broad s, 2x 3H, C^9*Me*$_2$), 1.25 (s, 9H, C^{2}C*Me*$_3$), 1.17 (s, 9H, C^{7}C*Me*$_3$). **^{13}C{^{1}H} NMR: (150.9 MHz, CD_2Cl_2):** δ = 155.05 (s, *C*^{2}CMe$_3$), 151.58, 149.43 (broad s, *C*^{5} & *ipso*-B*Ph*$_2$), 151.01 (s, *C*^{7}CMe$_3$), 150.50 (s, *C*^{12}), 145.84 (d, $J_{C\text{-}P}$ = 12 Hz, *C*^{10}), 140.96 (s, *C*^{13}), 137.86 (s, *C*^{11}), 135.9 (s), 135.2(s), 134.6(s), 134.1(s), 133.0(s), 132.9(s), 129.2(s), 127.5(s), 127.4(s), 126.7(s, 12 x Ph), 133.97 (s, *C*H^6), 131.65 (d, $J_{C\text{-}P}$ = 66 Hz, *C*^{4}), 129.21 (s, *C*H^3), 127.11 (s, *C*H^1), 121.17 (s, *C*H^8), 43.03 (s, C^9*Me*$_2$), 35.64 (s,

C^2CMe_3), 35.28 (s, C^7CMe_3), 31.68 (s, C^7CMe_3), 31.42 (s, C^2CMe_3), 28.36, 26.19 (s, C^9Me_2). **$^{31}P\{^1H\}$ NMR (80.0 MHz, CD_2Cl_2)** : δ = 32.4 (s, $J_{P\text{-}Pt}$ = 3880 Hz)

2,7-di-(tert-butyl)-9,9-dimethyl-4-(methylphenylboryl)-(5-diphenylphosphino)-thioxanthene phenylmethylplatinum(II) [PtPhMe(TXPB^{Me,Ph})], (2)

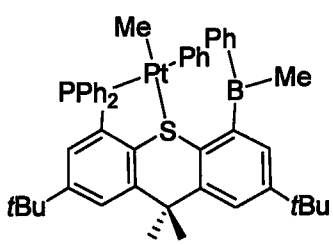

100 mg (0.15mmol) of 2,7-di-(*tert*-butyl)-9,9-dimethyl-4-diphenylboryl-5-diphenylphosphinothioxanthene and 49 mg (0.15 mmol) of [PMe_2(COD)] were dissolved in CH_2Cl_2. The solution was then stirred at room temperature for one hour. A yellow solid was produced following removal of the solvent. The solid was sonicated with 10ml hexanes, then filtered and dried, leaving an off-white solid, 90 mg, 60% yield. Crystals of the product were grown from DCE/hexanes at -30° C. **^1H NMR (600.13 MHz, CD_2Cl_2)** : δ = 7.81 (s, 1H, CH^1), 7.67 (s, 1H, CH^8), 7.46 – 7.40 (m, 6H, *ortho*-PPh_2 and *para*-PPh_2), 7.46-7.34 (m, 4H, BPh/PtPh), 7.40 (s, 1H, CH^3), 7.37 (app. t, $J_{H\text{-}H}$= 7.2 Hz, 4H, *meta*-PPh_2), 6.94-6.82 (m, 6H, BPh/PtPh), 6.91 (s, 1H, CH^6), 2.03 (broad s, 6H, C^9Me_2), 1.29 (s, 9H, C^2CMe_3), 1.26 (s, 9H, C^7CMe_3), 0.51 (d, $J_{H\text{-}Pt}$ = 83.3 Hz, $J_{H\text{-}P}$ =

5.68,1H, Pt*Me*), -0.46 (broad s, 1H, B*Me*). **$^{13}C\{^1H\}$ NMR: (150.9 MHz, CD_2Cl_2):** δ = 153.05 (s, C^2CMe_3), 150.17 (s, C^7CMe_3), 146.88 (d, $J_{C\text{-}P}$= 11.3 Hz, C^{10}), 144.36 (s, C^{13}), 141.00 (d, $J_{C\text{-}P}$ = 30.0 Hz, C^{11}), 136.98 (broad s, *Ph*), 133.90 (d, $J_{C\text{-}P}$ = 10.4 Hz, *ortho*-PPh_2), 133.16 (d, *J*= 50 Hz, C^4 or *ipso*-PPh_2), 130.86 (s, *para*-PPh_2), 130.71 (s, C^{12}), 129.64 (s, C^3), 128.91 (d, $J_{C\text{-}P}$=10 Hz, *m*-PPh_2), 128.01 (broad s, *Ph*), 126.62 (s, C^6), 125.95 (s, C^1), 122.30 (s, C^8), 43.71 (s, C^9Me_2), 35.51 (s, C^2CMe_3), 35.29 (s, C^7CMe_3), 31.68 (s, C^7CMe_3), 31.60 (s, C^2Me_3), 26.21 (s, C^9Me_2), 14.47 (s, PtMe), 13.06 (broad s, *B*Me), **$^{31}P\{1H\}$ NMR (80.0 MHz, CD_2Cl_2)** : δ = 54.5 (s, $J_{P\text{-}Pt}$= 2285 Hz)

2,7-di-(*tert*-butyl)-4-bromo-5-diphenylphosphino-9,9-dimethylxanthene (XPBr)

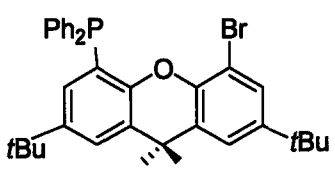

XPBr

2.0 g (4.2 mmol) of 2,7-di-(*tert*-butyl)-4,5-dibromo-9,9-dimethylxanthene was dissolved in 25 ml of THF, and the solution was cooled to -78 ° C. Following the drop wise addition of 2.6 ml (4.4 mmol) of *t*Buli, the solution changed from colourless to a pale yellow, and was allowed to warm to -15° C slowly over approximately three hours. The solution was again cooled to -78° C, and 0.78ml (4.4 mmol) of $ClPh_2B$ was added, turning the solution a paler yellow colour. After slowly warming to room temperature overnight, the LiCl salt was filtered off, and the solvent was removed *in vacuo*. The

remaining solid was then washed with 10ml of hexanes, cooled to -78° C, then filtered to give 1.5g of a white powder (75 % yield). By ^{1}H NMR, the product is approximately 98 % pure, with 2,7-di-(*tert*-butyl)-4,5-dibromo-9,9-dimethylxanthene starting material as the impurity. Subsequent recrystallisation from a variety of solvents did not yield a purer product. ^{1}H-NMR data for this compound in $CDCl_3$ match the literature.[145]

2,7-di(*tert*-butyl)xanthene-9,9- dimethyl-4-diphenylboryl-5-diphenylphosphino-xanthene (XPB) (3)

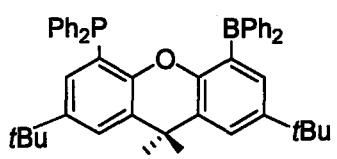

1.0g (1.75mmol) of 2,7-di(*tert*-butyl) -9,9-dimethyl-4-bromo -5-diphenylphosphino-xanthene was dissolved in 20 ml of EtO_2, and the solution was then cooled to -78 °C. The solution changed from colourless to dark yellow upon the drop wise addition of 2 ml (3.38 mmol) of *t*BuLi, and was allowed to warm to -10° C slowly over approximately three hours. The solution was again cooled to -78° C, and 0.340 mg (1.71 mmol) of $ClPh_2B$ was added, turning the solution a paler yellow. After slowly warming to room temperature overnight, the LiCl salt was filtered off and the solvent was removed, leaving a light yellow oily solid. The precipitate was dissolved in 10ml of MeCN and stirred for 1hr to form the solid MeCN adduct. The resulting slurry was cooled to -30° C and filtered to collect a white solid which was dried in vacuo to give 650mg of MeCN-free product

(65% yield). **^{1}H NMR (600.13 MHz, CD_2Cl_2)** : δ = 7.54 (dd, J_{H-H} = 27.9 Hz, J_{H-P} = 1.11 Hz, 4H, *meta*-Ph_2,) 7.51 (d, J_{H-H} = 2.47 Hz, 1H, C*H*^{1}), 7.48 (m, 2H, *para*-Ph_2), 7.39 (d, J_{H-H} = 2.47 Hz, 1H, C*H*^{8}), 7.35 (m, 4H, *ortho*-B*Ph*$_2$), 7.14 (m, 2H, *para*-Ph_2), 7.09 (m, 4H, *ortho*-P*Ph*$_2$), 6.96 (m, 4H, *meta*-Ph_2), 6.944 (d, J_{H-H} = 2.35 Hz, 1H, C*H*^{6}), 6.65 (dd, J_{H-H} = 4.32 Hz, J_{H-P} = 2.22 Hz, 1H, C*H*^{3}), 1.32 (s, 6H, C^9*Me*$_2$), 1.28 (s, 9H, *C*^{7}C*Me*$_3$), 1.12 (s, 9H, C^{2}C*Me*$_3$). **^{13}C{^{1}H} NMR (150.9 MHz, CD_2Cl_2)** : δ = 151.0 (s, *C*^{4}), 145.9 (s, *C*^{7}CMe$_3$), 145.5 (s, *C*^{2}CMe$_3$), 139.4 (s, *meta*-B*PPh*$_2$), 138.1 (d, J_{C-P} = 15.5 Hz, *C*^{11}), 134.5 (d, J_{C-P} = 19.9 Hz, *meta-PPh*$_2$), 132.1(s, *para-BPh*$_2$), 130.0 (s, *C*^{6}), 129.6 (s, *C*^{13}), 129.4 (s, *C*^{3}), 129.2 (s, *C*^{9}), 129.0 (s, *para*- PPh_2), 128.89 (d, J_{C-P}= 6.6 Hz, *ortho*-PPh_2), 128.0 (s, *ortho*-B*Ph*$_2$), 125.0 (br. s, *C*^{10}), 124.3 (s, *C*^{1}), 123.9(s, *C*^{8}), 35.459 (s, C^7*C*Me$_3$), 35.080 (s, C^2*C*Me$_3$). 32.8(s, *C*^{9}CMe$_3$), 32.0 (s, C^{7}C*Me*$_3$), 31.7 (s, C^{2}C*Me*$_3$). **^{31}P NMR (80.0 MHz, CD_2Cl_2):** δ -10.2.

[Pt(nbe)$_2$(XPB)] (4)

100 mg (0.211 mmol) of XPB and 44 mg (0.211 mmol) of Pt(nbe)$_3$ were dissolved in CD_2Cl_2, and the resulting brown solution was stirred at room temperature for 3 hours. The solvent was then removed *in vacuo*, and the solid brown product was washed twice with hexanes at -78° C, then filtered and dried *in vacuo*. This yielded 20.2 mg (22%) of product which contained approximately 0.2 equivalents of free nbe. The product was dissolved in CH_2Cl_2 and crystals were grown by slow diffusion of hexanes at -30 °C. **^{1}H NMR (600.13 MHz, CD_2Cl_2)** : δ 7.51 (d, J_{H-H} = 2.35 Hz, 1H, C*H*^{8}), 7.50 (d, J_{H-H} = 2.10

Hz, C*H*^{1}), 7.38 (m, 4H, *para*-P*Ph*$_2$), 7.25 (d, $J_{H\text{-}H}$ = 7.41 Hz, 2H, *ortho*-P*Ph*$_2$), 7.19 (m, 4H, *meta*-P*Ph*$_2$), 7.11-6.98 (br, 10H, B*Ph*$_2$), 6.944 (d, $J_{H\text{-}H}$ =2.22 Hz, 1H, C*H*^{6}), 6.65 (app. d, $J_{H\text{-}P}$ =11.23 Hz, 1H, C*H*^{3}), 1.32 (s, 6H, *C*^{9}Me$_2$), 1.28 (s, 9H, C^{7}C*Me*$_3$), 1.12 (s, 9H, C^{2}C*Me*$_3$), 0.45 (d, $J_{H\text{-}Pt}$ = 6.79 Hz, 2H, nbe), -0.1 (d, $J_{H\text{-}Pt}$ = 7.98 Hz, 2H, nbe). **^{13}C{^{1}H} NMR (150.9 MHz, CD_2Cl_2)** : δ = 150.5 (s, *C*^{7}CMe$_3$), 149.8 (s, *C*^{2}CMe$_3$), 145.0 (s, *C*), 144.7 (s, *C*), 141.2 (s, *C*), 140.7 (s, *C*), 139.4 (s, *C*), 139.2 (br. s, *C*), 135.8 (s, *C*) 134.5 (br. s., *BPh*$_2$), 131.7 (s, *para-PPh*$_2$), 130.0 (s, *C*^{6}), 129.7 (s, *C*), 129.5 (s, *C*^{3}), 128.0 (d, $J_{C\text{-}P}$ = 8.8 Hz, *ortho*-PPh$_2$), 127.6 (s, *meta*-P*Ph*$_2$), 123.8 (s, *C*^{8}), 123.2 (s, *C*^{1}), 40.2 (s, nbe), 39.1 (s, *C*^{9}Me$_2$), 34.1 (s, C^{2}*C*Me$_3$), 33.3 (d, $J_{C\text{-}P}$ =16.6 Hz, nbe), 32.8(s, C^{7}*C*Me$_3$), 32.0(s, C^{7}C*Me*$_3$), 31.7(s, C^{2}Me$_3$), 29.76 (br. S, nbe) **^{31}P NMR (80.0 MHz, CD_2Cl_2):** δ = 24.0 (s, $J_{P\text{-}Pt}$ = 3265 Hz).

4-fluoro-3-iodotoluene (5)

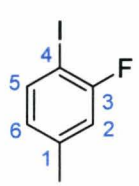

5

2.84 g (0.02 mol) of NaI, 100 mg (0.5 mmol) of CuI, 10ml of 1,4-dioxane, 2 ml (0.01 mol) of 3-bromo-4-fluorotoluene and 0.10 ml (1.0 mmol) of *N,N'*-dimethylethylenediamine were added to a sealable flask. The flask was evacuated, filled with argon, then and heated at 160° C for 3 days. The resulting dark brown product was allowed to cool before addition to 80 ml of conc. NH_4OH, to which 100 ml of H_2O was

added. The product was extracted three times with 50 ml of $CHCl_3$, followed by distillation to remove $CHCl_3$. The remaining solution was dissolved in hexanes, filtered through a plug of silica, and then distilled to remove the solvent. Yield: 15.1g of a colourless, oily product 4-fluoro-3-iodotoluene **(5)** (82 % yield). **^{1}H NMR (600.13 MHz, $CDCl_3$)** : δ = 7.58 (dd, $J_{H\text{-}H}$ = 8.02 Hz, $J_{H\text{-}F}$ = 6.79 Hz, 1H, CH^5), 6.87 (dd, $J_{H\text{-}H}$ = 9.14 Hz, $J_{H\text{-}F}$ = 1.98 Hz, 1H, CH^6), 6.73 (dd, $J_{H\text{-}H}$ = 7.90 Hz, $J_{H\text{-}F}$ = 1.11 Hz, 1H, CH^2), 2.36 (br. s, 3H, C^1*Me*). **^{13}C{^{1}H} NMR (150.9 MHz, $CDCl_3$)** : δ = 161.8 (s, C^3), 160.2 (s, C^1), 140.4 (s, C^4), 138.3 (s, C^5), 126.3 (s, C^6), 116.0 (s, C^2), 20.5 (s, C^1*Me*). **^{19}F NMR (188.3 MHz, $CDCl_3$)** : δ = -94.6. **HRMS** for C_7H_6FI: (M^+): Found 235.9422, Calcd. 235.9498.

2-(2'-fluoro-4'-methylphenylamino)-3-bromo-5-methylbenzoic acid (6)

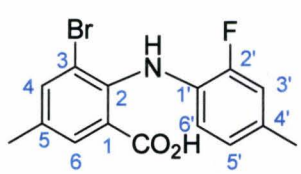

6

9.0g (0.39 mmol) of 3-bromo-5-methylanthranilic acid and 10.0g (0.42mmol) of 4-iodo-3-fluorotoluene were added to a flask, along with 540 mg (0.84mol) of Cu powder, 6.15g (0.44 mol) of K_2CO_3 and 300 ml of cyclohexanol. This mixture was refluxed for 36 hrs under N_2. The dark brown viscous product was steam distilled to remove the cylcohexanol, the resulting solution then was filtered to remove any solid, and then acidified with 0.1M HCl. The precipitate which formed was filtered, dried and then sublimed. This produced 6.4g of a yellow powder (48 % yield). **^{1}H NMR (600.13**

MHz, $CDCl_3$) : δ = 7.99 (d, $J_{H\text{-}F}$ = 1.48 Hz, 1H, CH^4, 7.66 (d, $J_{H\text{-}H}$ = 1.73 Hz, 1H, CH^6), 6.93 (dd, $J_{H\text{-}H}$ = 11.85 Hz, $J_{H\text{-}F}$ = 1.3 Hz, 1H, C$H^{3'}$), 6.4 (dd, $J_{H\text{-}H}$ = 17.0 Hz, $J_{H\text{-}F}$ = 3.6 Hz, 1H, C$H^{5'}$), 6.41 (s, 1H, C$H^{6'}$), 2.38 (s, 1H, C$^{4'}$*Me*), 2.25 (s, 1H, C^5*Me*). **$^{13}C\{^1H\}$ NMR: (150.9 MHz, $CDCl_3$)**: δ = 168 (s, CO_2H), 153.0 (d, $J_{C\text{-}F}$ = 243.3 Hz, $C^{2'}$), 139.1 (s, C^4), 138.8 (s, C^2), 135.7 (s, C^5Me), 132.7 (s, $C^{4'}$Me), 132.4 (s, C^6), 129.0 (d, $J_{C\text{-}F}$ = 12.2 Hz, $C^{1'}$), 125.0 (s, C^1) 124.7 (s, $C^{5'}$), 121.1 (s, C^3), 118.4 (s, $C^{6'}$), 116.9 (d, $J_{C\text{-}F}$ = 18.2 Hz, $C^{3'}$), 20.17, 19.8 (s, 2H, C^5*Me* & C$^{4'}$*Me*), **^{19}F NMR (188.3 MHz, $CDCl_3$)** : δ = -131.0. **HRMS** for $C_{15}H_{15}BrFNO_2$: (M^+): Found 338.9833, Calcd. 339.0093

4-bromo-9-chloro-5-fluoro-2,7-dimethylacridine (7)

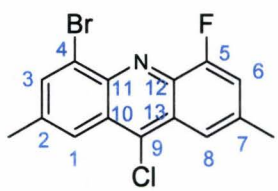

7

6.4g (0.018 mol) of 4-bromo-5-fluoro-2,7-dimethylanthranilic acid was suspended in 200 ml of freshly distilled $POCl_3$ and heated at reflux for 3.5 hrs, turning from a yellow slurry to a dark brown solution after about 30 min of heating. The excess $POCl_3$ was distilled off, and the resulting viscous, dark brown product was dissolved in 50 ml of chloroform and added drop-wise to an ice cold solution of conc. NH_4OH. The organic layer was separated and the remaining aqueous layer was washed twice with 200ml of chloroform. The organic layers were combined and the solvent was removed to produce a brown solid. This solid was sublimed, rinsed with hexanes and then dried to produce 3.72 g of a yellow powder (60% yield). **^1H NMR (600.13 MHz, $CDCl_3$)** : δ = 8.14 (s, 1H, CH^3),

8.05 (s,1H, C*H*^{1}), 7.95 (s, 1H, C*H*^{8}), 7.39 (dd, $J_{H\text{-}H,}$ = 12.3 Hz, $J_{H\text{-}F}$ = 2.0Hz, 1H, C*H*^{6}), 2.61 (s, 6H, C^{2}*Me* & C^{7}*Me*). **13C{^{1}H} NMR: (150.9 MHz, $CDCl_3$)**: δ = 157.9 (d, JC-F = 153.8 Hz, *C*^{5}), 139.7 (s, *C*^{2}Me & *C*^{7}Me), 138.0 (d, $J_{C\text{-}F}$ = 49.2 Hz, *C*^{12}), 137.0 (s, *C*^{1}), 125.2 (s, *C*^{4}), 123.0 (s, *C*^{3}), 118.9 (s, *C*^{8}), 116.3 (d, $J_{C\text{-}F}$ = 17.2 Hz, *C*^{6}), 22.8 (s, C^{2}*Me*), 22.2 (s, C^{7}*Me*). **^{19}F NMR (188.3 MHz, $CDCl_3$)** : δ = -123.1. **HRMS** for $C_{15}H_{10}BrClFN$: (M^+): Found 338.9833, Calcd. 338.9648

4-bromo-2,7-dimethyl-5-fluoroacridine (9)

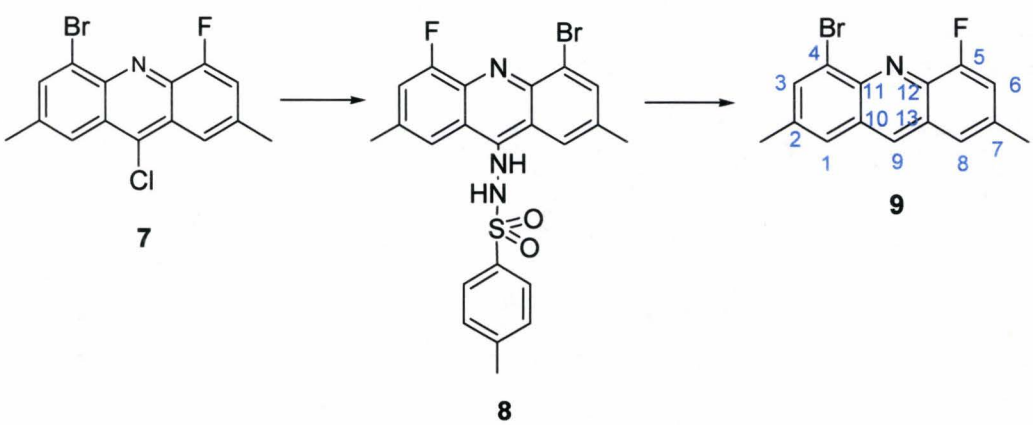

60 mg (0.32 mmol) of para-toluenesulfonic hydrazide was suspended in 10ml of anhydrous chloroform and heated to 50° C. 100mg (0.29 mmol) of 4-bromo-9-chloro-2,7-dimethyl-5-fluoroacridine was dissolved in 10 ml of anhydrous chloroform, and then added drop wise to the p-toluenesulfonic hydrazide suspension. The resulting yellow mixture was then allowed to stir at room temperature for 3 days. After two days, an orange precipitate had formed, and this precipitate was filtered, washed with water, dried

and finally sublimed to give 130 mg of the orange solid, 4-bromo-2,7-dimethyl-5-fluoro-9-(*p*-tosylhydrazide)acridine, (**8**, 90 % yield).

130 mg of **8** was suspended in 40 ml of ethylene glycol and 1.3 g of NaOH, dissolved in 10 ml of water, was added. The mixture was heated at reflux for 3.5 hrs, and a dark red precipitate formed. After cooling, 100 ml of water was added to the mixture, and the solid was filtered, washed with water and dried. The red product was sublimed to give 60 mg of a yellow solid, (**9**, 67 % yield). **^{1}H NMR (600.13 MHz, $CDCl_3$)** : δ = 8.5(s, 1H, CH^9), 8.0 (d, $J_{H\text{-}H}$ =1.2 Hz, 1H, CH^3), 7.6 (s, 1H, CH^1), 7.5 (s,1H, CH^8), 7.3 (dd, $J_{H\text{-}H}$ = 12.8 Hz, $J_{H\text{-}F}$ = 0.8 Hz, 1H, CH^6), 2.6 (s, 6H, C^2Me & C^7Me). **^{13}C{^{1}H} NMR: (150.9 MHz, $CDCl_3$):** δ = 157.3 (d, $J_{C\text{-}F}$ = 259.8 Hz, C^5), 144.0 (s, C^{12}), 143.8 (s, *C*), 139.0 (s, C^{11}), 137.0 (s, C^7), 136.5 (s, C^9), 134.7 (s, C^3), 128.4 (s, C^2), 127.9 (s, *C*), 126.3 (s, C^1) 125.0 (s, *C*), 121.2 (s, C^8), 115.9(d, $J_{C\text{-}F}$ = 17.7 Hz, C^6), 22.3 (s, C^7) 21.6(s, C^2). **^{19}F NMR (188.3 MHz, $CDCl_3$):** δ = -124.7. **HRMS** for $C_{15}H_{11}BrFN$: (M^+): Found 305.0052, Calcd. 305.0038

References

1 Lewis G. N. *Development of Modern Chemistry*, Dover Books, NY, **1984.**

2 For examples see (a) Ooi, T.; Tayama, E.; Takahashi, M.; Maruoka, K. *Tetrahedron Lett.* **1997**, *38*, 7403. (b) Kjærsgaard, A.; Anker, K. *J., Org. and Biomol. Chem.* **2005**, *5*, 804.(c). Myers A. G.; Siu, M. *Tetrahedron* **2002**, *58*, 6397.

3 For example: Rauk, A.; Hunt, I. R.; Keay, B. A. *J. Org. Chem.* **1994**, *59*, 6808. (b) McCoy, R. E.; Bauer, S. H. *J. Am. Chem. Soc.* **1956**, *78*, 2061. (c) Legon, A. C.; Werner, H. E. *J. Chem. Soc., Chem. Commun.* **1991**, 53210.

4 For example: Aubauer, C.; Irran, E.; Klapötke, T. M.; Schnick, W.; Schulz, A.; Senker, J. *Inorg. Chem.* **2001**, *40*, 4956. (b) Anane, H.; Boutalib A. *J. Phys. Chem. A*, **1997**, *101*, 7879. (c) Fitzpatrick, N. J.; Fanning, M. O. *J. Mol. Structure* **1978**, *50*, 127.

5 Liu, C.; Wang, X.; Pei, T.; Widenhoefer, R. A. *Chem. Eur. J.* **2004**, *10*, 6343. (b) Pei, T.; Wang, X.; Widenhoefer, R. A. *J. Am. Chem. Soc.* **2003**, *125*, 648.

6 Borodkoa, Y.; Somorjai G. A. *Appl. Catal. A: Gen.* **1999**, *186*, 355. (b) Ouha, L.; Müllerb T. E.;Yan, Y.K. *J. Organomet. Chem.* **2005**, *690*, 3774.(c) Bajracharya, G. B; Nakamura, I.; Yamamoto Y. *J. Org. Chem.* **2005**, *70*, 892.(d) Zhao, P.; Xu, L.; Xia C. *Synlett.* **2004**, *5*, 846.(d) Asao, N.; Nogami, T.; Takahashi, K., *J. Am. Chem. Soc.* **2002**, *124*, 764.

7 Massera, C.; Frenking, G. *Organometallics* **2003**, *22*, 2758.(b) Lynea ,P. D. D.; Mingos, M. P. *J. Organomet. Chem.* **1994**, *478*, 141.

8 Shi, M.; Chen, L. Li, C. *J. Am. Chem. Soc.* **2005**, *127*, 3790.(b) Couturier, M.; Ménard, F.; Ragan, J. A.; Riou, M.; Dauphin, E.; Andresen, B. M.; Ghosh, A.; Dupont-Gaudet, K.; Girardin, M. *Org. Lett.* **2004**, *6*, 1857.(c) Shi, Y.; Xu, Y.; Shi, M. *Adv. Synth. Catal.* **2004**, *346,* 1220.

9 Pearson, R.G. *J. Am. Chem. Soc.* **1963**, *85*, 3533.

10 Yang, S.; Li, X.;Huang, Y. *J. Organomet Chem.* **2002**, *658*, 9.

11 Shriver, D. J. *J. Am. Chem. Soc.* **1963**, *85*, 3509.

12 Johnson, M. P.; Shriver, D. F. *J. Am. Chem. Soc.* **1966**, *88*, 301.

13 Braunschweig, H.; Wagner, T., *Chem. Ber.* **1994**, *127*, 1613.(b) Braunschweig, H.; Wagner T. *Z. Naturforsch. Teil B* **1996**, *51*, 1618.

14 Hill, A. F.; Owen, G. R.; White, A. J. P.; Williams, D. J. *Angew. Chem. Int. Ed.* **1999**, *38*, 2759.(b) Foreman, A. F; Hill, A. J.; Owen, G. R.; White, A. J. P.; Williams, D. J. *Organometallics* 2003, 22, 4446.

15 Foreman, M. R. St.-J.; Hill, A. F.; White, A. J. P.; Williams, D. J. *Organometallics* **2004**, *23*, 913.

16 Crossley, I.R,; Foreman, M.R.St.-J., Hill, A.F., White, A.J.P., Williams, D.J. Chem. Commun. **2005**, *2*, 221.

17 Crossley, I.R.; Hill, A.F., *Organometallics* **2004**, *23*, 5656.

18 Crossley, I.R.; Hill, A.F.; Willis, A.C. *Organometallics* **2005**, *24*, 1062.

19 Crossley, I. R.; Hill, A. F.; Humphrey, E. R.; Smith M. K.;Tshabang, N.; Willis, A. C. *Chem. Commun.* **2004,** 1878.

20 Crossley, I. R.; Hill, A. F.; Humphrey, E. R.; Willis, A. C. *Organometallics* **2006**, *25*, 289.

21 Crossley, I. R.; Hill, A. F.; Humphrey, E. R.; Willis, A. C. *Organometallics* **2005**, *24*, 4083.
22 Mihalcik, D. J.;White, J.L.; Tanski, J. M.; Zakharov, L. N.; Yap, G. P. A.; Incarvito C. D.; Rheingold, A. L; Rabinovich, D. *Dalton Trans.* **2004**, 1626.
23 Bontemps, S.; Gornitzka, H.; Bouhadir, G.; Miqueu, K.; Bourissou, D. *Angew. Chem.* **2006**, *118*, 1641.
24 Burlitch, J. M.; Burk, J. H.; Leonowicz, M. E.; Hughes, R.E., *Inorg. Chem.* **1979**, *18*, 1702.
25 Braunscheig, H.; Radacki, K.; Rais, D.; Whittell, G. R. *Angew. Chem. Int. Ed.* **2005**, *44*, 1192.
26 Westcott, S. A. Marder T. B; Baker, R. T.; Harlow, R. L.; Calabrese, J. C.; Lam, K. C.; Lin, Z. *Polyhedron* **2004**, *23*, 2665.
27 Curtis, D.; Lesley, M. J. G.; Norman, N. C.; Orpen, A. G.; Starbuck, J. *J. Chem. Soc. Dalton Trans.* **1999**, 1687.
28 Mayer, J. M.; Calabrese, J. C. *Organometallics* **1984**, *3*, 1292.
29 Steinke, T.; Gemel, C.; Cokoja, M.; Winter, M.; Fischer, R. A. J. Chem. Soc., Chem. Commun. **2003**, 1066.
30 Leiner, E.; Hampe, O.; Scheer, M., *Eur. J. Inorg. Chem.* **2002**, *3*, 584.
31 Clarkson, L. M.; Clegg, W.; Norman, A. J.; Tucker, P. M., *Inorg. Chem.* **1988**, *27*, 2653.
32 Golden, J.T.; Peterson, T. H.; Holland, P.L.; Bergman, R.G.; Anderson, R. A. *J. Am. Chem. Soc.* **1998**, 120.
33 Linti, G.; Li, G.; Pritzkow, H., *J. Organomet. Chem.* **2001**, *626*, 82.
34 Nuber, B.; Schaltz, W.; Ziegler, M. L. *Z. Naturforsch B* **1990**, *45*, 508.
35 Fischer, R. A.; Miehr A.; Hoffmann H.; Roggee, W.; Boehme, C.; Frenking, G.; Herdtweck, E. A. *Z. Anorg. Allg. Chem.* **1999**, *625*, 1466.
36 Scott, R. N,.;Schriver, D.F.; Lehmann, D. D. *Inorg. Chim. Acta.* **1970**, *4*, 73.
37 Dahlenburg, L.; Hoeck, N.; Berke, H. *Chem. Ber.* **1988**, *121*, 2083.
38 Fryzuk, M. D.; McManus, N. T.; Paglia, P.; Rettig, S.J.; Whitell, G. S. *Organometallics* **1992**, *11*, 2979.
39 Stender, M.; Oesen, H.; Blaurock, S.; Hay-Hawkins, A. *Z. Anorg. Allg. Chem.* **2001**, *627*, 980.
40 Cook, K. S.; Piers, W. E.; McDonald, R. *J. Am. Chem. Soc.* **2002**, *124*, 5411.
41 Braunscheig H.; Radacki K.; Seeler F.; Whittell G. R. *Organometallics* **2004**, *23*, 4178.
42 Crossley I. R.; Hill A. F.; Willis A. C. *Organometallics* **2006**, *25*, 289.
43 Aldridge, S.; Bresner C. *Coord. Chem. Rev.* **2003**, *244*, 71.
44 Appel, A.; Jäkle F.; Priermeier, T.; Schmid, R.; Wagner, M. *Organometallics 1996*, **15**, 1188.
45 Carpenter, B. E.; Piers, W. E.; Parvez, M.; Yap, G. P. A.; Rettig, S. J. *Can. J. Chem.* **2001**, *79*, 857.
46 Appel, A.; Noth, H.; Schmidt, M. *Chem. Ber.* **1995**, *128*, 621.
47 Agou, T.; Kobayashi, J.; Kawashima, T. *Org. Lett.* **2005**, *7*, 4373.(b) Liu, Z.; Fang, Q.; Wang, D.; Cao, D.; Xue, G.; Yu, W.; Lei, H. *Chem. Eur. J.* **2003**, *9*, 5074. ((c)

Albrecht, K.; Kaiser, V; Boese, R.; Adams, J. D. E. Kaufmann A. *J. Chem. Soc.-Perkin Trans. 2* **2000**, 2153. (d) Z. Yuan, N. J. Taylor, Y. Sun, T. B. Marder, I. D. Williams, L. T. Cheng *J. Organomet. Chem.* **1993**, *449*, 27. (e) Z. Yuan, N. J. Taylor, T. B. Marder, I. D. Williams, S. K. Kurtz, L.-T. Cheng *Chem. Comm.* **1990**, 1489. (f) Y. Sugihara, T. Yagi, I. Murata, *J. Am. Chem. Soc.* **1992**, *114*, 1479. (g) Wrackmeyer, B.; Milius, W.;.Molla, E, *Z. Natur.* **1996**, *51b*, 1811. (h) Giles, R. L.; Howard, J. A. K.; Patrick, L. G. F.; Probert, M. R.; Smith, G. E.; Whiting, A. *J. Organomet. Chem.* **2003**, *680*, 257. (i) Roesler, R.; Piers, W. E.; Parvez, M. *J. Organomet. Chem.* **2003**, *680*, 218. (j) Herberich, G. E.; Fischer, A. Organometallics 1996, 15, 58. (k) Karsch, H. H.; Appelt, A.; Kohler, F. H.; Muller, G. *Organometallics* **1985**, *4*, 231.

48 Lesley, M. J. G.; Woodward, A.; Taylor, N. J.; Marder, T. B. *Chem. Mater.* **1998**, *10*, 1355.

49 Beachley O. T.; Tessier-Youngs, C. *Organometallics* **1983**, *2*, 736.

50 Labinger, J. A.; Bonfiglio J. N.; Grimmett, D. L.; Masuo S. T.; Shearin, E.; Miller J. S., *Organometallics* **1983**, *2*, 733.

51 Fontaine, F.; Zargarian D. *J. Am. Chem. Soc.* **2004**, *126*, 8786.

52 Roesler, R; Piers, W. E.;. Parvez, M. *J. Organomet. Chem.* **2003**, *680*, 218.

53 Agou, T.; Kobayashi, J.; Kawashima, T. *Org. Lett.* **2005**, *7*, 4373.

54 For example : Liu, H.; Du, D.; Xu, J. *Helv. Chim. Acta.* **2006**, *89*, 1067. Crudden, C. M.; Hleba Y. B.; Chen A. C. *J. Am. Chem. Soc.* **2004**, *126*, 92010. Hu J.; Zhao G.; Yang G.; Ding Z. *J. Org. Chem.* **2001**, *66*, 303.

55 Yates, P.; Eaton P. *J. Am. Chem. Soc.* **1960**, *82*, 4436.

56 Piers, W. E.; Chivers, T. *Chem. Soc. Rev.* **1997**, 345.

57 Ishihara, K.;Yamamoto, H. *Eur. J. Org. Chem.* **1999**, *527*, 7.

58 Chen, Y..-X.; Stern, C. L.; Yang, S. T.; Marks, J. *J. Am. Chem. Soc.* **1996**, *118*, 12451.

59 Gevorgan, V.; Liu, J. –X.; Rubin, M.; Benson, S.; Yamamoto, Y. *Tetrahedron Lett.* **1999**, *40*, 8919.

60 Rubin, M.; Gevorgyan, V. *Org Lett.* **2001**, *3*, 2705.

61 Blackwell, J. M.; Piers, W. E.; Parvez, M. *Org. Lett.* **2000**, *2*, 695.

62 Deck, P. A.; Beswick, C. L.; Marks, T. J. *J. Am. Chem. Soc.* **1998**, *120*, 1772.

63 Erker, G. *Dalton Trans.* **2005**, *11*, 1883.

64 Good, C. D.; Ritter, M. D. *J. Am. Chem. Soc.* **1962**, *84*, 1162.

65 Layton,W. J.;Niedenzu, N.; Niedenzu, F. M.; Trofimenko, S. *Inorg. Chem.* **1985**, 24, 1454.

66 Thompson, R. J.;Davis, J. C. Jr. *Inorg. Chem.* **1965**, *4*, 1464.

67 Young, D. E.; McAchran, G. E.; Shore, S. G. *J. Am. Chem. Soc.* **1966**, *88* , 4390.

68 Massey, A. G.; Park A. J. *J. Organomet. Chem.* **1966**, *5*, 218.

69 Wrackmeyer, S. B.; Noth, H. *Chem, Ber.* **1976**, *109*, 1011.

70 (a) Cui, Q.; Musaev, D.G.; Morokuma, K. *Organometallics*, **1998**, *17*, 1383. (b) Demoulin, O.; Seunier, I.; Navez M.; Ruiz P. *Appl. Catal. A: Gen.* **2006**, *300*, 41.

71 Malatesa, L.;Angoletta, C., *J. Chem. Soc.* **1957**, 1186.

72 Wolfgang, P.; Kutschera S.; Neumüller, B. *Organometallics* **2005**, *24*, 5038.

73 Boag, N. M.; Green, M.; Grove, D. M.; Howard, J. A. K.; Spencer, J. L.; Stone, F. G. A. *J. Chem. Soc., Dalton Trans.* **1980**, 2170.

74 Existing stable Pd(0) reagents : [Pd2(dba)3] (Rettig, M. F.; Maitlis, P. M. *Inorg. Synth.* **1990**, *28,* 110); [[Pd(COD)(bq)] and [{Pd(nbe)(bq)}2] (bq = p-benzoquinone) (Yamamoto, Y.; Ohno, T.; Itoh, Kenji. *Organometallics* **2003**, *22*, 2267); [$Pd_2(dvds)_3$] (dvds = tetramethyldivinyldisiloxane) (Krause, J.; Cestaric, G.; Haack, K-J.; Seevogel, K.; Storm. W, Porschke, K-R. *J. Am. Chem. Soc.* **1999**, *121*, 9807. Other known but very unstable reagents include: [$Pd(COD)_2$], [$Pd(nbe)_3$] and [$Pd(C_2H_4)_3$] (Green, M.; Howard, J. A. K.; Spencer, J. L.; Stone, F. G. A. *Dalton* **1977**, 273.)
75 Mendez, M.; Munoz M. P.; Nevado C.; Cardenas D. J.; Echavarren A. M. *J. Am Chem. Soc.* **2001**, *123*, 10511.
76 Kalantara, A.; Backmana,H.; Caruccia J. H.; Salmia T.; Murzina Y. D. *J. Catal,* **2004**, *227*, 60.
77 Prati, L.; Rossi M. *Appl. Catal. B: Environmental*, **1999**, *23*, 135.
78 Kataoka, Y.; Matsumoto O.; Tani K. *Organometallics* **1996**, *15*, 5246.
79 Roy, U. K.; Roy S. *Tetrahedron*, **2006**, *62*, 678.
80 Sprengers, J. W.; Greef M.; Duin M. A.; Elsevier, C. J. *Eur. J. Inorg. Chem.* **2003**, *20*, 3811.
81 Anderson, G. K.; Clark, H. C.; Davies, J. A.; Ferguson, G. & Parvez, M. J. *Crystallogr. Spectrosc. Res.* **1982**, *12*, 449.
82 Johansson, M. H.; Otto, S. *Acta Cryst. C* **2000**, *56*, e12–e15.
83 Goodfellow, R. J.; Knight, J. R.; Norton, M.G Taylor, B.F. *J. Chem. Soc., Dalton Trans.* **1972**, 2518.
84 Matern, E.; Pikies, J.; Frit, G. *Z. Anorg. Allg. Chem.* **2000**, *626*, 2136.
85 Fontaine, F.; Zargarian D. *J. Am. Chem. Soc.* **2004**, *126*, 8786.
86 Kamer, P. C. J.; van Leeuwen, P. W. N. M. *Acc. Chem. Res.* **2001**, *34*, 895.
87 Haenel, M. W.; Jakubik, D.; Krüger, C.; Betz, P. *Chem. Ber.* **1991**, *124*, 333.
88 (a) Caviezel, R.; Eichenberger, E.; Kunzle, F.; Schmultz, *J. Pharm. Act. Helv.* **1958**, *33*, 447. (b) Botte, L. *Acta Psychia. Belg.* **1983**, *83*, 397. (c) Muren, J. F.; Bloom, B. M. *J. Med. Chem.* **1970**, *13*,17. (d) Jeyaseelia, L.; Asish, G.; Kumara, D. K.; Mazumdarb, A. K.; Duttab N. K.; Dastidar. S. G. *Int. J. Antimicrob. Agents* **2006**, *27*, 58.
89 Guari, Y.; van Strijdonck, G. P. F., Boele M. D. K;, Reek J. N. H. *Chem. Eur. J.* **2001**, *7*, 475.
90 Emslie, D.; Blackwell, J. M.; Britten, J. F.; Harrington, L. E. *Organometallics* **2006**, *25*, 2412.
91 Emslie group, unpublished data.
92 Katz, M. E. *Organometallics* **1987**, *6*, 1134.
93 Ancillotti, F.; Lami M.; Marchionna, M. *J. Mol. Catal.* **1991**, 66, 37.
94 Lewis, L. N.; Sy, K. G.; Bryant, G. L.; Donahue, P. E. *Orgametallics* **1991**, *10*, 3750.
95 Kelkar, A. A.; *Tetrahedron Lett.* **1996**, *37*, 8917.
96 Connelly, N. G.; Emslie, D. J. H.; Metz, B.; Orpen, A. G.; Quayle, M. *J. Chem. Commun.* **1996**, *19*, 2289.
97 (a) van Benschoten, J. J.; Lewis, J. Y.; Heineman, W. R.; Rosten, D. A.; Kissinger, P. T.; *J. Chem. Ed.* **1983**, *60*, 772. (b) Kissinger, P. T.; Heineman, W. R. *J. Chem. Ed.* **1983**, *60*, 702.

98 Aranzaes, J. R.; Daniel, M.; Astruc, D. *Can. J. Chem.* **2006**, *84*. 288.
99 Wen, F.; Bonnemann, H. *App. Organomet. Chem.* **2005**, *19*, 94.
100 Cotton, F. A.; Wilkinson, G.; Murillo, C. A.; Bochmann, M. *Advanced Inorganic Chemistry*, 6th ed.; Wiley: New York, **1999**.
101 For example: (a) Jia, L.; Yang, X.; Stern, C.; Marks, T. J. *Organometallics* **1994**, *13*, 3755. (b) Metz, M. V.; Schwartz, D. J.; Stern, C. L.; Nickias, P. N.; Marks, T. J. *Angew. Chem., Int. Ed.* **2000**, *39*, 1312.
102 Appel, A.; Noth, H.; Schmidt, M. *Chem. Ber.* **1995**, *128*, 621.
103 For example: Pt-P= 2.290(1) Å in [PMe_3PtMe_2], Pt-P = 2.344(1) Å in [PCy_3PtMe_3], Haar, C. M.; Nolan , S. P. *Organometallics* **1990**, *18*, 474; Pt-P = 2.2730(10) Å in trans-[$PtPhMe(PPh_3)_2$], Nilsson, P.; Plamper, F.; Wendt, O. F. *Organometallics* **2003**, *22*, 5235.
104 Green, M.; Howard, J. A. K.; Spencer, J.L.; Stone, F. G. A. *J. Chem.Soc., Dalton Trans.* **1977**, 271.
105 (a) Crossley, I.R.; Hill, A.F.,; Willis, A.C. *Organometallics* **2005**, *24*, 1062. (b) Chatt, J.; Mason, R, Meek D. W. *J. Am. Chem. Soc.* **1975**, 3826.(c) Baralt, E. Lukehart, C. M. *Inorg. Chem.* **1990**, *29*, 2870.
106 (a) *Chemical compound*, Encyclopædia Britannica, **2006**. (b) Yang, Y. J.; Escobedo, J. O.; Wong, A.; Schowalter, C. M.; Touchy, M. C.; Jiao, L. J.; Crowe W. E.; Fronczek, F. R.; Strongin, R. M. *J. Org. Chem.* **2005**, *70*, 6907.
107 Sakia, N.; Dincb, T.; Akkayab, E.U. *Tetetrahedron*, **2006**, *62*, 2721.
108 Nowick, J., Ballester, P., Ebmeyer, F., Rebek, J. *J.Am.Chem.* Soc. **1990**, *112*, 8902.
109 Chang, C. J.; Yeh, C.; Nocera, D. G. *J. Org. Chem.* **2002**, *67*, 1403.
110 van der Veen, L. A.; Keeven P. K.; Kamer, P. C. J.; van Leeuwen, P. W. *Chem. Soc., Dalton Trans.* **2000**, 2105.
111 van Leeuwen, P. W. N. M.; Kamer, P. C. J.; Reek J. N. H. *Pure Appl. Chem.* **1999**, *71*, 1443.
112 Harris, M.C.; Geis, O.; Buchwald, S. L. *J. Org. Chem.* **1999**, *64*, 6.
113 Sergeev, A. G.; Artamkina, G.A.; Beletskaya, I.P. *Tetrahedron Lett.* **2003**, *44*, 4719.
114 Johns, A.M.; Utsunomiya, M.; Incarvito, C.D.; Hartwig, J. F. *J. Am. Chem. Soc.* **2006**, *128*, 1828.
115 Reetz, M.T.; Li, X. J. *Am. Chem. Soc.* **2006**, *128*, 1044.
116 Petocz, G.; Berente, Z.; Kegl, T.; Kollar, L. *J. Organomet. Chem.* **2004**, *689*, 1188.
117 Iwasa, S.; Ishima, Y.; Widagdo, H.S.; Aoki, K.; Nishiyama, H. *Tetrahedron Lett.* **2004**, *45*, 2121.
118 Goedheijt, M.S.; Reek, J. N. H.; Kramer, C. J. P.; van Leeuwen P. W. N. M. *Chem Commun.* **1998**, 2431.
119 Zuidevelda, M. A.; Swennenhuisa, B. H. G.; Boelea, M. D. K.; Guaria, Y.; van Strijdoncka, G. P. F.; Reeka, J. N. H.; Kamera, P. C. J.; Goubitzb, K.; Fraanjeb, J.; Lutzc, M.; Spekc A. L.; van Leeuwen, P. W. N. M. *J. Chem. Soc., Dalton Trans.* **2002**, *11*, 2308.
120 van der Veen, L. A.; Keeven, P. K.; Kamer, P. C. J.; van Leeuwen, P. W. N. M. *Chem. Commun.* **2000**, 3333.
121 Boag, N M.; Revetz, M. S. *J. Chem. Soc. S. Dalton Trans.* **1995**, 3473.

122 Albert, A., *The Acridines*, 2nd Ed.,Edward Arnold Publishes, **1966**.
123 Hillebrand S.; BArtkowska B.; Bruckmann J.; Kruger C.; Haenel M. W. *Tetrahedron Lett.* **1998**, *39*, 813.
124 Haenel, M. W.; Hillebrand, S.; Bartkowska, B. United States Patent, US 6,290,926 B1, **2001**.
125 Belmont, P.; Andrez, J.; Allan, C. S. M. *Tetrahedron Lett.* **2004**, *45*, 2783.
126 Gamage, S. A.; Spicer, J. A.; Rewcastle, G. W.; Denny,W.A. *Tetrahedron Lett.* **1997**, 38, 699.
127 Acheson, R. M. *An Introduction to the Chemistry of Heterocyclic Compounds*, 3rd ed.; Wiley-Interscience: New York, **1976**.
128 Jourdan, F. *Ber.* **1885**, *18*, 1444.
129 Ullmann, F.; Bielecki, J. *Chem. Ber.* **1901**, *34*, 2174.
130 Malhotra, S.; Koul, S. K.; Singh, S.; Singh, G. B.; Dhar, K. *Int. J. Chem., Section B: Org. Chem.* **1989**, *1*, 100.
131 Kollmar, R.; Parlitz, R.; Oevers, S. R.; Helmchen, G. *Organic Syntheses*, **2003**, *79*, 196.
132 (a) Louie, J.; Hartwig, J. F. *Tetrahedron Lett.* **1995**, *36*, 3609. (b) Guram, A. S. *Angew. Chem, Int. Ed.* **1995**, *34*, 1348. (c) MacNeil S. L. *Synlett* **1998**, 419. (d) Hartwig, J. F. *Angew, Chem. Int. Ed.* **1998**, *37*, 2046
133 Clews, J.; Curtis, A. D. M.; Malkin, H. *Tetrahedron* **2000**, *56*, 8735.
134 Marino, S.T.; Stachurska-Buczek, D.; Huggins, D. A.; Krywult, B. M.; Sheehan, C. S.; Nguyen, T.; Choi N.; Parsons, J. G.; Griffiths, P.; James, I. J.; Bray, A. M.; White J. M.; Boyce R. *Molecules* **2004**, *9*, 405.
135 Klapars, A. Buchwald, S. L. *J. Am. Chem. Soc.* **2002**, *124*, 14844.
136 Magidson, O. J. *Ber.* **1933**, *66*, 866. (b) Albert. A.; Ritchie B. *Organic Syntheses, Coll.* **1955**, *3*, 53.
137 Albert, A,; Willis, J. B. *J. Soc. Chem. Indust.* **1946**, *65*, 26.
138 Albert, A.; Royer, R. P. *J. Chem. Soc. (Resumed)*, **1965**, 4653.
139 Escales, R. *Ber.* **1885**, *18*, 893.
140 Albert A, Royer, R. P. *J. Chem. Soc.* **1949**, 1148.
141 Ren, H.; Knochel, P. *Chem. Commun.* **2006**, *7*, 726.
142 Wen, F.; Bonnemann, H. *Appl. Organomet. Chem.* **2005**, *19*, 94.
143 Green, M.; Howard, J. A. K.; Spencer, J.L.; Stone, F. G. A. *J. Chem.Soc., Dalton Trans.* **1977**, 271.
144 Thomas J. C.; Peters J. C. *Inorg. Chem.* **2003**, *42*, 5055
145 van der Veen, L. A.; Keeven, P. K.; Kamer, P. C. J.; van Leeuwen, P. W. N. M. *Chem. Commun.* **2000**, 3333.

Appendix : Crystallographic data

1. Molecular Structure and Crystallographic Data for [PtX(μ-Cl)(TXPB)]·DCE (X = 80% Cl/ 20% Br)

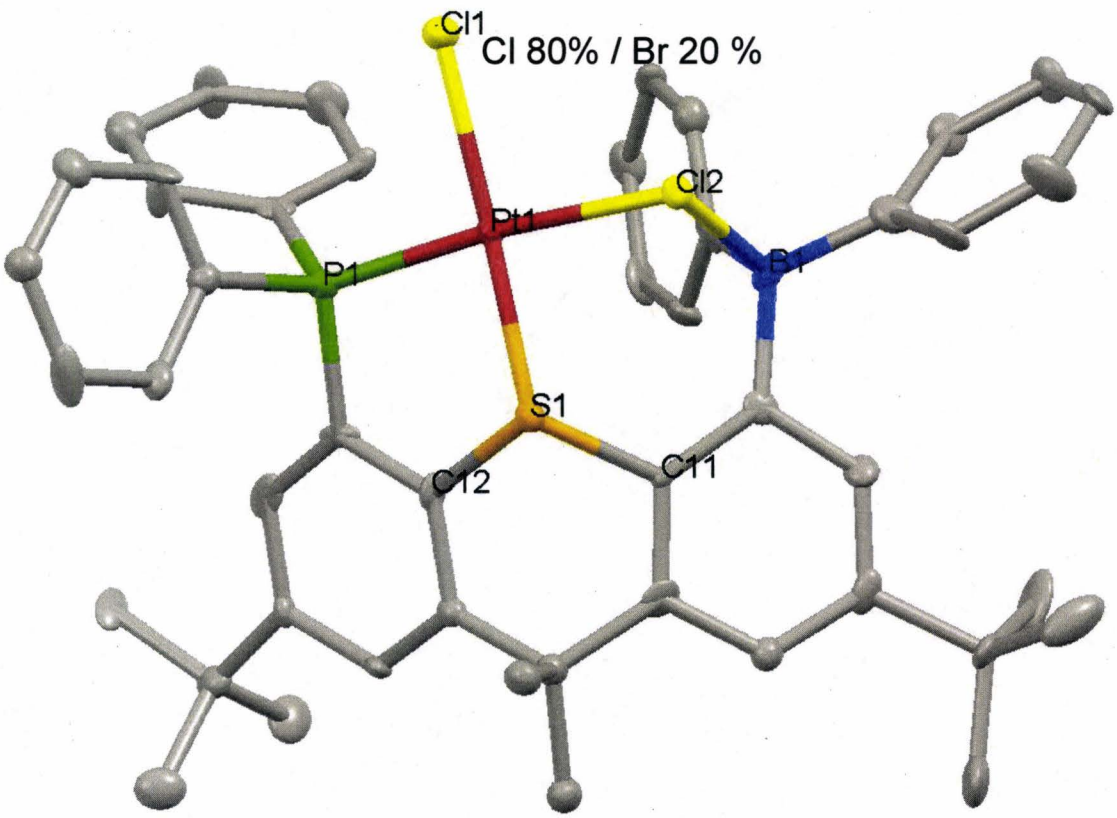

Crystal data and structure refinement for [PtCl(μ-Cl)(TXPB)]·DCE

Empirical formula	$C_{49}H_{52}BBrCl_4PPtS$	
Formula weight	1131.55	
Temperature	123(2) K	
Wavelength	0.71073 Å	
Crystal system	Orthorhombic	
Space group	P2(1)2(1)2(1)	
Unit cell dimensions	a = 8.956(7) Å	α= 90°.

	b = 20.665(16) Å	β= 90°.
	c = 24.552(16) Å	γ = 90°.
Volume	4544(6) $Å^3$	
Z	4	
Density (calculated)	1.654 Mg/m^3	
Absorption coefficient	4.318 mm^{-1}	
F(000)	2252	
Crystal size	0.20 x 0.09 x 0.03 mm^3	
θ range for data collection	1.29 to 27.48°.	
Index ranges	$-10 \leq h \leq 11, -26 \leq k \leq 25, -31 \leq l \leq 31$	
Reflections collected	37142	
Independent reflections	10378 [R(int) = 0.0788]	
Completeness to θ = 27.48°	100.0 %	
Absorption correction	Sadabs	
Refinement method	Full-matrix least-squares on F^2	
Data / restraints / parameters	10378 / 60 / 516	
Goodness-of-fit on F^2	1.158	
Final R indices [I>2σ(I)]	R1 = 0.0665, wR2 = 0.1253	
R indices (all data)	R1 = 0.0834, wR2 = 0.1299	
Absolute structure parameter	0.055(9)	
Extinction coefficient	0.00187(16)	
Largest diff. peak and hole	1.925 and -4.899 $e.Å^{-3}$	

Bond lengths [Å] and angles [°] for [PtCl(μ-Cl)(TXPB)]•DCE

Pt(1)-P(1)	2.206(3)	C(1)-C(13)	1.355(13)
Pt(1)-S(1)	2.219(3)	C(1)-C(2)	1.427(13)
Pt(1)-Cl(1)	2.356(2)	B(1)-C(36)	1.600(15)
Pt(1)-Cl(2)	2.360(2)	B(1)-C(42)	1.604(15)
S(1)-C(12)	1.769(9)	B(1)-C(5)	1.608(15)
S(1)-C(11)	1.797(8)	B(1)-Cl(2)	2.144(11)
P(1)-C(24)	1.809(9)	C(2)-C(3)	1.376(14)
P(1)-C(30)	1.817(10)	C(2)-C(16)	1.512(13)
P(1)-C(4)	1.827(10)	C(3)-C(4)	1.372(14)

Cl(3)-C(48)	1.805(12)	C(38)-C(39)	1.385(15)
Cl(4)-C(49)	1.783(10)	C(39)-C(40)	1.383(14)
C(4)-C(12)	1.382(12)	C(40)-C(41)	1.386(15)
C(5)-C(6)	1.408(12)	C(42)-C(43)	1.406(13)
C(5)-C(11)	1.418(12)	C(42)-C(47)	1.413(14)
C(6)-C(7)	1.396(14)	C(43)-C(44)	1.383(13)
C(7)-C(8)	1.359(13)	C(44)-C(45)	1.362(16)
C(7)-C(20)	1.580(11)	C(45)-C(46)	1.351(15)
C(8)-C(10)	1.419(12)	C(46)-C(47)	1.377(14)
C(9)-C(10)	1.519(13)	C(48)-C(49)	1.485(16)
C(9)-C(13)	1.540(12)		
C(9)-C(14)	1.539(13)	P(1)-Pt(1)-S(1)	87.99(10)
C(9)-C(15)	1.540(13)	P(1)-Pt(1)-Cl(1)	93.81(9)
C(10)-C(11)	1.402(13)	S(1)-Pt(1)-Cl(1)	170.81(7)
C(12)-C(13)	1.412(13)	P(1)-Pt(1)-Cl(2)	174.16(10)
C(16)-C(19)	1.512(13)	S(1)-Pt(1)-Cl(2)	86.95(9)
C(16)-C(18)	1.533(14)	Cl(1)-Pt(1)-Cl(2)	91.65(8)
C(16)-C(17)	1.558(13)	C(12)-S(1)-C(11)	98.8(4)
C(20)-C(21)	1.493(15)	C(12)-S(1)-Pt(1)	105.7(3)
C(20)-C(22)	1.509(16)	C(11)-S(1)-Pt(1)	121.1(3)
C(20)-C(23)	1.538(15)	C(24)-P(1)-C(30)	106.1(4)
C(24)-C(29)	1.380(13)	C(24)-P(1)-C(4)	106.8(4)
C(24)-C(25)	1.397(13)	C(30)-P(1)-C(4)	106.8(4)
C(25)-C(26)	1.404(13)	C(24)-P(1)-Pt(1)	114.9(3)
C(26)-C(27)	1.435(16)	C(30)-P(1)-Pt(1)	116.1(3)
C(27)-C(28)	1.341(14)	C(4)-P(1)-Pt(1)	105.6(3)
C(28)-C(29)	1.377(13)	C(13)-C(1)-C(2)	123.3(8)
C(30)-C(31)	1.374(12)	C(36)-B(1)-C(42)	117.3(8)
C(30)-C(35)	1.388(12)	C(36)-B(1)-C(5)	113.0(8)
C(31)-C(32)	1.390(14)	C(42)-B(1)-C(5)	114.6(8)
C(32)-C(33)	1.398(12)	C(36)-B(1)-Cl(2)	108.6(6)
C(33)-C(34)	1.369(13)	C(42)-B(1)-Cl(2)	95.1(7)
C(34)-C(35)	1.386(13)	C(5)-B(1)-Cl(2)	105.7(6)
C(36)-C(37)	1.381(13)	B(1)-Cl(2)-Pt(1)	96.6(3)
C(36)-C(41)	1.389(14)	C(3)-C(2)-C(1)	117.0(8)
C(37)-C(38)	1.394(14)	C(3)-C(2)-C(16)	125.7(8)

C(1)-C(2)-C(16)	117.3(8)	C(18)-C(16)-C(17)	105.9(8)
C(4)-C(3)-C(2)	122.0(9)	C(21)-C(20)-C(22)	111.4(10)
C(3)-C(4)-C(12)	118.9(9)	C(21)-C(20)-C(23)	108.0(10)
C(3)-C(4)-P(1)	125.1(8)	C(22)-C(20)-C(23)	108.0(9)
C(12)-C(4)-P(1)	116.0(8)	C(21)-C(20)-C(7)	111.4(8)
C(6)-C(5)-C(11)	113.3(9)	C(22)-C(20)-C(7)	109.1(9)
C(6)-C(5)-B(1)	116.2(8)	C(23)-C(20)-C(7)	108.9(9)
C(11)-C(5)-B(1)	129.5(8)	C(29)-C(24)-C(25)	120.6(8)
C(7)-C(6)-C(5)	124.2(9)	C(29)-C(24)-P(1)	119.7(7)
C(8)-C(7)-C(6)	119.3(8)	C(25)-C(24)-P(1)	119.6(7)
C(8)-C(7)-C(20)	122.4(9)	C(24)-C(25)-C(26)	119.8(10)
C(6)-C(7)-C(20)	118.3(8)	C(25)-C(26)-C(27)	117.6(10)
C(7)-C(8)-C(10)	121.5(9)	C(28)-C(27)-C(26)	120.4(8)
C(10)-C(9)-C(13)	108.6(7)	C(27)-C(28)-C(29)	122.0(10)
C(10)-C(9)-C(14)	111.9(8)	C(28)-C(29)-C(24)	119.5(9)
C(13)-C(9)-C(14)	109.7(7)	C(31)-C(30)-C(35)	121.8(8)
C(10)-C(9)-C(15)	111.9(7)	C(31)-C(30)-P(1)	120.8(7)
C(13)-C(9)-C(15)	108.3(7)	C(35)-C(30)-P(1)	117.4(7)
C(14)-C(9)-C(15)	106.5(8)	C(30)-C(31)-C(32)	120.2(8)
C(11)-C(10)-C(8)	116.6(8)	C(31)-C(32)-C(33)	117.6(9)
C(11)-C(10)-C(9)	122.6(8)	C(34)-C(33)-C(32)	121.9(9)
C(8)-C(10)-C(9)	120.8(9)	C(33)-C(34)-C(35)	120.1(9)
C(10)-C(11)-C(5)	125.0(8)	C(34)-C(35)-C(30)	118.2(8)
C(10)-C(11)-S(1)	113.7(6)	C(37)-C(36)-C(41)	118.3(9)
C(5)-C(11)-S(1)	121.0(7)	C(37)-C(36)-B(1)	120.3(9)
C(4)-C(12)-C(13)	122.2(9)	C(41)-C(36)-B(1)	121.2(9)
C(4)-C(12)-S(1)	120.1(8)	C(36)-C(37)-C(38)	121.3(10)
C(13)-C(12)-S(1)	117.8(6)	C(39)-C(38)-C(37)	118.9(10)
C(1)-C(13)-C(12)	116.5(8)	C(40)-C(39)-C(38)	121.0(9)
C(1)-C(13)-C(9)	125.3(8)	C(39)-C(40)-C(41)	118.8(9)
C(12)-C(13)-C(9)	118.2(8)	C(40)-C(41)-C(36)	121.6(9)
C(2)-C(16)-C(19)	109.3(8)	C(43)-C(42)-C(47)	115.0(9)
C(2)-C(16)-C(18)	111.8(8)	C(43)-C(42)-B(1)	122.2(9)
C(19)-C(16)-C(18)	110.5(9)	C(47)-C(42)-B(1)	122.7(9)
C(2)-C(16)-C(17)	110.5(8)	C(44)-C(43)-C(42)	121.4(9)
C(19)-C(16)-C(17)	108.7(8)	C(45)-C(44)-C(43)	120.8(9)

C(46)-C(45)-C(44)	120.3(10)
C(45)-C(46)-C(47)	119.9(11)
C(46)-C(47)-C(42)	122.6(9)
C(49)-C(48)-Cl(3)	112.8(8)
C(48)-C(49)-Cl(4)	112.3(8)

2. Molecular Structure and Crystallographic Data for [PtPhMe(TXPB^{Me,Ph})]

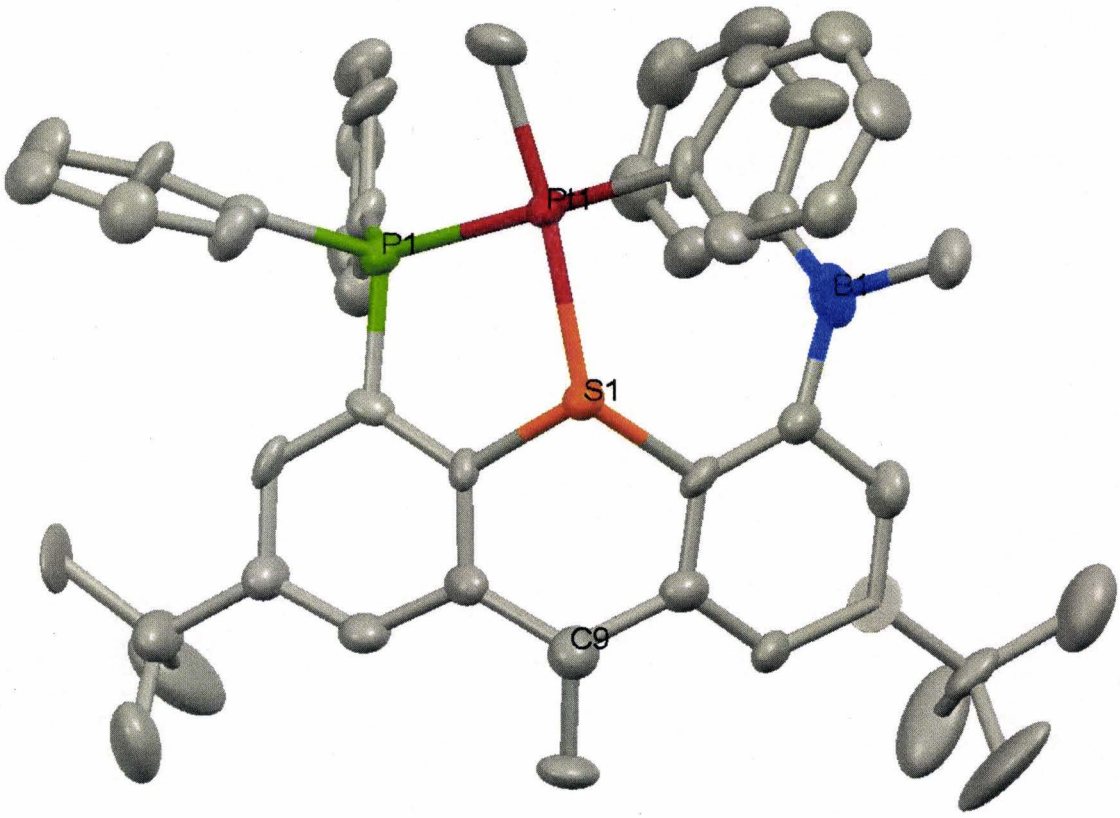

Crystal data and structure refinement for [PtPhMe(TXPB^{Me,Ph})].

Empirical formula	$C_{49}H_{54}BPPtS - 2C_6H_{14}$	
Formula weight	1082.18	
Temperature	173(2) K	
Wavelength	0.71073 Å	
Crystal system	Triclinic	
Space group	P1	
Unit cell dimensions	a = 9.5588(6) Å	α = 102.289(4)°.
	b = 13.1499(8) Å	β= 90.835(4)°.
	c = 20.7998(14) Å	γ = 96.268(4)°.
Volume	2537.4(3) Å^3	
Z	2	
Density (calculated)	1.416 Mg/m^3	
Absorption coefficient	2.877 mm^{-1}	
F(000)	1120	

Crystal size	0.17 x 0.12 x 0.02 mm^3
θ range for data collection	1.60 to 28.89°.
Index ranges	$-12 \leq h \leq 12, -16 \leq k \leq 17, -27 \leq l \leq 27$
Reflections collected	21217
Independent reflections	11154 [R(int) = 0.0734]
Completeness to θ = 28.89°	83.7 %
Absorption correction	Sadabs
Refinement method	Full-matrix least-squares on F^2
Data / restraints / parameters	11154 / 24 / 479
Goodness-of-fit on F^2	1.011
Final R indices [I>2σ(I)]	R1 = 0.0741, wR2 = 0.1387
R indices (all data)	R1 = 0.1244, wR2 = 0.1524
Largest diff. peak and hole	1.447 and -3.533 e.$Å^{-3}$
Ratio of min. to max. apparent transmission	0.7191

Bond lengths [Å] and angles [°] for [PtPhMe(TXPB^{Me,Ph})].

Pt(1)-C(42)	2.035(9)	C(1)-C(2)	1.363(13)
Pt(1)-C(49)	2.050(9)	C(1)-C(10)	1.398(12)
Pt(1)-P(1)	2.266(2)	C(1)-H(1A)	0.9500
Pt(1)-S(1)	2.322(2)	C(2)-C(3)	1.384(12)
P(1)-C(24)	1.812(10)	C(2)-C(16)	1.503(13)
P(1)-C(4)	1.818(8)	C(3)-C(4)	1.396(12)
P(1)-C(30)	1.842(8)	C(3)-H(3A)	0.9500
S(1)-C(11)	1.779(8)	C(4)-C(11)	1.383(11)
S(1)-C(12)	1.822(9)	C(5)-C(12)	1.378(12)
B(1)-C(36)	1.530(15)	C(5)-C(6)	1.393(13)
B(1)-C(5)	1.562(14)	C(6)-C(7)	1.373(12)
B(1)-C(48)	1.595(14)	C(6)-H(6A)	0.9500

C(7)-C(8)	1.374(12)	C(19)-H(19B)	0.9800
C(7)-C(20)	1.531(13)	C(19)-H(19C)	0.9800
C(8)-C(13)	1.356(13)	C(18)-H(18A)	0.9800
C(8)-H(8A)	0.9500	C(18)-H(18B)	0.9800
C(9)-C(10)	1.504(12)	C(18)-H(18C)	0.9800
C(9)-C(15)	1.547(11)	C(20)-C(22)	1.498(14)
C(9)-C(14)	1.562(12)	C(20)-C(23)	1.541(16)
C(9)-C(13)	1.566(12)	C(20)-C(21)	1.545(15)
C(10)-C(11)	1.391(11)	C(21)-H(21A)	0.9800
C(12)-C(13)	1.384(11)	C(21)-H(21B)	0.9800
C(14)-H(14A)	0.9800	C(21)-H(21C)	0.9800
C(14)-H(14B)	0.9800	C(22)-H(22A)	0.9800
C(14)-H(14C)	0.9800	C(22)-H(22B)	0.9800
C(15)-H(15A)	0.9800	C(22)-H(22C)	0.9800
C(15)-H(15B)	0.9800	C(23)-H(23A)	0.9800
C(15)-H(15C)	0.9800	C(23)-H(23B)	0.9800
C(16)-C(19)	1.502(17)	C(23)-H(23C)	0.9800
C(16)-C(18)	1.507(15)	C(24)-C(25)	1.381(12)
C(16)-C(17)	1.51(2)	C(24)-C(29)	1.414(12)
C(17)-H(17A)	0.9800	C(25)-C(26)	1.383(14)
C(17)-H(17B)	0.9800	C(25)-H(25A)	0.9500
C(17)-H(17C)	0.9800	C(26)-C(27)	1.428(14)
C(19)-H(19A)	0.9800	C(26)-H(26A)	0.9500

C(27)-C(28)	1.384(14)	C(39)-H(39A)	0.9500
C(27)-H(27A)	0.9500	C(40)-C(41)	1.424(15)
C(28)-C(29)	1.357(14)	C(40)-H(40A)	0.9500
C(28)-H(28A)	0.9500	C(41)-H(41A)	0.9500
C(29)-H(29A)	0.9500	C(42)-C(47)	1.399(12)
C(30)-C(31)	1.381(12)	C(42)-C(43)	1.416(12)
C(30)-C(35)	1.382(11)	C(43)-C(44)	1.350(13)
C(31)-C(32)	1.334(12)	C(43)-H(43A)	0.9500
C(31)-H(31A)	0.9500	C(44)-C(45)	1.392(14)
C(32)-C(33)	1.384(13)	C(44)-H(44A)	0.9500
C(32)-H(32A)	0.9500	C(45)-C(46)	1.360(13)
C(33)-C(34)	1.413(13)	C(45)-H(45A)	0.9500
C(33)-H(33A)	0.9500	C(46)-C(47)	1.415(13)
C(34)-C(35)	1.371(12)	C(46)-H(46A)	0.9500
C(34)-H(34A)	0.9500	C(47)-H(47A)	0.9500
C(35)-H(35A)	0.9500	C(48)-H(48A)	0.9800
C(36)-C(37)	1.382(13)	C(48)-H(48B)	0.9800
C(36)-C(41)	1.411(13)	C(48)-H(48C)	0.9800
C(37)-C(38)	1.373(13)	C(49)-H(49A)	0.9800
C(37)-H(37A)	0.9500	C(49)-H(49B)	0.9800
C(38)-C(39)	1.403(15)	C(49)-H(49C)	0.9800
C(38)-H(38A)	0.9500		
C(39)-C(40)	1.402(16)	C(42)-Pt(1)-C(49)	87.6(4)

C(42)-Pt(1)-P(1)	175.1(3)	C(2)-C(3)-C(4)	121.2(8)
C(49)-Pt(1)-P(1)	91.4(3)	C(2)-C(3)-H(3A)	119.4
C(42)-Pt(1)-S(1)	94.1(3)	C(4)-C(3)-H(3A)	119.4
C(49)-Pt(1)-S(1)	171.8(3)	C(11)-C(4)-C(3)	119.0(7)
P(1)-Pt(1)-S(1)	86.23(8)	C(11)-C(4)-P(1)	118.9(6)
C(24)-P(1)-C(4)	102.0(4)	C(3)-C(4)-P(1)	122.1(7)
C(24)-P(1)-C(30)	103.1(4)	C(12)-C(5)-C(6)	116.0(8)
C(4)-P(1)-C(30)	104.7(4)	C(12)-C(5)-B(1)	132.4(9)
C(24)-P(1)-Pt(1)	118.6(3)	C(6)-C(5)-B(1)	111.5(9)
C(4)-P(1)-Pt(1)	107.6(3)	C(7)-C(6)-C(5)	121.3(9)
C(30)-P(1)-Pt(1)	118.8(3)	C(7)-C(6)-H(6A)	119.4
C(11)-S(1)-C(12)	98.2(4)	C(5)-C(6)-H(6A)	119.4
C(11)-S(1)-Pt(1)	107.5(3)	C(6)-C(7)-C(8)	120.0(9)
C(12)-S(1)-Pt(1)	127.9(3)	C(6)-C(7)-C(20)	120.2(9)
C(36)-B(1)-C(5)	120.2(9)	C(8)-C(7)-C(20)	119.6(9)
C(36)-B(1)-C(48)	120.4(9)	C(13)-C(8)-C(7)	121.0(8)
C(5)-B(1)-C(48)	117.6(10)	C(13)-C(8)-H(8A)	119.5
C(2)-C(1)-C(10)	125.6(8)	C(7)-C(8)-H(8A)	119.5
C(2)-C(1)-H(1A)	117.2	C(10)-C(9)-C(15)	112.4(8)
C(10)-C(1)-H(1A)	117.2	C(10)-C(9)-C(14)	109.9(8)
C(1)-C(2)-C(3)	116.8(8)	C(15)-C(9)-C(14)	103.4(7)
C(1)-C(2)-C(16)	121.7(8)	C(10)-C(9)-C(13)	110.3(7)
C(3)-C(2)-C(16)	121.5(9)	C(15)-C(9)-C(13)	110.3(8)

C(14)-C(9)-C(13)	110.4(7)	H(15A)-C(15)-H(15C)	109.5
C(11)-C(10)-C(1)	115.0(9)	H(15B)-C(15)-H(15C)	109.5
C(11)-C(10)-C(9)	119.7(8)	C(2)-C(16)-C(19)	110.7(9)
C(1)-C(10)-C(9)	125.1(8)	C(2)-C(16)-C(18)	113.0(10)
C(4)-C(11)-C(10)	122.1(7)	C(19)-C(16)-C(18)	115.2(13)
C(4)-C(11)-S(1)	119.1(6)	C(2)-C(16)-C(17)	107.5(11)
C(10)-C(11)-S(1)	118.8(7)	C(19)-C(16)-C(17)	104.2(14)
C(5)-C(12)-C(13)	123.7(9)	C(18)-C(16)-C(17)	105.5(11)
C(5)-C(12)-S(1)	120.0(7)	C(16)-C(17)-H(17A)	109.5
C(13)-C(12)-S(1)	116.2(7)	C(16)-C(17)-H(17B)	109.5
C(8)-C(13)-C(12)	117.9(9)	H(17A)-C(17)-H(17B)	109.5
C(8)-C(13)-C(9)	121.2(8)	C(16)-C(17)-H(17C)	109.5
C(12)-C(13)-C(9)	120.9(8)	H(17A)-C(17)-H(17C)	109.5
C(9)-C(14)-H(14A)	109.5	H(17B)-C(17)-H(17C)	109.5
C(9)-C(14)-H(14B)	109.5	C(16)-C(19)-H(19A)	109.5
H(14A)-C(14)-H(14B)	109.5	C(16)-C(19)-H(19B)	109.5
C(9)-C(14)-H(14C)	109.5	H(19A)-C(19)-H(19B)	109.5
H(14A)-C(14)-H(14C)	109.5	C(16)-C(19)-H(19C)	109.5
H(14B)-C(14)-H(14C)	109.5	H(19A)-C(19)-H(19C)	109.5
C(9)-C(15)-H(15A)	109.5	H(19B)-C(19)-H(19C)	109.5
C(9)-C(15)-H(15B)	109.5	C(16)-C(18)-H(18A)	109.5
H(15A)-C(15)-H(15B)	109.5	C(16)-C(18)-H(18B)	109.5
C(9)-C(15)-H(15C)	109.5	H(18A)-C(18)-H(18B)	109.5

C(16)-C(18)-H(18C)	109.5	H(23A)-C(23)-H(23B)	109.5
H(18A)-C(18)-H(18C)	109.5	C(20)-C(23)-H(23C)	109.5
H(18B)-C(18)-H(18C)	109.5	H(23A)-C(23)-H(23C)	109.5
C(22)-C(20)-C(7)	110.5(9)	H(23B)-C(23)-H(23C)	109.5
C(22)-C(20)-C(23)	106.2(10)	C(25)-C(24)-C(29)	119.3(9)
C(7)-C(20)-C(23)	113.5(9)	C(25)-C(24)-P(1)	125.0(7)
C(22)-C(20)-C(21)	110.3(11)	C(29)-C(24)-P(1)	115.5(7)
C(7)-C(20)-C(21)	110.1(9)	C(24)-C(25)-C(26)	121.3(10)
C(23)-C(20)-C(21)	106.1(10)	C(24)-C(25)-H(25A)	119.3
C(20)-C(21)-H(21A)	109.5	C(26)-C(25)-H(25A)	119.3
C(20)-C(21)-H(21B)	109.5	C(25)-C(26)-C(27)	118.5(11)
H(21A)-C(21)-H(21B)	109.5	C(25)-C(26)-H(26A)	120.7
C(20)-C(21)-H(21C)	109.5	C(27)-C(26)-H(26A)	120.7
H(21A)-C(21)-H(21C)	109.5	C(28)-C(27)-C(26)	119.3(10)
H(21B)-C(21)-H(21C)	109.5	C(28)-C(27)-H(27A)	120.4
C(20)-C(22)-H(22A)	109.5	C(26)-C(27)-H(27A)	120.4
C(20)-C(22)-H(22B)	109.5	C(29)-C(28)-C(27)	121.5(10)
H(22A)-C(22)-H(22B)	109.5	C(29)-C(28)-H(28A)	119.3
C(20)-C(22)-H(22C)	109.5	C(27)-C(28)-H(28A)	119.3
H(22A)-C(22)-H(22C)	109.5	C(28)-C(29)-C(24)	119.9(9)
H(22B)-C(22)-H(22C)	109.5	C(28)-C(29)-H(29A)	120.1
C(20)-C(23)-H(23A)	109.5	C(24)-C(29)-H(29A)	120.1
C(20)-C(23)-H(23B)	109.5	C(31)-C(30)-C(35)	118.5(8)

C(31)-C(30)-P(1)	124.2(7)	C(37)-C(38)-C(39)	118.3(11)
C(35)-C(30)-P(1)	117.2(7)	C(37)-C(38)-H(38A)	120.9
C(32)-C(31)-C(30)	122.2(9)	C(39)-C(38)-H(38A)	120.9
C(32)-C(31)-H(31A)	118.9	C(40)-C(39)-C(38)	119.2(11)
C(30)-C(31)-H(31A)	118.9	C(40)-C(39)-H(39A)	120.4
C(31)-C(32)-C(33)	121.5(9)	C(38)-C(39)-H(39A)	120.4
C(31)-C(32)-H(32A)	119.2	C(39)-C(40)-C(41)	121.1(11)
C(33)-C(32)-H(32A)	119.2	C(39)-C(40)-H(40A)	119.5
C(32)-C(33)-C(34)	116.4(8)	C(41)-C(40)-H(40A)	119.5
C(32)-C(33)-H(33A)	121.8	C(36)-C(41)-C(40)	118.9(12)
C(34)-C(33)-H(33A)	121.8	C(36)-C(41)-H(41A)	120.5
C(35)-C(34)-C(33)	121.7(9)	C(40)-C(41)-H(41A)	120.5
C(35)-C(34)-H(34A)	119.1	C(47)-C(42)-C(43)	113.3(8)
C(33)-C(34)-H(34A)	119.1	C(47)-C(42)-Pt(1)	122.8(7)
C(34)-C(35)-C(30)	119.4(9)	C(43)-C(42)-Pt(1)	123.9(7)
C(34)-C(35)-H(35A)	120.3	C(44)-C(43)-C(42)	125.2(10)
C(30)-C(35)-H(35A)	120.3	C(44)-C(43)-H(43A)	117.4
C(37)-C(36)-C(41)	117.5(10)	C(42)-C(43)-H(43A)	117.4
C(37)-C(36)-B(1)	121.9(9)	C(43)-C(44)-C(45)	119.0(10)
C(41)-C(36)-B(1)	120.5(10)	C(43)-C(44)-H(44A)	120.5
C(38)-C(37)-C(36)	124.8(10)	C(45)-C(44)-H(44A)	120.5
C(38)-C(37)-H(37A)	117.6	C(46)-C(45)-C(44)	120.3(9)
C(36)-C(37)-H(37A)	117.6	C(46)-C(45)-H(45A)	119.8

C(44)-C(45)-H(45A)	119.8
C(45)-C(46)-C(47)	119.2(9)
C(45)-C(46)-H(46A)	120.4
C(47)-C(46)-H(46A)	120.4
C(42)-C(47)-C(46)	123.1(9)
C(42)-C(47)-H(47A)	118.5
C(46)-C(47)-H(47A)	118.5
B(1)-C(48)-H(48A)	109.5
B(1)-C(48)-H(48B)	109.5
H(48A)-C(48)-H(48B)	109.5
B(1)-C(48)-H(48C)	109.5
H(48A)-C(48)-H(48C)	109.5
H(48B)-C(48)-H(48C)	109.5
Pt(1)-C(49)-H(49A)	109.5
Pt(1)-C(49)-H(49B)	109.5
H(49A)-C(49)-H(49B)	109.5
Pt(1)-C(49)-H(49C)	109.5
H(49A)-C(49)-H(49C)	109.5
H(49B)-C(49)-H(49C)	109.5

3. Molecular Structure and Crystallographic Data for XPB (3)

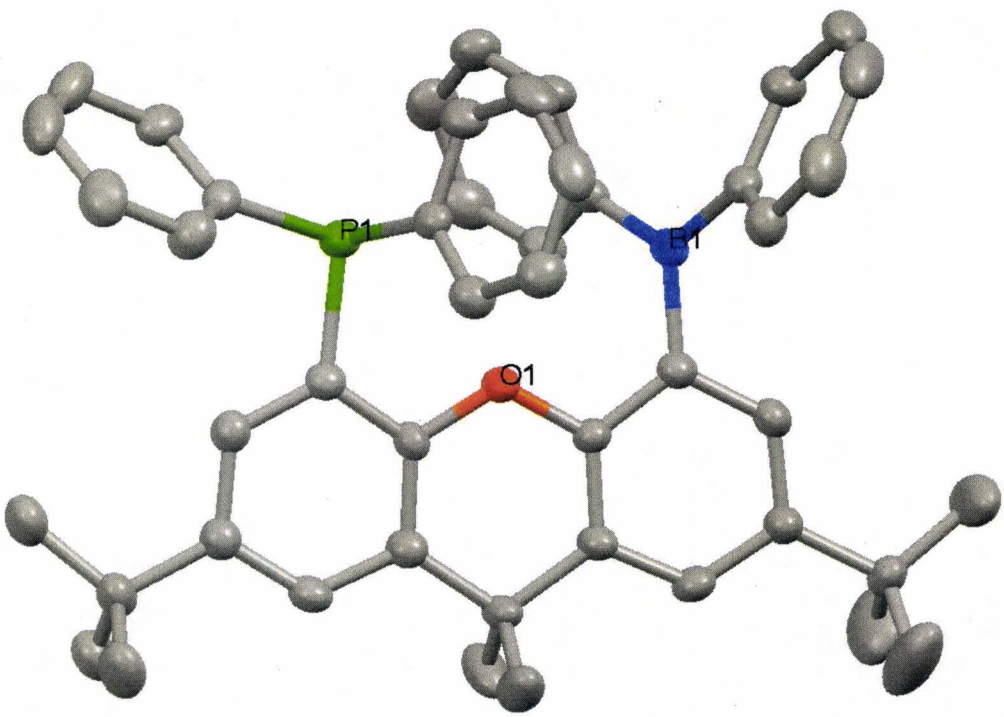

Crystal data and structure refinement for XPB

Empirical formula	$C_{47}H_{48}BOP$	
Formula weight	670.63	
Temperature	173(2) K	
Wavelength	0.71073 Å	
Crystal system	Triclinic	
Space group	P-1	
Unit cell dimensions	a = 10.9636(4) Å	α = 68.618(2)°.
	b = 12.2390(4) Å	β = 85.822(2)°.
	c = 16.1997(6) Å	γ = 75.059(2)°.
Volume	1955.14(12) $Å^3$	
Z	2	
Density (calculated)	1.139 Mg/m^3	
Absorption coefficient	0.104 mm^{-1}	

F(000)	716
Crystal size	0.40 x 0.40 x 0.40 mm^3
θ range for data collection	1.35 to 28.29°.
Index ranges	$-14 \leq h \leq 14, -15 \leq k \leq 15, -20 \leq l \leq 21$
Reflections collected	31755
Independent reflections	9024 [R(int) = 0.1389]
Completeness to θ = 28.29°	92.7 %
Absorption correction	Sadabs
Refinement method	Full-matrix least-squares on F^2
Data / restraints / parameters	9024 / 0 / 548
Goodness-of-fit on F^2	0.983
Final R indices [$I>2\sigma(I)$]	R1 = 0.0614, wR2 = 0.1283
R indices (all data)	R1 = 0.1937, wR2 = 0.1634
Extinction coefficient	0.0032(9)
Largest diff. peak and hole	0.640 and -0.326 e.$Å^{-3}$
Ratio of min. to max. apparent transmission	0.83

Bond lengths [Å] and angles [°] for XPB

P(1)-C(30)	1.836(3)	C(5)-C(12)	1.395(3)
P(1)-C(24)	1.838(3)	C(5)-C(6)	1.397(4)
P(1)-C(4)	1.839(3)	C(6)-C(7)	1.388(4)
O(1)-C(11)	1.378(3)	C(6)-H(6A)	0.99(3)
O(1)-C(12)	1.383(3)	C(7)-C(8)	1.392(4)
C(1)-C(2)	1.390(4)	C(7)-C(20)	1.531(4)
C(1)-C(10)	1.396(4)	C(8)-C(13)	1.390(4)
C(1)-H(1A)	0.96(3)	C(8)-H(8A)	0.95(2)
B(1)-C(42)	1.557(4)	C(9)-C(10)	1.524(4)
B(1)-C(36)	1.564(4)	C(9)-C(13)	1.535(4)
B(1)-C(5)	1.576(4)	C(9)-C(14)	1.545(4)
C(2)-C(3)	1.393(4)	C(9)-C(15)	1.546(4)
C(2)-C(16)	1.532(4)	C(10)-C(11)	1.386(4)
C(3)-C(4)	1.390(4)	C(12)-C(13)	1.383(3)
C(3)-H(3A)	0.97(2)	C(14)-H(14A)	0.9800
C(4)-C(11)	1.396(3)	C(14)-H(14B)	0.9800

C(14)-H(14C)	0.9800	C(28)-C(29)	1.378(4)
C(15)-H(15A)	0.9800	C(28)-H(28A)	0.93(3)
C(15)-H(15B)	0.9800	C(29)-H(29A)	0.96(3)
C(15)-H(15C)	0.9800	C(30)-C(31)	1.388(4)
C(16)-C(19)	1.523(4)	C(30)-C(35)	1.389(4)
C(16)-C(17)	1.537(4)	C(31)-C(32)	1.385(4)
C(16)-C(18)	1.539(4)	C(31)-H(31A)	0.99(3)
C(17)-H(17A)	0.9800	C(32)-C(33)	1.382(4)
C(17)-H(17B)	0.9800	C(32)-H(32A)	0.98(3)
C(17)-H(17C)	0.9800	C(33)-C(34)	1.378(5)
C(18)-H(18A)	0.9800	C(33)-H(33A)	0.97(3)
C(18)-H(18B)	0.9800	C(34)-C(35)	1.378(4)
C(18)-H(18C)	0.9800	C(34)-H(34A)	0.87(3)
C(19)-H(19A)	0.9800	C(35)-H(35A)	1.03(3)
C(19)-H(19B)	0.9800	C(36)-C(37)	1.392(4)
C(19)-H(19C)	0.9800	C(36)-C(41)	1.401(4)
C(20)-C(21)	1.495(4)	C(37)-C(38)	1.382(4)
C(20)-C(23)	1.500(4)	C(37)-H(37A)	0.97(3)
C(20)-C(22)	1.550(5)	C(38)-C(39)	1.381(5)
C(21)-H(21A)	0.9800	C(38)-H(38A)	1.03(3)
C(21)-H(21B)	0.9800	C(39)-C(40)	1.372(5)
C(21)-H(21C)	0.9800	C(39)-H(39A)	0.98(3)
C(22)-H(22A)	0.9800	C(40)-C(41)	1.391(4)
C(22)-H(22B)	0.9800	C(40)-H(40A)	0.90(3)
C(22)-H(22C)	0.9800	C(41)-H(41A)	0.96(2)
C(23)-H(23A)	0.9800	C(42)-C(43)	1.396(4)
C(23)-H(23B)	0.9800	C(42)-C(47)	1.402(4)
C(23)-H(23C)	0.9800	C(43)-C(44)	1.383(4)
C(24)-C(25)	1.385(4)	C(43)-H(43A)	0.96(3)
C(24)-C(29)	1.399(4)	C(44)-C(45)	1.371(4)
C(25)-C(26)	1.382(4)	C(44)-H(44A)	1.02(3)
C(25)-H(25A)	0.99(2)	C(45)-C(46)	1.381(4)
C(26)-C(27)	1.370(5)	C(45)-H(45A)	0.94(3)
C(26)-H(26A)	0.88(3)	C(46)-C(47)	1.369(4)
C(27)-C(28)	1.372(5)	C(46)-H(46A)	1.06(3)
C(27)-H(27A)	0.97(3)	C(47)-H(47A)	0.96(2)

C(30)-P(1)-C(24)	98.75(11)	C(14)-C(9)-C(15)	110.3(3)
C(30)-P(1)-C(4)	103.40(12)	C(11)-C(10)-C(1)	116.6(3)
C(24)-P(1)-C(4)	102.11(12)	C(11)-C(10)-C(9)	122.2(2)
C(11)-O(1)-C(12)	119.5(2)	C(1)-C(10)-C(9)	121.2(3)
C(2)-C(1)-C(10)	123.4(3)	O(1)-C(11)-C(10)	123.0(2)
C(2)-C(1)-H(1A)	118.4(16)	O(1)-C(11)-C(4)	114.3(2)
C(10)-C(1)-H(1A)	118.1(16)	C(10)-C(11)-C(4)	122.7(2)
C(42)-B(1)-C(36)	121.9(2)	O(1)-C(12)-C(13)	122.5(2)
C(42)-B(1)-C(5)	119.3(2)	O(1)-C(12)-C(5)	114.2(2)
C(36)-B(1)-C(5)	118.7(3)	C(13)-C(12)-C(5)	123.2(2)
C(1)-C(2)-C(3)	117.2(3)	C(12)-C(13)-C(8)	116.7(3)
C(1)-C(2)-C(16)	120.0(3)	C(12)-C(13)-C(9)	122.4(2)
C(3)-C(2)-C(16)	122.7(2)	C(8)-C(13)-C(9)	120.9(2)
C(4)-C(3)-C(2)	122.0(3)	C(9)-C(14)-H(14A)	109.5
C(4)-C(3)-H(3A)	116.7(15)	C(9)-C(14)-H(14B)	109.5
C(2)-C(3)-H(3A)	121.2(15)	H(14A)-C(14)-H(14B)	109.5
C(3)-C(4)-C(11)	117.9(3)	C(9)-C(14)-H(14C)	109.5
C(3)-C(4)-P(1)	123.5(2)	H(14A)-C(14)-H(14C)	109.5
C(11)-C(4)-P(1)	118.2(2)	H(14B)-C(14)-H(14C)	109.5
C(12)-C(5)-C(6)	116.7(2)	C(9)-C(15)-H(15A)	109.5
C(12)-C(5)-B(1)	123.5(2)	C(9)-C(15)-H(15B)	109.5
C(6)-C(5)-B(1)	119.6(2)	H(15A)-C(15)-H(15B)	109.5
C(7)-C(6)-C(5)	123.1(3)	C(9)-C(15)-H(15C)	109.5
C(7)-C(6)-H(6A)	122.1(14)	H(15A)-C(15)-H(15C)	109.5
C(5)-C(6)-H(6A)	114.8(14)	H(15B)-C(15)-H(15C)	109.5
C(6)-C(7)-C(8)	116.5(3)	C(19)-C(16)-C(2)	112.4(2)
C(6)-C(7)-C(20)	123.0(3)	C(19)-C(16)-C(17)	108.0(2)
C(8)-C(7)-C(20)	120.5(3)	C(2)-C(16)-C(17)	109.5(2)
C(13)-C(8)-C(7)	123.6(3)	C(19)-C(16)-C(18)	108.9(2)
C(13)-C(8)-H(8A)	121.3(15)	C(2)-C(16)-C(18)	109.1(2)
C(7)-C(8)-H(8A)	114.9(15)	C(17)-C(16)-C(18)	108.8(3)
C(10)-C(9)-C(13)	110.2(2)	C(16)-C(17)-H(17A)	109.5
C(10)-C(9)-C(14)	109.0(2)	C(16)-C(17)-H(17B)	109.5
C(13)-C(9)-C(14)	108.9(2)	H(17A)-C(17)-H(17B)	109.5
C(10)-C(9)-C(15)	109.3(2)	C(16)-C(17)-H(17C)	109.5
C(13)-C(9)-C(15)	109.1(2)	H(17A)-C(17)-H(17C)	109.5

H(17B)-C(17)-H(17C)	109.5	H(23B)-C(23)-H(23C)	109.5
C(16)-C(18)-H(18A)	109.5	C(25)-C(24)-C(29)	118.0(3)
C(16)-C(18)-H(18B)	109.5	C(25)-C(24)-P(1)	117.8(2)
H(18A)-C(18)-H(18B)	109.5	C(29)-C(24)-P(1)	124.2(2)
C(16)-C(18)-H(18C)	109.5	C(26)-C(25)-C(24)	121.3(3)
H(18A)-C(18)-H(18C)	109.5	C(26)-C(25)-H(25A)	119.9(14)
H(18B)-C(18)-H(18C)	109.5	C(24)-C(25)-H(25A)	118.8(14)
C(16)-C(19)-H(19A)	109.5	C(27)-C(26)-C(25)	119.4(4)
C(16)-C(19)-H(19B)	109.5	C(27)-C(26)-H(26A)	123(2)
H(19A)-C(19)-H(19B)	109.5	C(25)-C(26)-H(26A)	117(2)
C(16)-C(19)-H(19C)	109.5	C(26)-C(27)-C(28)	120.8(3)
H(19A)-C(19)-H(19C)	109.5	C(26)-C(27)-H(27A)	122.5(18)
H(19B)-C(19)-H(19C)	109.5	C(28)-C(27)-H(27A)	116.7(18)
C(21)-C(20)-C(23)	110.2(3)	C(27)-C(28)-C(29)	119.9(3)
C(21)-C(20)-C(7)	111.1(2)	C(27)-C(28)-H(28A)	121.1(17)
C(23)-C(20)-C(7)	113.6(3)	C(29)-C(28)-H(28A)	119.0(17)
C(21)-C(20)-C(22)	108.0(3)	C(28)-C(29)-C(24)	120.6(3)
C(23)-C(20)-C(22)	105.3(3)	C(28)-C(29)-H(29A)	122.0(17)
C(7)-C(20)-C(22)	108.2(3)	C(24)-C(29)-H(29A)	117.4(16)
C(20)-C(21)-H(21A)	109.5	C(31)-C(30)-C(35)	118.0(3)
C(20)-C(21)-H(21B)	109.5	C(31)-C(30)-P(1)	125.9(2)
H(21A)-C(21)-H(21B)	109.5	C(35)-C(30)-P(1)	116.0(2)
C(20)-C(21)-H(21C)	109.5	C(32)-C(31)-C(30)	121.0(3)
H(21A)-C(21)-H(21C)	109.5	C(32)-C(31)-H(31A)	119.2(16)
H(21B)-C(21)-H(21C)	109.5	C(30)-C(31)-H(31A)	119.8(16)
C(20)-C(22)-H(22A)	109.5	C(33)-C(32)-C(31)	120.6(3)
C(20)-C(22)-H(22B)	109.5	C(33)-C(32)-H(32A)	119.5(18)
H(22A)-C(22)-H(22B)	109.5	C(31)-C(32)-H(32A)	119.9(18)
C(20)-C(22)-H(22C)	109.5	C(34)-C(33)-C(32)	118.6(3)
H(22A)-C(22)-H(22C)	109.5	C(34)-C(33)-H(33A)	121.0(18)
H(22B)-C(22)-H(22C)	109.5	C(32)-C(33)-H(33A)	120.5(18)
C(20)-C(23)-H(23A)	109.5	C(33)-C(34)-C(35)	121.2(3)
C(20)-C(23)-H(23B)	109.5	C(33)-C(34)-H(34A)	119.9(19)
H(23A)-C(23)-H(23B)	109.5	C(35)-C(34)-H(34A)	118.9(19)
C(20)-C(23)-H(23C)	109.5	C(34)-C(35)-C(30)	120.7(3)
H(23A)-C(23)-H(23C)	109.5	C(34)-C(35)-H(35A)	121.6(17)

C(30)-C(35)-H(35A)	117.7(17)	C(42)-C(47)-H(47A)	113.5(15)
C(37)-C(36)-C(41)	116.5(3)		
C(37)-C(36)-B(1)	118.8(3)		
C(41)-C(36)-B(1)	124.5(3)		
C(38)-C(37)-C(36)	122.1(3)		
C(38)-C(37)-H(37A)	118.1(18)		
C(36)-C(37)-H(37A)	119.7(18)		
C(39)-C(38)-C(37)	119.7(4)		
C(39)-C(38)-H(38A)	119.5(19)		
C(37)-C(38)-H(38A)	120.8(19)		
C(40)-C(39)-C(38)	120.2(3)		
C(40)-C(39)-H(39A)	117.3(18)		
C(38)-C(39)-H(39A)	122.5(18)		
C(39)-C(40)-C(41)	119.6(4)		
C(39)-C(40)-H(40A)	123(2)		
C(41)-C(40)-H(40A)	118(2)		
C(40)-C(41)-C(36)	121.8(3)		
C(40)-C(41)-H(41A)	120.3(16)		
C(36)-C(41)-H(41A)	117.9(16)		
C(43)-C(42)-C(47)	116.1(3)		
C(43)-C(42)-B(1)	122.3(2)		
C(47)-C(42)-B(1)	121.5(3)		
C(44)-C(43)-C(42)	122.0(3)		
C(44)-C(43)-H(43A)	118.1(15)		
C(42)-C(43)-H(43A)	119.9(16)		
C(45)-C(44)-C(43)	119.9(3)		
C(45)-C(44)-H(44A)	122.0(17)		
C(43)-C(44)-H(44A)	118.0(17)		
C(44)-C(45)-C(46)	119.8(3)		
C(44)-C(45)-H(45A)	118.2(18)		
C(46)-C(45)-H(45A)	122.0(18)		
C(47)-C(46)-C(45)	120.0(3)		
C(47)-C(46)-H(46A)	121.3(17)		
C(45)-C(46)-H(46A)	118.6(17)		
C(46)-C(47)-C(42)	122.2(3)		
C(46)-C(47)-H(47A)	119.5(15)		